JAERI-Tech
2002-053

ALTERNATIVES OF ITER VACUUM VESSEL SUPPORT SYSTEM

July 2002

Junji OHMORI, Kazunori KITAMURA
Masanori ARAKI, Isamu OHNO and Teruaki SHOJI

日本原子力研究所
Japan Atomic Energy Research Institute

本レポートは，日本原子力研究所が不定期に公刊している研究報告書です。
入手の問合わせは，日本原子力研究所研究情報部研究情報課（〒319－1195 茨城県那珂郡東海村）あて，お申し越しください。なお，このほかに財団法人原子力弘済会資料センター（〒319－1195　茨城県那珂郡東海村日本原子力研究所内）で複写による実費頒布をおこなっております。

This report is issued irregularly.
Inquiries about availability of the reports should be addressed to Research Information Division, Department of Intellectual Resources, Japan Atomic Energy Research Institute, Tokai-mura, Naka-gun, Ibaraki-ken 〒319－1195, Japan.

編集兼発行　日本原子力研究所

Alternatives of ITER Vacuum Vessel Support System

Junji OHMORI, Kazunori KITAMURA, Masanori ARAKI,
Isamu OHNO and Teruaki SHOJI

Department of ITER Project
Naka Fusion Research Establishment
Japan Atomic Energy Research Institute
Naka-machi, Naka-gun, Ibaraki-ken

(Received May 2,2002)

Optional designs of vacuum vessel (VV) support have been performed for the International Thermonuclear Experimental Reactor (ITER) to reduce stresses and buckling concern of the flexible plate structure in ITER-FDR.

One of the optional designs is hanging type VV support concept that consists of top hanging supports at the top of VV and middle radial stoppers in the middle of outboard VV. The hanging supports are located at the toroidal field (TF) coil inboard top region (R~5400 mm) using the narrow window space surrounded by a poloidal field coil (PF1) and TF coil. The radial stoppers are located inside TF coil cases in the TF coil outboard middle region (R~9300 mm). The upper flange connection of the radial stoppers should slide in vertical direction to eliminate thermal stress produced by relative thermal displacement between VV wall and TF coil case. Both supports consist of flexible plates and are mounted on 18 locations in toroidal direction. The radial and toroidal reaction forces are shared with the hanging supports and the radial stoppers. However, the vertical force is sustained by only the hanging supports.

The others are compressive type support concept that consists of nine VV supports located in alternate divertor port regions in toroidal direction. Two designs have been performed for the VV support concept. One is mounted on TF inter-coil structures (OIS) and the other is on cryostat ring. The compressive support on TF coil OIS is dependent on TF coil movement but that on cryostat ring is independent.

In the optional designs, the bending stress due to the relative thermal displacement between TF coil and VV is classified to primary stress according to ASME Sec. III NF. The stress due to TF coil displacement is also considered as primary stress. The stress due to non-uniform temperature distribution of the flexible plate is classified to secondary stress.

The preliminary structural assessments for the optional designs have been performed for all load combinations to confirm the structural feasibility. Three optional designs have enough structural integrity for all load combinations.

The restriction of the hanging type support is that there is no space for port in upper region of VV and the upper shape of VV should be flattened and moved

downward by 100 mm to attach the support flanges. The top Correction Coil (CC) radial spans need to be modified from the side edge to the center of the TF coil case. For the designs of the compressive type support, alternate divertor port should be eliminated in toroidal direction.

Keywords : Fusion, ITER, Vacuum Vessel, Support Structure, Structural Assessment

JAERI-Tech 2002-053

真空容器支持構造の代替設計

日本原子力研究所那珂研究所 ITER 開発室
大森　順次・喜多村　和憲・荒木　政則・大野　勇・荘司　昭朗

（2002 年 5 月 2 日受理）

国際熱核融合実験炉(ITER)の真空容器(VV)支持構造として、現在の板バネ構造の発生応力を下げるためと座屈裕度を持たせるため、支持構造の代替設計を行った。

設計案の一つは、VV 上部に設ける吊り下げ支持構造と、VV 中央部に設ける振れ止めから成る。吊り下げ支持構造は、TF コイルのインボード上部でポロイダル磁場（PF）コイルと TF コイルにに囲まれた領域(R～5400mm)に設けられる。振れ止めは、TF コイルの外周側中央部の TF コイルの内側(R～9300mm)に設けられる。振れ止めの上部の接続フランジでは、VV と TF コイルケースとの相対的な熱変位によって生ずる熱応力をなくすため、垂直方向にスライドする構造である。両支持部材共、多層板バネ構造で、トーラス 18 箇所に設置する。半径方向、トーラス周方向荷重は上下の支持機構で分担支持されるが、垂直方向荷重は上部支持機構のみで支持される。

他の設計案は、圧縮型の支持構造で、トーラス方向には 9 カ所で、ダイバータポート部の一つおきに設ける。２つの設計がこの圧縮型についてなされ、一つは TF コイルのコイル間構造物から支持するもので、他はクライオスタットリングから支持するものである。TF コイルのコイル間構造物から支持する方式は、TF コイルの動きに従属であるが、クライオスタットから支持する方式では独立である。

本設計では、ASME Sec. III NF に沿って、TF コイルと VV との熱膨張差に伴う曲げ応力と、TF コイルの変位による応力を一次応力で評価する。板バネの温度分布の不均一による熱応力は、二次応力とする。

構造の成立性を確認するため、全ての荷重組合せについて評価を行った結果では、いずれの支持脚も十分な構造強度を有している。

これらの支持脚を適用するための制約として、上部 TF コイル間から吊り下げる支持脚では真空容器の上部にはポートが設けられないことと、真空容器上部のフランジ締結のために上部形状の平坦化と上部位置の 100mm 下方移動修正が必要となることである。さらに、上部補正コイルの半径方向のスパンを TF コイルケースの端部から中央に変更する必要がある。一方、ダイバータポート部に設ける支持脚では、ダイバータポートがトロイダル方向に一つおきになることである。

那珂研究所：〒311-0193　茨城県那珂郡那珂町向山 801-1

This is a blank page.

Contents

1. Introduction ---------- 1
2. Comparison of Structural Design Criteria for VV Support Design---------- 1
2.1 Introduction ---------- 1
2.2 Differences among Codes ---------- 2
3. Investigation of Hanging Type Support System ---------- 6
3.1 Configuration of Support System ---------- 6
3.1.1 Configuration ---------- 6
3.1.2 Interference with Top Correction Coil ---------- 7
3.2 Initial Assembly Procedures in the Site ---------- 7
3.3. Structural Assessments of Support System ---------- 8
3.3.1 Spring Constants of VV Support ---------- 8
3.3.2 Reaction Forces on the Support ---------- 9
3.3.3 Bolt Stress Assessments ---------- 15
3.3.4 Numerical Calculations ---------- 16
3.3.5 Stress Assessment of VV Support ---------- 17
3.3.6 Buckling Strength of VV Support for Vertical Loads ---------- 18
3.3.7 Natural Frequency of VV Support System ---------- 19
3.4. Heat Load Assessment of Support System ---------- 19
3.4.1 Conduction Heat Load ---------- 19
3.4.2 Radiation Heat Load ---------- 20
3.5. Summary ---------- 21
4. Investigation of Compressive Type Support in Divertor Region---------- 55
4.1 Support System on TF Coil OIS---------- 55
4.1.1 Configuration ---------- 55
4.1.2 Structural Assessment of Support System---------- 55
4.1.3 Buckling Assessment ---------- 58
4.1.4 Natural Frequency ---------- 59
4.1.5 Heat Load Assessment of Support System ---------- 59
4.1.6 Bolt Stress Assessment ---------- 59
4.2 Support System on Cryostat Ring ---------- 72
4.2.1 Configuration ---------- 72
4.2.2 Structural Assessment of Support System---------- 73
4.2.3 Natural Frequency ---------- 73
4.3. Summary ---------- 73
5. Conclusions ---------- 85
Acknowledgement ---------- 85
References ---------- 86

目　次

1. 緒言 ---------- 1
2. 真空容器支持脚設計の構造設計基準の比較---------- 1
2.1 まえがき ---------- 1
2.2 設計基準の相違 ---------- 2
3.上部吊り下げ形支持構造の設計 ---------- 6
3.1 支持構造の設計・形状 ---------- 6
3.1.1 支持構造 ---------- 6
3.1.2 補正コイルとの干渉 ---------- 7
3.2 現地初期組立手順 ---------- 7
3.3 上部吊り下げ形支持構造の構造強度評価 ---------- 8
3.3.1 支持構造のバネ定数 ---------- 8
3.3.2 支持構造に掛かる反力 ---------- 9
3. 3.3 ボルト応力評価 ---------- 15
3.3.4 数値計算による各部応力値 ---------- 16
3.3.5 真空容器支持構造の応力評価 ---------- 17
3.3.6 垂直荷重に対する支持構造の座屈強度 ---------- 18
3.3.7 支持構造の固有振動数 ---------- 19
3.4. 上部吊り下げ形支持構造からの侵入熱評価 ---------- 19
3.4.1 伝導侵入熱 ---------- 19
3.4.2 輻射侵入熱 ---------- 20
3.5. まとめ ---------- 21
4.ダイバータポートの位置に設ける圧縮形支持構造の設計---------- 55
4.1TF コイル OIS に設ける支持構造 ---------- 55
4.1.1 支持構造の設計・形状 ---------- 55
4.1.2 支持構造の構造強度評価 ---------- 55
4.1.3 座屈評価 ---------- 58
4.1.4 固有振動数 ---------- 59
4.1.5 支持構造からの侵入熱評価 ---------- 59
4.1.6 ボルトの応力評価 ---------- 59
4.2 クライオスタットリングに設ける支持構造---------- 72
4.2.1 支持構造の設計・形状 ---------- 72
4.2.2 支持構造の構造強度評価 ---------- 73
4.2.3 固有振動数 ---------- 73
4.3. まとめ ---------- 73
5. 結　言 ---------- 85
謝辞 ---------- 85
参考文献 ---------- 86

1. Introduction

In the DDD of the FDR for ITER design [1], the outboard mid-support concept was adopted as the VV support system. The VV supports consist of the flexible plate mounted between VV wall and TF coil case around the outboard mid plane. However, the large compressive force is produced on the flexible plates during the operation modes, mainly due to the VV and in-vessel dead weight of -100 MN, the downward VDE III force of -72 MN and seismic load of -60 MN. In addition, the VV support has to withstand the large VDE and seismic horizontal load component of 25 MN and 60 MN, respectively. Moreover, the support is loaded by radial bending moments produced by relative thermal displacement between the VV and TF coil of about 50 mm (at R=9300 mm). For these loads, there is some concern about structural integrity for the produced stress and the buckling.

Two VV support concepts have been studied as optional support structures to avoid the structural concern of the support.

One is hanging type VV support concept that consists of top hanging supports at the top of VV and middle radial stoppers at the middle of outboard VV. Both supports are formed with flexible plates and are mounted on 18 locations in toroidal direction.

The other is a compressive type support concept that consists of nine VV supports located in alternate divertor port region in toroidal direction. Two designs are investigated for the compressive VV support concept. One is mounted on TF inter-coil structures (OIS) and the other is on cryostat ring. The compressive support on TF coil OIS is dependent on TF coil movement but that on cryostat ring is independent

The preliminary structural assessment of the optional VV support has been also performed to confirm the feasibility.

2. Comparison of Structural Design Criteria for VV Support Design

2.1. Introduction

Several design criteria are considered to apply to the structural design for the support structures in the fusion tokamak machine, such as ASME Sec. VIII-Div. 2, ASME Sec. III-NB, -NC, -NF and RCC-MR, etc., while they have both reasonable and unreasonable points for their structural assessments. For instance, the ASME Sec VIII-Div.2 and ASME Sec. III-NC codes are selected for the structural design of vacuum vessel (VV) and its support structure in ITER. The former is applied to the stress assessment for the Cat. I and II loads (corresponding to normal operation and anticipated upset condition, respectively), which is used for the structural component design of the non-nuclear power plant. The latter is selected for the Cat. III and IV loads (corresponding to unlikely upset condition and extremely unlikely event, respectively), which is applied to the class 2 component design for the nuclear power plant. This is one of solutions to establish the new design criteria for the VV and its support structural design in the ITER, since the ASME Sec VIII-Div.2 code prescribes nothing on the assessment for the Cat. III and IV loads.

The ASME Sec. III-NF Code reasonably covers the assessment on the static primary stress components for all Category loads, but does not describe in detail on the assessment for the secondary stress such as the thermal stress and cyclic stress (fatigue assessment). In addition, there is no description on the pre-loading on the bolt assessment in the code. As for the ASME Sec. III-NB Code, which is applied to the

class 1 component design for the nuclear power plant, it covers all requirements for the VV structural design assessments, while the application leads to the increase of its fabrication cost. As mentioned above, there is no design code applied perfectly to the design of the VV support.

Therefore, the differences among the design criteria in these codes are compared, and the additional items are considered for the application to the design criteria for the VV support.

2.2. Differences among Codes

Differences on the design criteria among several design codes are summarized in Table 2.2-1 for the flexible plates, and in Table 2.2-2 for connecting bolts. The design criteria used in DDD of ITER FDR and alternative designs are also shown in the Tables.

(1) For Flexible Plates on VV Support

The ITER VV support design basically adopts the ASME Sec VIII-Div.2 as the design criteria of Category I and II loads, and the ASME Sec. III-NC as those for Category III and IV loads. However, ITER-SDC (Structural Design Criteria) prescribes to select the ASME Sec. III-NF code as the design criteria for the VV support design.

The buckling load factors in the RCC-MR French code, safety margin to the critical load, are used for the buckling assessment. Comparing with the criteria in the ASME Sec. III-NF code, the current design criteria of the ITER VV support is found to be more conservative for the VV support design. In addition, thermal expansion stress is assessed to be the secondary stress category in the ITER VV support design, because it is taken to be the secondary one in the ASME Sec VIII-Div.2. So, the flexible plates design might be less conservative, because the flexible plates have a large compressive stress to induce the buckling concern under the plastic bending stress region.

For the alternative design, the bending stress due to the relative thermal displacement between TF coil and VV is classified to primary stress according to ASME Sec. III NF. The stress due to TF coil displacement is also considered as primary stress. The thermal stress due to non-uniform temperature distribution of the flexible plate, which is not defined in ASME Sec III NF, is classified to secondary. The bucking criteria are based on ASME Sec III NH Appendix-T. Plastic buckling is not considered because the plastic region of the flexible plate is limited.

(2) For Connecting Bolts on VV Support

The structural design of the connecting bolts in the ITER VV support is performed by keeping relatively high pre-loading stress on the bolt at the initial assembly. Namely, the induced stress on the bolts at the external loads is kept to be less than the pre-loading stress, so that the alternative stress range on the bolt at the operation is estimated to be negligibly small, resulting that the fatigue assessment of the bolts is not required. However, maximum stress on the bolts must be kept below the allowable stress limits in accordance with Category loads in other design codes such as ASME, so the bolt stress should be kept lower than that in the ITER design. From Table 2.2-2, the allowable bolt stress limits in the ASME Sec. III-NF is found to be lowest among the design codes, and it seems to be most conservative code for the connecting bolt design among the several design codes mentioned above.

(3) For Gravity Support Design

The toroidal field (TF) gravity support design, with the flexible plates and connecting bolts, is basically performed in the same manner as that for the VV support, while the operating temperature is slightly different. The ASME Sec. III-NF code is applied to the structural design assessment for the gravity support. The application of the NF code includes the several issues, as previously described the NF code has no description on the secondary stress and fatigue assessment in detail. The secondary stress, of the thermal stress due to thermal gradient on the plates, is considered as the primary stress in the gravity support, while the thermal expansion stress (Free End Displacement Stress) is prescribed as the primary stress in the ASME Sec. III-NF code. This consideration seems to be slightly conservative, though the thermal stress value was considerably lower than the stress values due to other external loads. The fatigue assessment was performed based on the ASME Sec. III-NB code because of no description on the detailed fatigue assessment procedure in the NF code. The buckling assessment was also conducted with the ASME Sec. III Appendix-T, for no detailed description on NF code.

On the other hand, the connecting bolt stress on the gravity support was also conservatively assessed by using the ASME Sec. III-NF code, so the safety margin of the connecting bolt against the allowable limits is small but it is less than the limits.

Table 2.2-1 Differences on Design Criteria among Design Codes for Flexible Plates

		Stress Component	Sec III-NB	Sec III-NC	Sec III-NF	Sec VIIIDiv.2 Alternative Rules	**ITER VV Support(DDD)**	**Optional VV Support**
Static Stress		Sm	Min.(2/3 Sy, 1/3 Su)					
	Cat. I	Pm	1.0 Sm	1.0 Sm	1.0 Sm	1.0 Sm	1.0 Sm	1.0 Sm
		Qτ	0.6x1.0 Sm	0.6x1.0 Sm	0.6x1.0 Sm	0.6x1.0 Sm	0.6x1.0 Sm	0.6x1.0 Sm
		Pm + Pb	1.5x1.0 Sm	1.5x1.0 Sm	1.5x1.0 Sm	1.5x1.0 Sm	1.5x1.0 Sm	1.5x1.0 Sm
		Pm + Pb +Pe	3.0x1.0 Sm	3.0x1.0 Sm	1.5x1.0 Sm	3.0x1.0 Sm	**3.0x1.0 Sm**	**1.5x1.0 Sm**
		Pm+Pb+Pe+Q	3.0x1.0 Sm	3.0x1.0 Sm	-	3.0x1.0 Sm	3.0x1.0 Sm	3.0x1.0 Sm
		Buckling, mk	3.0	3.0	2.0	3.0	**2.5** [2)]	**3.0**
	Cat. II	Pm	1.1 Sm	1.1 Sm	1.33 Sm	1.0 Sm	1.0 Sm	1.0 Sm
		Qτ	0.6x1.1 Sm	0.6x1.1 Sm	0.6x1.33 Sm	0.6x1.0 Sm	0.6x1.0 Sm	0.6x1.0 Sm
		Pm + Pb	1.5x1.1 Sm	1.5x1.1 Sm	1.5x1.33 Sm	1.5x1.0 Sm	1.5x1.0 Sm	1.5x1.0 Sm
		Pm + Pb +Pe	3.0x1.1 Sm	3.0x1.1 Sm	1.5x1.33 Sm	3.0x1.0 Sm	**3.0x1.0 Sm**	**1.5x1.0 Sm**
		Pm + Pb + Q	3.0x1.1 Sm	3.0x1.1 Sm	-	3.0x1.0 Sm	3.0x1.0 Sm	3.0x1.0 Sm
		Buckling, mk	3.0	3.0	2.0	3.0	**2.0** [2)]	**3.0**
	Cat. III	Pm	1.2 Sm	1.2 Sm	1.5 Sm		1.2 Sm	1.2 Sm
		Qτ	0.6x1.2 Sm	0.6x1.2 Sm	0.6x1.5 Sm		0.6x1.2 Sm	0.6x1.2 Sm
		Pm + Pb	1.5x1.2 Sm	1.5x1.2 Sm	1.5x1.5 Sm		1.5x1.2 Sm	1.5x1.2 Sm
		Pm + Pb +Pe	-	-	1.5x1.5 Sm		-	1.5x1.2 Sm
		Pm + Pb + Q	-	-	-		-	-
		Buckling, mk	2.5	2.5	2.0		**1.3** [2)]	**2.5**
	Cat. IV	Pm	Max(1.5Sm, 1.2Sy), but <0.7Su	2.0 Sm	Max(1.5Sm, 1.2Sy), but <0.7Su		2.0 Sm	2.0 Sm
		Qτ	0.42 Su	0.6x2.0 Sm	0.42 Su		0.6x2.0 Sm	0.6x2.0 Sm
		Pm + Pb	1.5x(Max(1.5 Sm,1.2Sy), but <0.7Su)	1.5x2.0 Sm	1.5x(Max(1.5 Sm,1.2Sy), but <0.7Su)		1.5x2.0 Sm	1.5x2.0 Sm
		Pm + Pb +Pe	-	-	1.5x(Max(1.5 Sm,1.2Sy), but <0.7Su)		-	1.5x2.0 Sm
		Pm + Pb + Q	-	-	-		-	-
		Buckling, mk	1.5	1.5	-		-	1.5
Cyclic Stress		Fatigue Assessment Procedure	Based on S-N Fatigue Curve, and For Pm+Pb+Q+F (Cumulative Damage)	Based on S-N Fatigue Curve, and For Pm+Pb+Q+F (Cumulative Damage)	No Description in Detail	Based on S-N Fatigue Curve, and For Pm+Pb+Q+F (Cumulative Damage)	Not Assessed	Not Assessed

Note: 1) Pm : Primary Membrane Stress, Qτ : Primary Shear Stress, Pb : Bending Stress, Pe ; Thermal Expansion Stress (Free End Displacement Stress), Q : Secondary Stress and F : Peak Stress (Expansion Stress of Pe is considered to be Secondary Stress in ASME Sec. III-NB, -NC, Sec VIII and in ITER Design, but to be Primary one in ASME Sec. III-NF)

2) In ITER VV support design, load factors based on RCC-MR French Code, for Fast Breeder Reactor, are applied as a buckling limit. Those in other codes are based on ASME Sec III NF Appendix-T.

Table 2.2-2 Differences on Design Criteria among Design Codes for Bolts

		Stress Component	Sec III-NB	Sec III-NC	Sec III-NF	SecVIIIDiv.2 Alternative Rules	**ITER VV Support**	**Optional VV Support**
Static Stress		Smb	1/3 Sy	1/3 Sy	1/3.33 Su	1/3 Sy	-	1/3 Sy
		P0 (Pre-load Stress)	2 Smb0	-	Smb0	Smb0	0.8 Sy0	2 Smb0
	Cat. I	Pt	1.0 Smb	1.0 Smb	1.0 Smb	1.0 Smb	0.8 Sy	1.0 Smb
		Qτ	-	-	0.62xSu / 5	-	-	-
		P0 + Pt	2.0x1.0 Sm	1.0 Smb	-	2.0x1.0 Sm	0.8 Sy	2.0x1.0 Sm
		P0+ Pt + Pb	3.0x1.0 Sm	1.0 Smb	-	3.0x1.0 Sm	0.8 Sy	3.0x1.0 Sm
	Cat. II	Pt	1.0 Smb	-	1.15 Smb	1.0 Sm	0.8 Sy	1.0 Smb
		Qτ	-	-	1.15x0.62 xSu / 5	-	-	-
		P0 + Pt	2.0x1.0 Sm	-	-	2.0x1.0 Sm	0.8 Sy	2.0x1.0 Sm
		P0+ Pt + Pb	3.0x1.0 Sm	-	-	3.0x1.0 Sm	0.8 Sy	3.0x1.0 Sm
	Cat. III	Pt	1.0 Smb	-	1.25 Smb	-	0.8 Sy	1.0 Smb
		Qτ	-	-	1.25x0.62 xSu / 5	-	-	-
		P0 + Pt	2.0x1.0 Sm	-	-	-	0.8 Sy	2.0x1.0 Sm
		P0+ Pt + Pb	3.0x1.0 Sm	-	-	-	0.8 Sy	3.0x1.0 Sm
	Cat. IV	Pt	Min.(0.7Su, Sy)	-	Min.(0.7Su, Sy)	-	0.8 Sy	Min.(0.7Su, Sy)
		Qτ	Min(0.42 Su, 0.6Sy)	-	Min(0.42 Su, 0.6Sy)	-	-	Min(0.42 Su, 0.6Sy)
		P0 + Pt	Su, but Su > 700 MPa	-	Su, but Su > 700 MPa	-	0.8 Sy	Su, but Su > 700 MPa
		P0+ Pt + Pb	Su, but Su > 700 MPa	-	Su, but Su > 700 MPa	-	0.8 Sy	Su, but Su > 700 MPa
Cyclic Stress		Fatigue Assessment Procedure	Based on S-N Fatigue Curve, and For Pm+Pb+Q+F , Fatigue Strength Reduction Factor of 4, (Cumulative Damage)	No Description in Detail	No Description in Detail	Based on S-N Fatigue Curve, and For Pm+Pb+Q+F , Fatigue Strength Reduction Factor of 4, (Cumulative Damage)	No Description in Detail	No Description in Detail

Notes : 1) P0 ; Pre-loading Stress at Assembly, Pt : Tensile Stress due to External Load, Qτ : Shearing Stress due to External Load, and Pb : Bending Stress due to External Load

2) Bolt is designed by formula in ASME Sec. III-NC Code, in which bolt stress is not classified in accordance with load category.

3) Sy : Yield Strength at Service Temperature, Sy0 : Yield Strength at Room Temperature, Su : Ultimate Strength at Service Temperature

3. Investigation of Hanging Type Support System

3.1 Configuration of Support System

3.1.1 Configuration

The hanging support system of the vacuum vessel from the top of the TF coil case is shown in Figs. 3.1-1 to 3.1-3. The vertical window space dimensions to see the VV main body from the top of the TF coils are the inboard toroidal length of 600mm, outboard toroidal one of 1000mm and both radial lengths of 1100mm with the trapezoidal shape, which is surrounded with the adjacent TF coil cases. The top VV support consists of 18-30 mm thick flexible plates with the vertical length of about 2.1m and average toroidal width of 500mm, and top and bottom trapezoidal flanges with 100 and 150mm thickness, respectively. The top flange mounted 80 K cooling paths as the thermal anchor is bridged on the top edges of both side support posts. The bottom flange is connected with the top of the VV main body through 12-M72 connecting bolts, made of Inconel-718, at 18 locations between the adjacent TF coils. The Inconel-718 washer plate with hexagonal bolt holes to fix bolt head is installed on the back side of the VV outer wall, because high strength stopper, with strengthened material equivalent to the bolt heads, is necessary to fasten the bolts at the initial assembly. At both toroidal edges of the top TF coil cases, the support posts are mounted and fixed by the 6-M60 bolts. The VV support of the flexible plates is hung from the top of the support posts through the flange connection. The connection of the VV support top flange and support posts is conducted through the 20 mm thick electrical insulation made of glass epoxy laminate and 12-M72 dielectric bolts, to electrically insulate between the VV and TF coil case.

Four thermal shield panels mounted 80 K cooling paths are also hung from the support post top flange, so as to surround all the flexible plates. Each panel consists of lower and upper ones with a vertical length of ~1 m, and they are connected with the hinge joints and flexible cooling tubes for easy insertion from the narrow side spaces between the hanging VV support and TF coil case at the assembly. Four shield panels are jointed each other on the side edges with the screws and formed to be a box type panel. The schematic drawing of the thermal shield panel is shown in Fig.3.1-4.

In current design, there is a vertical gap of 200 mm between the VV outer wall and TF case inside surface in the top region at the initial assembly, however the vertical gap needs to be increased by an additional 100 mm for the bolt fastening and thermal shield installation spaces. The top VV location, therefore, should be moved downward by 100 mm and top VV outer wall configuration might be flattened for the easy assembly.

The hanging type VV support system may give a concern of the horizontal swaying with large deformation of the VV lower region at the large seismic loads. Then, the installation of the radial stopper with the 5-25 mm thick flexible plates, on which the 80 K cooling paths are mounted at the middle portion, is also proposed as the centering support mechanism at the lower portion on the TF coil case inside surface, as shown in Fig. 3.1-3. The radial stopper slides on the VV main body in the vertical direction at the joint portion, where the joint of both components is conducted by 4-M72 bolts through the clearance bolt holes. The sliding surfaces on the joint may need to have the sliding materials such as Teflon and/or Fiberslip.

Then, the radial and toroidal reaction forces are shared with the hanging support at the top and radial stopper at the middle. However, the vertical force is sustained by only the hanging support at the top.

3.1.2 Interference with Top Correction Coil

There is a design concern on the interference between the top hanging support and top correction coil (CC), consisting of 6 multi-turn coils arranged toroidally around outside of the TF coils but inside the PF1 coil. Each top CC covers a 60 degree sector and spans three TF coils in the toroidal direction. Because of this, each top CC is forms a electrical circuit with a inboard toroidal span at the PF1 coil, a outboard toroidal span around the PF2 coil, 2 radial spans located on the side edge of the TF coil case at 6 locations in the torus. In the current design, these radial spans are arranged just on the vertical opening window between the adjacent TF coil cases, and therefore have the interference with the top hanging support configuration. Figures 3.1-5(a) and (b) show the modifications of the top CC winding configuration and CC radial spans arrangement for the application of the hanging support structure to the VV support. If the location of the CC radial spans is modified from the side edge to the center of the TF coil case to avoid the interference with the hanging support, there is no interference between CC and the top hanging supports, as shown in Fig.3.1-5(b).

3.2 Initial Assembly Procedures in the Site

A sub-assembly unit of two VV sectors integrated with two TF coils is carried into the assembly site, as an assembly set of the tokamak. The 2 VV sectors in the sub-assembly unit have been already connected by the poloidal welding in the factory. At that time, the hanging support and radial stopper are also mounted and jointed between the VV sectors and TF coils in the factory. In addition, the setting of the bolts and bolt washer plates for the 9 remaining joints has to be also performed in the factory before the in-situ assembly, as follows.

1) Set the connecting bolts on the VV outer wall from the inside access
2) Fix the bolt heads with the washer plates, and weld the edge periphery of washer plates to VV outer wall
3) Seal-weld the cover plate on the bolt head holes

The 9 remaining joints and assemblies of the hanging supports and radial stoppers are conducted in the site after the in-situ VV sector welding assembly. The in-situ assembly procedures on the VV support are followings.

1) Fix the adjacent sub-assembly units consisting of 2 TF coils and 2 VV sectors
2) Poloidal welding assembly of VV outer wall using the splice plates
3) Insert and fix SS304 shield blocks into the space between VV outer and inner walls for the in-situ VV welding region
4) Poloidal welding assembly of VV inner wall using the splice plates
5) Carry down the hanging support to VV top joint portion from the window between TF coil cases, and connect VV outer wall and lower flange of hanging support with the bolts and nuts
   At that time, the shimming may need to be done between the VV top flange and hanging flange for fitting the flange surfaces
6) Insert 80K thermal shield panels between TF coil case and the hanging support. Mount the support posts on the both toroidal edges of the TF coil cases with the bolts and fix the box type 80 K thermal shield panel on the

support post top flange

7) Connect the upper flange and support posts with the di-electric connecting bolts through G-10 insulation sheet and adjustable shims
8) At same time, connect also the lower flange of radial stopper to attachment on the TF coil case with the connecting bolts through G-10 insulation sheet and adjustable shims
9) Mount and fix the 80 K thermal shield panels around the radial stopper

3.3. Structural Assessments of Support System

The structural assessment of the VV support have been performed assuming that the VV itself is rigid body and top base flange of the hanging support and the bottom base flange of the radial stopper on the TF coil case are completely fixed.

3.3.1 Spring Constants of VV Support

The radial stiffness of the VV top hanging support is given by the followings, taking into account the support installation.

Consider the force balance in the radial direction, when the radial force of Pr works on the bottom edge of the support. The radial displacement of δr is expressed by the followings under the condition with the rotation fixture on both edges, 'Build-in mode' [2].

$$\delta_r = \frac{P_r L_1^3}{12EI_{r1}} + \frac{P_r L_1}{A_1 G} = \left(\frac{L_1^3}{N_1 E w_1 t_1^3} + \frac{L_1}{N_1 G w_1 t_1}\right) \cdot P_r \qquad (3.3\text{-}1)$$

the spring constant of the top hanging support, k_{r1} can be obtained as follows.

$$k_{r1} = \frac{1}{\frac{L_1^3}{N_1 E w_1 t_1^3} + \frac{L_1}{N_1 G w_1 t_1}} \qquad (3.3\text{-}2)$$

Similarly, the spring constant of the radial stopper, k_{r2} can be calculated as follows.

$$k_{r2} = \frac{1}{\left(\frac{L_2^3}{N_2 E w_2 t_2^3} + \frac{L_2}{N_2 G w_2 t_2}\right) \cdot \cos^2\varphi + \frac{L_2}{N_2 E w_2 t_2} \cdot \sin^2\varphi} \qquad (3.3\text{-}3)$$

The radial spring constant of the hanging support, k_r is given by the following.

$$k_r = k_{r1} + k_{r2} \qquad (3.3\text{-}4)$$

Next, consider the force balance in the vertical direction, when the vertical force of Pz works on the bottom edge of the top hanging support.

$$\delta_z = \frac{L_1}{N_1 E w_1 t_1} \cdot P_z \qquad (3.3\text{-}5)$$

From the equation (3.3-5), the spring constant of the support in the vertical direction is calculated as follows, because the radial stopper has no contribution to the vertical stiffness of the hanging support system.

$$k_z = \frac{N_1 E w_1 t_1}{L_1} \tag{3.3-6}$$

The spring constant of the top hanging support in the toroidal direction is given by the following.

$$k_{\theta 1} = \frac{1}{\frac{L_1^3}{N_1 E t_1 w_1^3} + \frac{L_1}{N_1 G t_1 w_1}} \tag{3.3-7}$$

Similarly, the spring constant of the radial stopper, $k_{\theta 2}$ can be calculated as follows.

$$k_{\theta 2} = \frac{1}{\frac{L_2^3}{N_2 E t_2 w_2^3} + \frac{L_2}{N_2 G t_2 w_2}} \tag{3.3-8}$$

The toroidal spring constant of the hanging support, k_θ is given by the following.

$$k_\theta = k_{\theta 1} + k_{\theta 2} \tag{3.3-9}$$

where, E : Young's Modulus of Support Material (SS304, =200 Gpa)
G : Shear Modulus of Support Material (SS304, =78 Gpa)
N1 : Number of Plates on Top Hanging Support / sector (=18)
w1 : Width of Top Flexible Plate (=0.5 m in Average)
t 1: Thickness of Top Flexible -Plate (= 0.030 m)
L1 : Length of Flexible -Plate (=2.1 m)
N2 : Number of Plates on Radial Stopper / sector (=5)
w2 : Width of Lower Flexible Plate (=0.6 m in Average)
t 2: Thickness of Lower Flexible -Plate (= 0.025 m)
L2 : Length of Lower Flexible -Plate (=2.0 m)
φ : Inclined Angle of Lower Radial Stopper to Gravity Line (=15 deg.)
kr1 : Spring Constant of Top Flexible -Plates in Radial Direction(N/m)
kθ1 : Spring Constant of Top Flexible -Plates in Toroidal Direction(n/m)
kr2 : Spring Constant of Lower Flexible -Plates in Radial Direction(N/m)
kθ2 : Spring Constant of Lower Flexible -Plates in Toroidal Direction(n/m)
kr : Spring Constant of Hanging Support in Radial Direction(N/m)
kθ : Spring Constant of Hanging Support in Toroidal Direction(n/m)
kz : Spring Constant of Hanging Support in Vertical Direction(N/m)

3.3.2 Reaction Forces on the Support

(1) Initial Assembly

The relative displacement of δ_{r0} (assumed to be 5 mm) between the base pads of both the VV and TF coil is considered as the mismatch displacement in the radial direction at the initial assembly. The reaction force on the VV support at that time is estimated as follows.

$$f_{r0} = k_r \cdot \delta_{r0} \tag{3.3-10}$$

$$f_{r10} = \frac{k_{r1}}{k_{r1} + k_{r2}} \cdot \delta_{r0}, \quad f_{r20} = \frac{k_{r2}}{k_{r1} + k_{r2}} \cdot \delta_{r0} \tag{3.3-11}$$

$$f_{z0} = k_z \cdot \delta_{z0} = \frac{W}{Nc} \tag{3.3-12}$$

where, W is the total weight of VV and in-vessel components of 100 MN, and Nc is number of the VV support locations of 18.

(2) Normal Operation

(a) Relative Displacement between VV and TF Coil

At the normal operation, the relative displacement between the base pads of both the VV and TF coil increases because of the cool down of the TF coil and baking of the VV, in addition to that at the initial assembly. For the middle radial stopper support, the effect of the axis inclination to the gravity line has to be considered on the radial displacement component due to the relative vertical displacement between the VV and TF coil.

$$f_{r(op)} = k_r \cdot (\delta_{bk \cdot VV,i} + \delta_{CL \cdot TF,i}) \tag{3.3-13}$$

$$f_{r1(op)} = \frac{k_{r1}}{k_{r1} + k_{r2}} \cdot (\delta_{bk \cdot VV1} + \delta_{CL \cdot TF1}) \tag{3.3-14}$$

$$f_{r2(op)} = \frac{k_{r2}}{k_{r1} + k_{r2}} \cdot \left[(\delta_{bk \cdot VV,2} + \delta_{CL \cdot TF,2}) \cos\varphi + (\delta_{bk \cdot VV,2(Z)} + \delta_{CL \cdot TF,2(Z)}) \sin\varphi \right] \tag{3.3-15}$$

$$f_{zop} = k_z \cdot \delta_{z0} \tag{3.3-15}$$

where, $\delta_{bk.VV1}$: Radial Thermal expansion of VV at Top Hanging Support (=0.0073m)
$\delta_{CL.TF1}$: Radial Thermal shrinkage of TF coil at Top Hanging Support (=0.017m)
$\delta_{bk.VV2}$: Radial Thermal expansion of VV at Mid Stopper Support (=0.012m)
$\delta_{CL.TF2}$: Radial Thermal shrinkage of TF coil at Mid Stopper Support (=0.027m)
$\delta_{bk.VV2(Z)}$: Vertical Thermal expansion of VV at Mid Stopper Support (=0.0092m)
$\delta_{CL.TF2(Z)}$: Vertical Thermal shrinkage of TF coil at Mid Stopper Support (=0.0121m)

(b) In-Plane Thermal Stress on Plate due to Longitudinal Temperature Gradient

Here, the plate stress at the normal operation has to include the thermal stress due to the vertical temperature gradient of 80 K to 373 K on the upper hanging plates and that of 4 K to 373 K on the middle radial stopper, on which the temperature profile was calculated in detail by the FEM thermal analysis. Figure 3.3-1 shows the boundary conditions for the FEM thermal stress analysis. Figure 3.3-2 shows the stress profiles on the plate due to the vertical thermal gradient for the upper hanging support plate and middle radial stopper one.

As the results, maximum thermal stress on the plate due to the vertical temperature gradient is estimated to be 18 to 25 MPa according to the plate width for the top hanging support plate, and to be 64 MPa for the middle radial stopper plate.

(c) Support Stress due to TF Coil case Overturning Deformations

The TF coil case has the relatively significant deformation due to the overturning moment acting on the TF coil at the normal operation. The VV support, both top hanging support plates and middle radial stopper, is deformed from the TF coil case deformation, and may receive the large reaction forces. Then, the stress on the hanging supports due to the TF coil case deformations has been estimated based on the simple

calculation. The deformations on the both toroidal edges of the TF coil case for the VV support locations at the plasma operation (End of Burn mode: EOB1) are as follows [3].

Support Location	R-direction	θ-direction	Z-direction
Top (Left Side Edge)	1.37 mm	8.45 mm	7.65 mm
Top (Right Side Edge)	-1.74 mm	8.38 mm	7.61 mm
Mid (Left Side Edge)	4.11 mm	-2.64 mm	-1.95 mm
Mid (Right Side Edge)	2.54 mm	-2.80 mm	-4.17 mm

The difference between the displacements on the TF coil case left side edge and right side one causes the torsion moment, Tzi on the VV support plates around Z-axis by R- and θ-displacements, and toroidal bending moments, Mθi around R-axis by Z-displacement. Then, R-axis and Z-axis torsional and bending moments on the VV support locations are obtained by the following equation.

$$T_{z,i} = \frac{GJ_{i,z}\varphi_{i,z}}{L_i}, J_{z,i} = N_i w_i t_i^3 \left[\frac{1}{3} - 0.21\frac{t_i}{w_i}\left(1 - \frac{t_i^4}{12w_i^4}\right)\right] \quad (3.3\text{-}16)$$

$$M_{\theta,i} = \frac{EI_{\theta i}\varphi_{r,i}}{2L_i} = \frac{EN_i t_i w_i^3 \varphi_{r,i}}{24L_i} \quad (3.3\text{-}17)$$

where, the suffix, i=1 corresponds to upper hanging support and i=2 to middle radial stopper. The stresses on the hanging supports due to the TF coil case deformations are expressed by following equations using the bending moments obtained.

$$\tau_{z,i} = \frac{T_{z,i} t_i}{2J_{z,i}} \quad (3.3\text{-}18)$$

$$\sigma_{\theta,i} = \frac{M_{\theta,i} \cdot w_i}{2I_{\theta,i}} = \frac{6M_{\theta,i}}{N_i t_i w_i^2} \quad (3.3\text{-}19)$$

The Z- and R-rotations are estimated as follows from the TF coil case displacements mentioned above.

Support Location	Z-Rotation, φzi (Rad.) Z-Torsion, Tzi (MN m)	R-Rotation, φri (Rad.) θ-Moment, Mθi1 (MN m)
Top Support	$\varphi z1 = 3.005 \times 10^{-3}$ $Tz1 = 8.695 \times 10^{3}$	$\varphi r1 = 3.865 \times 10^{-5}$ $M\theta 1 = 1.036 \times 10^{4}$
Mid Support	$\varphi z2 = 1.517 \times 10^{-3}$ $Tz2 = 9.290 \times 10^{2}$	$\varphi r2 = 2.145 \times 10^{-3}$ $M\theta 2 = 2.414 \times 10^{5}$

The loads mentioned above are toroidally symmetrical. Next, consider asymmetric forces in toroidal direction such as VDE and seismic loads, as below.

(3) VDE Loads

The VDE loads include the vertical load of V_{VDE} and horizontal load of H_{VDE}, which act on the overall VV in the torus. Here, the V_{VDE} is assumed to act on the VV uniformly in the torus, and H_{VDE} to act on the overall VV in the torus.

$$f_{zVDE} = k_z \cdot \delta_{zVDE} = \frac{V_{VDE}}{Nc} \quad (3.3\text{-}20)$$

As for the H_{VDE}, the reaction force on the support can be obtained in same way as the seismic event. As shown in Fig. 3.3-3, the reaction force on each support due to the horizontal seismic load of H_{VDE} depends on its support location and stiffness in the load direction (X).

$$H_{VDE} = K_x \cdot \delta_{xVDE} = 2(k_r \sum_{i}^{Nc/2} \cos^2\theta_i + k_\theta \sum_{i}^{Nc/2} \sin^2\theta_i) \cdot \delta_{xVDE} = \frac{Nc}{2}(k_r + k_\theta)\delta_{xVDE} \quad (3.3\text{-}21)$$

$$\delta_{xVDE} = \frac{2H_{VDE}}{Nc(k_r + k_\theta)} \quad (3.3\text{-}22)$$

$$\delta_{r(VDE)i} = \delta_{xVDE} \cdot \cos\theta_i , \quad \delta_{\theta(VDE)i} = \delta_{xVDE} \cdot \sin\theta_i \quad (3.3\text{-}23)$$

$$f_{xVDEi} = (k_r \cos^2\theta_i + k_\theta \sin^2\theta_i)\delta_{xVDE} \quad (3.3\text{-}24)$$

The normal reaction force to the longitudinal direction on the middle radial stopper is expressed as follows. Here, the normal force to the longitudinal direction for the middle radial stopper is obtained with considering the inclination of 'cos(φ)'.

$$f_{r(VDE)i} = k_r \cdot (\delta_{r(VDE)i} + \delta_{r(op)} + \delta_{r0})$$

$$f_{r1(VDE)i} = \frac{k_{r1}}{k_{r1} + k_{r2}} \cdot f_{r(VDE)i}$$

$$f_{r2(VDE)i} = \frac{k_{r2}}{k_{r1} + k_{r2}} \cdot f_{r(VDE)i} \cdot \cos\varphi$$

$$f_{\theta(VDE)i} = k_\theta \cdot \delta_{\theta(VDE)i} \quad (3.3\text{-}25)$$

$$f_{\theta1(VDE)} = \frac{k_{\theta1}}{k_{\theta1} + k_{\theta2}} \cdot f_{\theta(VDE)i}$$

$$f_{\theta2(VDE)i} = \frac{k_{\theta2}}{k_{\theta1} + k_{\theta2}} \cdot f_{\theta(VDE)i}$$

$$f_{z(VDE)i} = f_{zVDE} + f_{z0}$$

where, V_{VDE} : Vertical Component of VDE Load (= 43, 54, 72 MN)
H_{VDE} : Horizontal Component of VDE Load (= 15, 19, 25 MN)

(4) SL1 and SL2 Seismic Events with ground accelerations of 0.05 G and 0.2 G

When the overall VV support in the torus receives the horizontal seismic load of H_{SEIS} (=0.15G and 0.6G, with amplification factor of 3) in X-direction and vertical load of V_{SEIS} (=0.15G and 0.6G, with amplification factor of 3), the reaction force on the support can be obtained as follows, in the same way as the horizontal VDE load.

$$H_{SEIS} = K_x \cdot \delta_{xSEIS} = 2(k_r \sum_{i}^{Nc/2} \cos^2\theta_i + k_\theta \sum_{i}^{Nc/2} \sin^2\theta_i) \cdot \delta_{xSEIS} = \frac{Nc}{2}(k_r + k_\theta)\delta_{xSEIS} \quad (3.3\text{-}26)$$

$$\delta_{xSEIS} = \frac{2H_{SEIS}}{Nc(k_r + k_\theta)} \quad (3.3\text{-}27)$$

$$\delta_{r(SEIS)i} = \delta_{xSEIS} \cdot \cos\theta_i , \quad \delta_{\theta(SEIS)i} = \delta_{xSEIS} \cdot \sin\theta_i \quad (3.3\text{-}28)$$

$$f_{xSEIS\,i} = (k_r \cos^2\theta_i + k_\theta \sin^2\theta_i)\delta_{xSEIS} \tag{3.3-29}$$

$$f_{z(SEIS)i} = k_z \cdot \delta_{z(SEIS)} = \frac{V_{SEIS}}{Nc} \tag{3.3-30}$$

Moreover, the reaction force in each direction is expressed as follows.

$$\begin{aligned}
f_{r(SEIS)i} &= k_r \cdot (\delta_{r(SEIS)i} + \delta_{r(op)} + \delta_{r0}) \\
f_{r1(SEIS)i} &= \frac{k_{r1}}{k_{r1} + k_{r2}} \cdot f_{r(SEIS)i} \\
f_{r2(SEIS)i} &= \frac{k_{r2}}{k_{r1} + k_{r2}} \cdot f_{r(SEIS)i} \cdot \cos\varphi \\
f_{\theta(SEIS)i} &= k_\theta \cdot \delta_{\theta(SEIS)i} \\
f_{\theta1(SEIS)i} &= \frac{k_{\theta1}}{k_{\theta1} + k_{\theta2}} \cdot f_{\theta(SEIS)i} \\
f_{\theta2(SEIS)i} &= \frac{k_{\theta2}}{k_{\theta1} + k_{\theta2}} \cdot f_{\theta(SEIS)i} \\
f_{z(SEIS)i} &= f_{z0} + f_{z(SEIS)}
\end{aligned} \tag{3.3-31}$$

(5) Seismic Event + VDE Loads

The reaction forces on the VV support at the seismic event and VDE loads can be obtained by linearly adding the reaction forces at both events, with expressions as follows.

$$\begin{aligned}
f_{r(SEIS)i} &= k_r \cdot (\delta_{r(SEIS)i} + \delta_{r(VDE)i} + \delta_{r(op)} + \delta_{r0}) \\
f_{r1(SEIS)i} &= \frac{k_{r1}}{k_{r1} + k_{r2}} \cdot f_{r(SEIS)i} \\
f_{r2(SEIS)i} &= \frac{k_{r2}}{k_{r1} + k_{r2}} \cdot f_{r(SEIS)i} \cdot \cos\varphi \\
f_{\theta(SEIS)i} &= k_\theta \cdot (\delta_{\theta(SEIS)i} + \delta_{\theta(VDE)i}) \\
f_{\theta1(SEIS)i} &= \frac{k_{\theta1}}{k_{\theta1} + k_{\theta2}} \cdot f_{\theta(SEIS)i} \\
f_{\theta2(SEIS)i} &= \frac{k_{\theta2}}{k_{\theta1} + k_{\theta2}} \cdot f_{\theta(SEIS)i} \\
f_{z(SEIS)i} &= f_{z(SEIS)i} + f_{z(VDE)i} + f_{z0}
\end{aligned} \tag{3.3-32}$$

Based on the reaction forces obtained by using the equations mentioned above, the bending moments, shearing forces and tensile/compressive forces, acting on the flexible plates of the top hanging support and middle radial stopper, are calculated and then the stress induced on the plates assessed as follows.

$$\sigma_{r,i} = M_r \cdot \frac{t_i}{2I_{r,i}} = \frac{f_{r,i}L}{2} \cdot \frac{t_i}{2I_{r,i}} = \frac{3f_{r,i}L_i}{N_i w_i t_i^2}$$

$$\sigma_{\theta,i} = M_\theta \cdot \frac{w_i}{2I_{\theta,i}} = \frac{3f_{\theta,i}L_i}{N_i t_i w_i^2}$$

$$\tau_{r,i} = \frac{f_{r,i}}{A_i} = \frac{f_{r,i}}{N_i w_i t_i} \qquad (3.3\text{-}33)$$

$$\tau_{\theta,i} = \frac{f_{\theta,i}}{A_i} = \frac{f_{\theta,i}}{N_i w_i t_i}$$

$$\sigma_{z,i} = \frac{f_{z,i}}{A_i} = \frac{f_{z,i}}{N_i w_i t_i}$$

Here, i=1and i=2 correspond to top hanging support plates and lower radial stopper, respectively. The equivalent stress on the plate, σeq is assessed as follow.

$$\sigma_{eq,j} = \sqrt{\sum_j \sigma_{i,j}^{\ 2} + \sum_j 4\tau_{i,j}^{\ 2}}, j = r,\theta,z \qquad (3.3\text{-}34)$$

(6) Vertical Force due to VV Rocking Movement

The rocking movement of the global VV main body should be also considered on the stress assessments of the VV support structures, which is caused by the horizontal load component of the VDE and seismic loads. Here, the global rocking moment is supported by the vertical tension and compression force on the supports, with the maximum force on θ=0, 180deg. support locations. Therefore, the global rocking moment is supported by only the top hanging supports because the middle radial stopper supports do not have the vertical stiffness.

$$M_{Rocking} = F_x \cdot LH_1 = f_{1,0(Z)} \cdot R_1 \cdot \sum_i^{Nc} \cos^2\theta_i$$

$$f_{1,0(Z)} = \frac{2 \cdot F_x \cdot LH_1}{Nc \cdot R_1} \qquad (3.3\text{-}35)$$

where, LH1 : Vertical Length from VV Center to Top Edge of Hanging Support (=7.762 m)

R1 : Center Radius of Top Hanging Support (=5.405 m)

$f_{rock,1,0}$: Vertical Tensile/Compressive Force on θ=0deg. Sector of Top Hanging Support

Fx : Total Horizontal Load in X-direction acting on Global VV body

Then, the stresses on the supports due to the VV rocking movement are obtained from the equations (3.3-35), as follows.

$$f_{rock,1,i(Z)} = f_{rock,1,0(Z)} \cdot \cos\theta_i$$

$$\sigma_{b,Rock,1,i(Z)} = \frac{f_{rock,1,i(Z)}}{A_1} = \frac{F_x \cdot LH_1 \cdot \cos\theta_i}{Nc \cdot R_1 \cdot N_1 w_1 t_1} \qquad (3.3\text{-}36)$$

3.3.3 Bolt Stress Assessments

Figure 3.3-4 shows a schematic drawing of the flange/bolts mechanical behavior at the loads of the bending moment and tensile force. White background area and oblique-lined one mean the uncontact surface (opening) region on the flange and contact surface region due to the loads mentioned above, which are corresponding to the regions inducing tensile force and compressive force, respectively. The loading moment, in other words, is shared by the tensile forces induced on the bolts in the former region, and by the compressive forces induced between the flange surfaces in latter one. Assuming the flange to be rigid body, there is nothing of the contact surface and the neutral axis is located on the right edge of the flange with Lc=0 shown in Fig. 3.3-4. The flange is conservatively considered to be rigid body for the bolt stress assessment.

When the forces of fr, fθ and fz work on the hanging support in radial, toroidal and vertical directions, following stresses are induced on the connecting bolts from the moment and force balances.

$$\sigma_{i,B(ro)} = \frac{M_{i,r} \cdot d_{i,B(ro)}}{A_{Bi} \sum_{j}^{N_{Bi}} d_{i,B(rj)}^{2}} = \frac{f_{i,r} \cdot L_i \cdot d_{i,B(ro)}}{A_{Bi} \sum_{j}^{N_{Bi}} d_{i,B(rj)}^{2}}$$

$$\sigma_{i,B(\theta o)} = \frac{f_{i,\theta} \cdot L_i \cdot d_{i,B(\theta o)}}{A_{Bi} \sum_{j}^{N_{Bi}} d_{i,B(\theta j)}^{2}},$$

$$\tau_{i,Br} = \frac{f_{i,r}}{N_{Bi} \cdot A_{Bi}} \qquad (3.3\text{-}37)$$

$$\tau_{i,B\theta} = \frac{f_{i,\theta}}{N_{Bi} \cdot A_{Bi}},$$

$$\sigma_{i,B(z)} = \frac{f_{i,z}}{N_{Bi} \cdot A_{Bi}}$$

where, N_{Bi} : Number of Bolts (=12 for Top Bolts, =14 for Mid Bolts)
dBrj : Radial Distance from neutral axis to each bolt center(m)
dBθj : Toroidal Distance from neutral axis to each bolt center(m)
A_{Bi} : Section Area of Bolt (=$0.25\pi d_{Bi}^{2}$)
d_{Bi} : Effective Bolt Diameter(=For example, 0.056 m for M60 bolt, 0.068 m for M72 one and 0.076 m for M80 one)

Here, i=1 and i=2 correspond to the bolts of the top hanging support and ones of the lower radial stopper, respectively. The equivalent bolt stress is expressed by the following.

$$\sigma_{B,eq,i} = \sqrt{\sum_{j} \sigma_{B,i,j}^{2} + \sum_{j} 4\tau_{B,i,j}^{2}}, j = r,\theta,z \qquad (3.3\text{-}38)$$

For the top hanging support bolts, the tensile and compression stress should be also assessed due to the rocking movement of the global VV body, as follows.

$$\sigma_{rock,k,B(z)} = \frac{f_{rock,1,k(z)}}{N_{B1} \cdot A_{B1}} = \frac{F_x \cdot LH_1 \cdot \cos\theta_k}{Nc \cdot R_1 \cdot N_{B1} \cdot A_{B1}} \quad \text{k=1,18 location} \qquad (3.3\text{-}39)$$

Moreover, the joint bolts are fastened with an appropriate pre-loading stress through the flanges at the initial assembly, so that the shearing force applied to the flanges in the horizontal direction is generally supported by the friction force induced on the flange interface. Therefore, the shearing stress does not occur on the bolt as long as the enough friction force can be expected between the flanges. However, the shearing stress on the bolts is conservatively assessed. The total friction force in the torus is estimated considering the bolt pre-loading stress to be 500 MPa, as follows.

$$Q_{friction} = \mu_S \cdot NcN_1 \cdot \frac{\pi}{4} d_{blt}{}^2 \cdot S_{blt,pre-loading} \qquad (3.3\text{-}40)$$

where, μs : Friction Coefficient between SS316 Flanges (=0.20-0.40)
D_{blt} : Effective Bolt Diameter (=0.068 m for M72 Bolt)
$S_{blt,pre\text{-}loading}$: Pre-loading Stress on Bolts at Initial Assembly (=500 MPa)

The total friction force in the torus is estimated to be 78-157 MN, which is enough beyond the horizontal force component of the applied forces at the operations. Then, the shearing stress does not occur on the bolt. Tables 3.3-5 (b) and (c) show the maximum bolt stresses for all load combinations with and without the friction forces between the joint flanges.

3.3.4 Numerical Calculations

(1) Load Combinations used in Structural Assessments

The following load combinations are taken in the structural assessments of the VV support as shown in Table 3.3-1, according to the VV support design described in the DDD of the FDR for ITER [4].

(2) Numerical Calculations

Using the equations (3.3-1) to (3.3-40), the reaction force on the each VV support has been calculated for several load combinations, and next stresses on the support also estimated.

At first, substituting the values into the equations (3.3-1) to (3.3-9), the spring constants of the top and bottom supports are given as follows.

kr1 = 5.244 x 10^6	N/m
kθ1= 1.273 x 10^9	N/m
kr2 = 1.255 x 10^6	N/m
kθ2= 5.484 x 10^8	N/m

The spring constants of the hanging support are given as followings.

kr = 6.499 x 10^6	N/m
kz = 2.571 x 10^{10}	N/m (= kz1)
kθ_= 1.821 x 10^9	N/m

Next, the tensile/compressive, bending and shearing stresses on the support can be

calculated using the equations (3.3-33) to (3.3-39).
Tables 3.3-3(a) to3.3-3(g) indicate the stress calculation results of the flexible plate on the upper hanging support and middle radial stopper for several load combinations. In addition, the stress calculation results of the joint bolts on the VV-side flange are also shown in Table 3.3-4 (a) to 3.3-4(f).

3.3.5 Stress Assessment of VV Support

(1) Structural Materials for VV Support

In general, austenitic stainless steels of SS316LN(IG) and SS304 are considered as the material candidates of the flexible plates for the case with relatively low stress values induced on the plates, however high Ni alloy of Inconel-625 should be also considered. From the stress assessment results shown in Table 3.3-3(a) to 3.3-3(g), Inconel-625 seems to be better for the flexible plate material. The material characteristics of the austenitic stainless steels are shown in Table 3.3-2(a), and those of Inconel-625 in Table 3.3-2(b), respectively. For the joint bolt materials, the austenitic stainless steels and Inconel-718 are considered. Table 3.3-2(c) shows the mechanical properties of Inconel-718. The limiting stress intensity values, Sm of these materials are shown in the Tables as a function of service temperatures from 4K to 573K, which are determined according to the design code of ASME Sec. VIII-Div. 2 [4], as follows.

$$Sm = \text{Min.}\ (2/3Sy,\ 1/3\ Su), \qquad \text{at Service Temperature}$$

(2) Allowable Stress Limits

The limiting stress intensity value of Sm can be applied to the shell components at the normal operation, but not to the joint bolts. The stress limits for the components except the bolts are as follows [4]:

Membrane Stress	$< 1.0K \times Sm$	(3.3-41)
Membrane + Bending Stress	$< 1.5K \times Sm$	
Pure Shearing Stress	$< 0.6K \times Sm$	

where, the limit factor of K is set to be 1.0 for the Normal conditions (Load Category-I), 1.0 for the Anticipated Upset conditions (Load Category-II),1.2 for the Unlikely Upset conditions (Load Category-III) and 2.0 for the Extremely Unlikely Event (Load Category-IV) [5]. For the secondary stress such as thermal stress due to thermal gradient on the plate, the following design criteria are taken in ASME Sec. VIII-Div.2 Code.

Primary + Secondary Stress $< 3.0 \times Sm$ (=2Sy), for Cat. I & II Loads

For the bolt materials, the limiting stress intensity of Smb and allowable stress limits for the loading of category I, are prescribed as the followings in the ASME Code, Sec. III-NB-3230 [6].

Limiting Stress Intensity	$Smb = Sy / 3$	(3.3-42)
Average Tensile Stress (Including pre-loading)	$< 2.0 \times Smb$ (=2/3 Sy)	
Tensile + Bending Stress	$< 3.0 \times Smb$ (=1.0 Sy)	

where, Sy means the yield strength of bolt material at service temperature.
Accordingly, maximum pre-load stress is limited to 0.67 times Sy at room temperature during the initial assembly, if additional external load on the bolt is negligibly small.

In addition, the same allowable limit is also used for the loads of categories II and

III. However, the allowable stress limits for the load of category-IV are determined as follows from the ASME Code, Sec. III-NB, APPENDIX-F [7].

Average Tensile Stress (Including pre-loading)	< Min. (Sy, 0.7×Su)	(3.3-43)
Tensile + Bending Stress	< Su, if Su > 700 MPa	

where, Su means the ultimate strength of bolt material at service temperature.

As the results, the VV support structure has an enough structural integrity for the most of the load combinations within the allowable stress limit of the material, except the primary stress on the middle radial stopper flexible plates with the maximum stress of 361 MPa for the load combination of DW + THL11 +VDE-I + SL-1. The maximum primary stresses on the flexible plates for the top hanging support and middle radial stopper are estimated as shown in Table 3.3-5 (a). The maximum stress in all cases appears on the VV support located at 45 deg. for the connecting bolts or 90 deg. for the flexible plates in the torus. Tables 3.3-5 (b) and (c) show maximum stresses of the connecting bolts on upper hanging support and middle radial stopper for all load combinations with and without the friction forces between the joint flanges, which are enough within the allowable stress limits.

(3) Sensitivity of Mechanical Stiffness Combination on Support Stress

The radial and toroidal reaction forces on each support of the upper hanging support and middle radial stopper are determined in the mechanical stiffness combination of the upper and middle supports as understood from the equations (3.3-13) to (3.3-15). The stress induced on each support also depends on the mechanical stiffness combination of the upper and middle supports. The proposed design of the hanging support has the mechanical stiffness ratios of 0.24 on kr2/kr1 and of 0.46 on kθ2/kθ1.

Then, the stresses on the each support has been investigated varying the mechanical stiffness ratios of kr2/kr1 and kθ2/kθ1. The calculated results are shown in Table 3.3-5(a) for the plate stress and in Table 3.3-5(b) for the bolt stress. For the design of mechanical stiffness ratios of 0.10 on kr2/kr1 and of 0.20 on kθ2/kθ1, the stress on flexible plates and bolts are within the allowable values for all of the load combinations.

3.3.6 Buckling Strength of VV Support for Vertical loads

In the hanging type VV support system, the flexible plate on the top hanging support essentially does not have the compressive loads, however the VV can have vertically upward loads at the upward VDE and seismic load. Then, the buckling strength of the flexible plates on the VV support has been assessed for the upward forces mentioned above. In addition, the radial stopper does not also have the compressive force because of its sliding mechanism in the vertical direction.

The calculation is based on the following Euler's equation [2]:

$$P_{CR} = \frac{4\pi^2 E I_r}{L^2} \qquad (3.3\text{-}44)$$

where, P_{CR} : Critical Buckling Load (N)
E : Young's Modulus of Stacked Plates (=200 GPa)
Ir : Radial Inertia Moment of Stacked Plates (=9.375x10^{-6} m^2)

L : Length of Stacked Plates (=2.10 m)

From the results shown in above Table 3.3-6, the VV support has the enough safety margin on the buckling strength for the VDE and seismic events.

3.3.7 Natural Frequency of VV Support System

The knowledge of the natural frequency of the global VV support system is basically important for the structural assessment against the horizontal seismic load, which can be calculated by the following equation.

$$f_k = \frac{1}{2\pi}\sqrt{\frac{K \cdot G}{W}} = \frac{1}{2\pi}\sqrt{\frac{Nc(k_r + k_\theta) \cdot G}{2W}} \qquad (3.3\text{-}45)$$

where, K : Spring Constant of Global VV Support System
G : Gravity Acceleration (=9.8 m/s^2)
W : Total Weight of Vessel and In-vessel Components (=100 MN)
Nc : Number of VV Support Locations (=18)
kr, kθ : Radial and Toroidal Spring Constants of each VV support
(=6.499 x10^6, 1.821 x10^9 N/m, respectively)

Substituting the valuables into the equation (3.3-45), the natural frequency of the global VV support system is estimated to be 6.39 Hz. This value is slightly larger than that of the global TF magnet support system of about 4 Hz.

3.4. Heat Load Assessment of Support System

3.4.1 Conduction Heat Load

It is important to estimate the conduction heat loads from the support structures thermal anchors on the VV supports to the magnets for the design of the cooling system of the magnet system, in addition to the heat load from the gravity support thermal anchor. Then, the conduction heat loads from the thermal anchors on the hanging type of VV supports have been estimated based on the simple calculation.

(1) Top Hanging Support

The thermal anchor is mounted on the upper flange of each flexible plate of the VV support, which is connected with the adjacent TF cases through the support posts with thickness of 100 mm, width of 1120 mm and height of about 1000 mm.

Then, the heat load to the TF coils is represented as follows.

$$q_L = Nc \cdot Nf \cdot \frac{W \cdot t_2}{L_2} \int_4^{80} \lambda(T) dT \qquad (3.4\text{-}1)$$

where, Nc : Number of VV Supports in the torus (= 18)
Nf : Number of Support Posts per Support (= 2)
W : Averaged Width of Support Post (= 1.12 m)
t2 : Thickness of Support Post (= 0.10 m)
L2 : Length of Support Post (= 1.0 m)
T : Temperature at the interface of Mid and Lower Plates (K)

$$\int_{4K}^{80K} \lambda_{SS}(T)dT = 349 \qquad \text{(w/m)}$$

From the equations (2.4-1), the following is obtained.

$$q_L = 18 \cdot 2 \cdot 1.12 \cdot \frac{0.10}{1.0} \cdot 0.349 = 1.407 \qquad \text{(kW)} \qquad (3.4\text{-}2)$$

(2) Radial Stopper

Thermal anchor with 80 K temperature is also mounted on the mid-location of the flexible plates, as well as the present design of the VV support described in DDD. Substituting the design dimensions of the radial stopper into equation (3.4-1), the conduction heat load from the radial stopper to TF coil is estimated to be 0.47 kW in total.

The conduction heat load from the thermal anchor to the TF case through the VV supports is estimated to be 1.88 kW in total, which is slightly increased by about 18 % from that (1.6 kW) in the current design of VV support in the DDD. Total conduction heat load to the TF coils is estimated to be 3.8 kW in addition to 1.9 kW of the heat load of the gravity support thermal anchor to the TF coils.

3.4.2 Radiation Heat Load

(1) Top Hanging Support

The radiation heat load, from 80 K thermal shield mounted on the surrounding of the top hanging VV support to the TF Case, has been preliminarily estimated based on the simple calculation. The thermal shied of the cooling panels, on which the cooling tubes with 80 K gas helium coolant are welded, is installed and covered surrounding the VV support structure. The radiation heat load is given by the following equation.

$$q_{(rad)} = Nc \sum_i \sigma \varepsilon_{i,j} A_i (T_i^4 - T_j^4) \qquad (3.4\text{-}3)$$

$$\varepsilon_{i,j} = \frac{1}{\frac{1}{\varepsilon_{i(Ti)}} + \frac{1}{\varepsilon_{j(Tj)}} - 1} \qquad \text{for Infinite Parallel Plates}$$

where, Nc : Number of TF coils (=18)

σ : Stephan-Boltzmann Constant (=5.99x10^{-7} W/m^{2}K^4)

Ai : Surface Area of Thermal Shield Panel (m^2)

εi,j : Equivalent Emissivity between Thermal Shield Panel and TF coil case Surface

$\varepsilon i_{(Ti)}$: Emmissivity of Stainless Steel (Thermal Shield Panel) at 80 K (= 0.05) [9]

$\varepsilon j_{(Tj)}$: Emmissivity of Stainless Steel (TF coil case Surface) at 4 K (= 1.0) [9]

Ti : Temperature on Thermal Shield Panel (= 80 K)

Tj : Temperature on TF coil case Surface (= 4 K)

Estimating roughly the radiation heat load with the use of the equation (3.4-3), it leads to about 0.16 kW.

(2) Radial Stopper

Similarly, the radiation heat load, from 80 K thermal shield mounted on the surrounding of the middle radial stopper to the TF coil case, has been preliminarily estimated based on the simple calculation, estimated to be 0.08 kW with Ai=3.2 m^2.

Therefore, the total radiation heat load from 80 K thermal shield mounted on the surrounding of the VV support to the TF coil case, is estimated 0.24 kW, which is corresponding to about 13 % of the conduction heat load.

3.5. Summary

The hanging type VV support concept has been studied as one of the VV support design options, instead of the outboard support with flexible plates mounted between the VV and TF coil case around the outboard mid plane. The preliminary structural design study of the hanging type VV support has been also performed to confirm the structural feasibility.

From the studies, following conclusions are drawn.

1) The hanging type VV support concept, consisting of top hanging flexible plates and middle radial stopper, has been studied to avoid the buckling structural concern of the flexible plates. They are mounted, on 18 locations in toroidal direction, at the TF inboard top region (R~5400 mm) using the narrow window space surrounded by PF1, top intercoil structure and TF coil cases, and around the TF outboard middle region (R~9700 mm), respectively. The radial and toroidal reaction forces are shared with the hanging support at the top and radial stopper at the middle, while the vertical force is sustained by only the hanging support at the top.
2) The initial assembly procedures of the hanging VV support have also been studied, including the pre-assemblies in the factory and in-situ assemblies. The 9 in-situ joints and assemblies of the hanging supports and radial stoppers are conducted in the site after the in-situ VV sector welding assembly. However the vertical gap, between the VV outer wall and TF coil case inside surface in the top region, needs to be increased by an additional 100 mm length for the joint bolt fastening and thermal shield installation spaces. The top VV location, therefore, should be moved downward by 100 mm and top VV outer wall configuration might be flattened for the easy assembly. In addition, the location of the top CC radial spans needs to be modified from the side edge to the center of the TF coil case to avoid the interference with the hanging support.
3) The structural assessments of the hanging support structures have been performed for all load combinations. For the reference design, the VV support structure of the flexible plates has enough structural integrity for the most of the load combinations except the primary stress on the middle radial stopper flexible plates for the load combination of DW (Dead Weight) + THL11 (Radial Displacements of VV and TF coil case) + VDE-I + SL-1.
   However, the optimization of the mechanical stiffness ratio combination of top hanging plate and mid radial stopper plate leads to relatively low stress within the allowable limit for all load combinations. The optimized stiffness ratio are

kr2'/kr1of 0.10 and kθ2'/kθ1 of 0.20, corresponding to 30 mm thick and 500 mm wide for top hanging plate and 20.5 mm thick and 490 mm wide for the mid radial stopper plate.

The joint bolts have enough structural integrity for all of the load combinations within the allowable stress limit

4) The conduction heat load from the thermal anchor to the TF coil case through the VV supports is estimated to be 1.88 kW in total, which is slightly increased by about 18 % from that (1.6 kW) in the current design of VV support in the DDD. Then, total conduction heat load to the TF coils is estimated to be 3.8 kW in addition to 1.9 kW of the heat load of the gravity support thermal anchor to the TF coils.
5) The restrictions to apply the hanging type support are as follows:
   (i) The vertical location of the VV outer wall in the top region must be moved downward by 100 mm;
   (ii) Top VV outer wall configuration might be flattened for the easy assembly;
   (iii) The top CC radial spans need to be modified from the side edge to the center of the TF coil case.

Table 3.3-1 Loads and Load Combinations considered for VV Support Structural Assessments

Cat.	Loads and Load Combinations	Load Magnitude (MN)		Allowable Stress Limit for Primary Membrane Stress , Sm (MPa)
		Vertical	Horizontal	
I	**Loads Considered**			**SS316LNIG:**
	1) Dead Weight (DW)	-100		Sm_I= 453, at 80 K
	2) Thermal Load1by R-Disp.		ΔR1= 0.024 m	= 137, at 100 C
	(100 C Expansion :THL11)		ΔR2= 0.040 m	= 130, at 200 C
	3) Temperature Gradient Load on	ΔT1=293 K		
	Plate (from 80K-373K :THL12)	ΔT2=369 K		
	4) Thermal Load1by R-Disp.		ΔR1= 0.033 m	**Inconel-625**
	(200 C Expansion :THL21)		ΔR2= 0.056 m	Sm_I= - , at 80 K
	5) Temperature Gradient Load on	ΔT1=393 K		= 217, at 100 C
	Plate (from 80K-473K :THL22)	ΔT2=469 K		= 193, at 200 C
	6) VDE-I	-43	15	
	Load Combinations			**Inconel-718**
	1) DW	-100		Sm_I= 523 , at 80 K
	2) DW + THL11+ THL12	-100		= 453, at 100 C
	3) DW + THL21+ THL22	-100		= 453, at 200 C
	4) DW + THL11 +THL12 + VDE-I	-143	15	
II	**Additional Loads**			Sm_{II}= Sm_I
	1) VDE-II	-54	19	
	2) SL-1	0.15 G	0.15 G	
	Load Combinations			
	DW + THL1 +VDE-II	-154	19	
	DW + THL1 +VDE-I + SL1	-158	30	
III	**Additional Loads**			Sm_{III}= 1.2 Sm_I
	1) VDE-III	-72	25	
	Load Combinations			
	1) DW + THL11 + VDE-III	-172	25	
	2) DW + THL11 + VDE-II + SL1	-169	34	
IV	**Additional Loads**			Sm_{IV}= 2.0 Sm_I
	1) SL-2	0.6 G	0.6 G	
	Load Combinations			
	1) DW + THL11 + VDE-I + SL2	-203	75	

Notes : 1) Thermal Loads 'THL1' means both the imposed radial displacement due to thermal expansion/contraction of VV main body and TF case 'THL11', and longitudinal temperature gradient load on the plate 'THL12'.

2) For the load categories III and IV, the secondary stresses do not need to be assessed, so that the longitudinal temperature gradient load on the plate of 'THL12' is eliminated for the load categories III and IV. In addition, the imposed radial displacement due to thermal expansion/contraction of VV main body and TF case 'THL11', corresponding to 'End Free Displacement', is taken as the primary stress.

3) The allowable stress limit for membrane stress component of the materials is determined based on the VV Design Criteria described in the ISDC on the FDR for ITER-FEAT.

Table 3.3-2(a) Mechanical Properties of Austenitic Stainless Steel for Flexible Plate Material-1

Material Properties of Austenitic Stainless Steel (SS316LNIG & SS304)						
Temp. [C]	-269	-193	20	100	200	300
Young's Modulus,E [GPa]	207	200	192	186	178	170
Poisson's Ratio, ν	0.28	0.29	0.30	0.30	0.30	0.30
Shear Modulus, G [GPa]	80.9	77.5	73.8	71.5	68.5	65.4
Thermal Expansion, $\alpha(1x10^{-6}/C)$	10.2	13.0	16.3	16.8	17.2	17.7
Ultimate Strength, Su (MPa)	1450	1360	517	517	510	500
Yield Strength, Sy (MPa)	900	820	206	206	195	173
Allowable Stress, Sm (MPa)	(483)	(453)	137	137	130	115

Table 3.3-2(b) Mechanical Properties of Inconel-625 for Flexible Plate Material-2

Material Properties of Inconel 625						
Temp. [C]	-269	-193	20	100	200	300
Young's Modulus,E [GPa]	200	200	197	191	182	175
Poisson's Ratio, ν	0.29	0.29	0.28	0.28	0.28	0.29
Shear Modulus, G [GPa]	77.5	77.5	77.0	74.6	71.1	67.8
Thermal Expansion, $\alpha(1x10^{-6}/C)$	-	-	12.0	12.3	12.6	12.7
Ultimate Strength, Su (MPa)	(-)	(-)	820	780	740	730
Yield Strength, Sy (MPa)	(-)	(-)	362	325	290	270
Allowable Stress, Sm (MPa)	(-)	(-)	241	217	193	180

Note : Here, the allowable stress of Sm value for plate material is determined according to the design code of ASME Sec. VIII, Div. 2, as follows.

Sm = Min. (2/3 Sy, 1/3 Su), at Service Temperature

Table 3.3-2(c) Mechanical Properties of Inconel-718 for Joint Bolt Material

Material Properties of Inconel 718						
Temp. [C]	-269	-193	20	100	200	300
Young's Modulus,E [GPa]	205	204	200	196	190	185
Poisson's Ratio, ν	0.29	0.29	0.30	0.30	0.30	0.30
Shear Modulus, G [GPa]	79.5	79.1	76.9	75.4	73.1	71.2
Thermal Expansion, $\alpha(1x10^{-6}/C)$	7.40	9.20	12.5	13.0	13.5	13.8
Ultimate Strength, Su (MPa)	1600	1570	1360	1370	1360	1340
Yield Strength, Sy (MPa)	1350	1280	1079	1030	990	980
Allowable Stress, Smb (MPa)	(450)	(427)	360	343	330	327

Note : Bolt limiting stress intensity of Smb is determined based on ASME Sec.III-NB (=1/3 Sy at service temperature).

Table 3.3-3(a) Stress on Flexible Plates for the load combinations.

Load Combinations	Torus Angle,θ	Stress Comp.	Plate Stress, MPa		Allowable Limit, MPa	
			Top	Middle	SS316LNIG	Inco-625
Category I (1) Assembly (DW and Radial Mismatch Disp. 5 mm)	-	Sbr	20	19	206	325
		Sτr	0.1	0.1	82	130
		Sz	21	0	137	217
		SS	41	19	206	325
Category I (2) Normal Operation-1 (DW+THL11 +THL12)	Primary Stress	Sbr	119	194	206	325
		Sbθdp	0.5	32	206	325
		Sτr	0.6	0.8	82	130
		Sτdp	1.7	0.7	82	130
		Sz	21	0	137	217
		SS	140	226	206	325
	Prim.+ Second.	Sth	25	64	411	650
		SS	165	290	411	650
Category I (3) Normal Operation-2 (DW+THL21 +THL22)	Primary Stress	Sbr	155	227	206	325
		Sbθdp	0.5	32	206	325
		Sτr	0.7	1.1	82	130
		Sτdp	1.7	0.7	82	130
		Sz	21	0	137	217
		SS	177	297	206	325
	Prim.+ Second.	Sth	33	84	411	650
		SS	210	381	411	650

Note: 1) Stress component of Sth means the in-plane thermal stress on the flexible plate due to the vertical temperature gradient of 80-400 K for the top support and of 4-400 K for middle one, which are assessed as the secondary stress.

2) Stress Components mean as follows;

Sz : Vertical Tensile Stress Component due to Vertical Force
Sbr : Radial Bending Stress Component due to Radial Force and Displacement
Sbθ : Toroidal Bending Stress Component due to Toroidal Force and Displacement
Sτr : Radial Shear Stress Component due to Radial Force and Displacement
Sτθ : Toroidal Shear Stress Component due to Toroidal Force and Displacement
Sbθdp : Toroidal Bending Stress Component due to TF Coil Overturning Displacement
Sτdp : Toroidal Shear Stress Component due to TF Coil Overturning Displacement
Szrok : Vertical Tensile Stress Component due to VV Rocking Movement
SS : Total Equivalent Stress

Table 3.3-3(b-1) Stress on Flexible Plates for the load combinations.

Load Combinations	Torus Angle,θ	Stress Components		Plate Stress, MPa		Allowable Limit, MPa	
				Top	Middle	SS316LNIG	Inco-625
Category I (4) Normal Operation -3 (DW + THL11 + THL12 + VDE-I)	θ = 0	Primary Stress	Sbr	122	198	206	325
			Sbθ	0	0	206	325
			Sτr	0.6	0.8	82	130
			Sτθ	0	0	82	130
			Sz	29	0	137	217
			Sbθdp	0.5	32	206	325
			Sτdp	1.7	0.7	82	130
			Srokz	9	0	137	217
			SS	161	230	206	325
		Prim.+ Second.	Sth	25	64	411	650
			SS	186	294	411	650
	θ = 45	Primary Stress	Sbr	121	197	206	325
			Sbθ	38	47	206	325
			Sτr	0.6	0.8	82	130
			Sτθ	3	5	82	130
			Sz	29	0	137	217
			Sbθdp	0.5	32	206	325
			Sτdp	1.7	0.7	82	130
			Srokz	6	0	137	217
			SS	196	276	206	325
			SS	203	293	206	325
		Prim.+ Second.	Sth	25	64	411	650
			SS	228	357	411	650

Note: Total Stress of SS includes the stresses due to TF case overturning deformation effect.

Table 3.3-3(b-2) Stress on Flexible Plates for the load combinations.

Load Combinations	Torus Angle,θ	Stress Components		Plate Stress, MPa		Allowable Limit, MPa	
				Top	Middle	SS316LNIG	Inco-625
Category I (4) Normal Operation -3 (DW + THL11 + THL12 + VDE-I)	θ = 135	Primary Stress	Sbr	116	192	206	325
			Sbθ	38	47	206	325
			Sτr	0.6	0.8	82	130
			Sτθ	3	5	82	130
			Sz	29	0	137	217
			Sbθdp	0.5	32	206	325
			Sτdp	1.7	0.7	82	130
			Srokz	-6	0	137	217
			SS	178	271	206	325
		Prim.+ Second.	Sth	25	64	411	650
			SS	203	335	411	650
	θ = 180	Primary Stress	Sbr	115	191	206	325
			Sbθ	0	0	206	325
			Sτr	0.5	0.8	82	130
			Sτθ	0	0	82	130
			Sz	29	0	137	217
			Sbθdp	0.5	32	206	325
			Sτdp	1.7	0.7	82	130
			Srokz	-9	0	137	217
			SS	136	223	206	325
		Prim.+ Second.	Sth	25	64	411	650
			SS	161	287	411	650

Table 3.3-3(c-1) Stress on Flexible Plates for the load combinations.

Load Combinations	Torus Angle,θ	Stress Components		Plate Stress, MPa		Allowable Limit, MPa	
				Top	Middle	SS316LNIG	Inco-625
Category II (1) Anticipated Upset Condition (DW + THL11 + THL12 + VDE-II)	θ = 0	Primary Stress	Sbr	123	199	206	325
			Sbθ	0	0	206	325
			Sτr	0.6	0.9	82	130
			Sτθ	0	0	82	130
			Sz	32	0	137	217
			Sbθdp	0.5	32	206	325
			Sτdp	1.7	0.7	82	130
			Srokz	11	0	137	217
			SS	167	231	206	325
		Prim.+ Second.	Sth	25	64	411	650
			SS	192	295	411	650
	θ = 45	Primary Stress	Sbr	122	197	206	325
			Sbθ	49	60	206	325
			Sτr	0.6	0.8	82	130
			Sτθ	4	6	82	130
			Sz	32	0	137	217
			Sbθdp	0.5	32	206	325
			Sτdp	1.7	0.7	82	130
			Srokz	8	0	137	217
			SS	211	289	206	325
		Prim.+ Second.	Sth	25	64	411	650
			SS	236	253	411	650
	θ = 90	Primary Stress	Sbr	119	194	206	325
			Sbθ	69	84	206	325
			Sτr	0.6	0.8	82	130
			Sτθ	5	8	82	130
			Sz	32	0	137	217
			Sbθdp	0.5	32	206	325
			Sτdp	1.7	0.7	82	130
			Srokz	0	0	137	217
			SS	220	311	206	325
		Prim.+ Second.	Sth	25	64	411	650
			SS	245	375	411	650

Table 3.3-3(c-2) Stress on Flexible Plates for the load combinations.

Load Combinations	Torus Angle,θ	Stress Components		Plate Stress, MPa		Allowable Limit, MPa	
				Top	Middle	SS316LNIG	Inco-625
Category II (1) Anticipated Upset Condition (DW + THL11 + THL12 + VDE-II)	θ = 135	Primary Stress	Sbr	115	191	206	325
			Sbθ	49	60	206	325
			Sτr	0.5	0.8	82	130
			Sτθ	4	6	82	130
			Sz	32	0	137	217
			Sbθdp	0.5	32	206	325
			Sτdp	1.7	0.7	82	130
			Srokz	-8	0	137	217
			SS	188	283	206	325
		Prim.+ Second.	Sth	25	64	411	650
			SS	213	347	411	650
	θ = 180	Primary Stress	Sbr	114	190	206	325
			Sbθ	0	0	206	325
			Sτr	0.5	0.8	82	130
			Sτθ	0	0	82	130
			Sz	32	0	137	217
			Sbθdp	0.5	32	206	325
			Sτdp	1.7	0.7	82	130
			Srokz	-11	0	137	217
			SS	135	222	206	325
		Prim.+ Second.	Sth	25	64	411	650
			SS	160	286	411	650

Table 3.3-3(d-1) Stress on Flexible Plates for the load combinations.

Load Combinations	Torus Angle,θ	Stress Components		Plate Stress, MPa		Allowable Limit, MPa	
				Top	Middle	SS316LNIG	Inco-625
Category II (2) Anticipated Upset Condition (DW + THL11 + THL12 + VDE-I + SL-1)	θ = 0	Primary Stress	Sbr	126	201	206	325
			Sbθ	0	0	206	325
			Sτr	0.6	0.8	82	130
			Sτθ	0	0	82	130
			Sz	33	0	137	217
			Sbθdp	0.5	32	206	325
			Sτdp	1.7	0.7	82	130
			Srokz	9	0	137	217
			SS	168	233	206	325
		Prim.+ Second.	Sth	25	64	411	650
			SS	193	297	411	650
	θ = 45	Primary Stress	Sbr	124	199	206	325
			Sbθ	77	94	206	325
			Sτr	0.6	0.8	82	130
			Sτθ	6	9	82	130
			Sz	33	0	137	217
			Sbθdp	0.5	32	206	325
			Sτdp	1.7	0.7	82	130
			Srokz	6	0	137	217
			SS	240	326	206	325
		Prim.+ Second.	Sth	25	64	411	650
			SS	265	390	411	650
	θ = 90	Primary Stress	Sbr	119	194	206	325
			Sbθ	108	133	206	325
			Sτr	0.6	0.8	82	130
			Sτθ	9	13	82	130
			Sz	33	0	137	217
			Sbθdp	0.5	32	206	325
			Sτdp	1.7	0.7	82	130
			Srokz	0	0	137	217
			SS	261	361	206	325
		Prim.+ Second.	Sth	25	64	411	650
			SS	286	425	411	650

Table 3.3-3(d-2) Stress on Flexible Plates for the load combinations.

Load Combinations	Torus Angle,θ	Stress Components		Plate Stress, MPa		Allowable Limit, MPa	
				Top	Middle	SS316LNIG	Inco-625
Category II (2) Anticipated Upset Condition (DW + THL11 + THL12 + VDE-I + SL-1)	θ = 135	Primary Stress	Sbr	113	189	206	325
			Sbθ	77	94	206	325
			Sτr	0.5	0.8	82	130
			Sτθ	6	9	82	130
			Sz	33	0	137	217
			Sbθdp	0.5	32	206	325
			Sτdp	1.7	0.7	82	130
			Srokz	-6	0	137	217
			SS	217	316	206	325
		Prim.+ Second.	Sth	25	64	411	650
			SS	242	380	411	650
	θ = 180	Primary Stress	Sbr	111	187	206	325
			Sbθ	0	0	206	325
			Sτr	0.5	0.8	82	130
			Sτθ	0	0	82	130
			Sz	33	0	137	217
			Sbθdp	0.5	32	206	325
			Sτdp	1.7	0.7	82	130
			Srokz	-9	0	137	217
			SS	177	219	206	325
		Prim.+ Second.	Sth	25	64	411	650
			SS	202	283	411	650

Table 3.3-3(e) Stress resultants on Flexible Plates for the load combinations.

Load Combinations	Torus Angle,θ	Stress Comp.	Plate Stress, MPa		Allowable Limit, MPa	
			Top	Middle	SS316LNIG	Inco-625
Category-III (1) (DW + THL11 + VDE-III) **Primary Stress Only**	θ = 0	Sbr	125	200	247	391
		Sbθ	0	0	247	391
		Sτr	0.6	0.8	97	156
		Sτθ	0	0	97	156
		Sz	35	0	164	260
		Sbθdp	0.5	32	247	391
		Sτdp	1.7	0.7	97	156
		Srokz	15	0	164	260
		SS	176	232	247	391
	θ = 45	Sbr	123	198	247	391
		Sbθ	64	79	247	391
		Sτr	0.6	0.8	97	156
		Sτθ	5	8	97	156
		Sz	35	0	164	260
		Sbθdp	0.5	32	247	391
		Sτdp	1.7	0.7	97	156
		Srokz	10	0	164	260
		SS	233	309	247	391
	θ = 90	Sbr	119	194	247	391
		Sbθ	90	111	247	391
		Sτr	0.6	0.8	97	156
		Sτθ	7	11	97	156
		Sz	35	0	164	260
		Sbθdp	0.5	32	247	391
		Sτdp	1.7	0.7	97	156
		Srokz	0	0	164	260
		SS	245	338	247	391
	θ = 135	Sbr	114	190	247	391
		Sbθ	64	79	247	391
		Sτr	0.5	0.8	97	156
		Sτθ	5	8	97	156
		Sz	35	0	164	260
		Sbθdp	0.5	32	247	391
		Sτdp	1.7	0.7	97	156
		Srokz	-10	0	164	260
		SS	204	301	247	391
	θ = 180	Sbr	113	188	247	391
		Sbθ	0	0	247	391
		Sτr	0.5	0.8	97	156
		Sτθ	0	0	97	156
		Sz	35	0	164	260
		Sbθdp	0.5	32	247	391
		Sτdp	1.7	0.7	97	156
		Srokz	-15	0	164	260
		SS	134	220	247	391

Table 3.3-3(f) Stress resultants on Flexible Plates for the load combinations.

Load Combinations	Torus Angle,θ	Stress Comp.	Plate Stress, MPa		Allowable Limit, MPa	
			Top	Middle	SS316LNIG	Inco-625
Category-III (2) (DW + THL11 + VDE-II + SL-1) **Primary Stress Only**	θ = 0	Sbr	127	202	247	391
		Sbθ	0	0	247	391
		Sτr	0.6	0.8	97	156
		Sτθ	0	0	97	156
		Sz	35	0	164	260
		Sbθdp	0.5	32	247	391
		Sτdp	1.7	0.7	97	156
		Srokz	9	0	164	260
		SS	171	234	247	391
	θ = 45	Sbr	125	200	247	391
		Sbθ	87	107	247	391
		Sτr	0.6	0.8	97	156
		Sτθ	7	11	97	156
		Sz	35	0	164	260
		Sbθdp	0.5	32	247	391
		Sτdp	1.7	0.7	97	156
		Srokz	6	0	164	260
		SS	253	340	247	391
	θ = 90	Sbr	119	194	247	391
		Sbθ	123	151	247	391
		Sτr	0.6	0.8	97	156
		Sτθ	10	15	97	156
		Sz	35	0	164	260
		Sbθdp	0.5	32	247	391
		Sτdp	1.7	0.7	97	156
		Srokz	0	0	164	260
		SS	277	379	247	391
	θ = 135	Sbr	113	188	247	391
		Sbθ	87	107	247	391
		Sτr	0.5	0.8	97	156
		Sτθ	7	11	97	156
		Sz	35	0	164	260
		Sbθdp	0.5	32	247	391
		Sτdp	1.7	0.7	97	156
		Srokz	-6	0	164	260
		SS	229	328	247	391
	θ = 180	Sbr	110	186	247	391
		Sbθ	0	0	247	391
		Sτr	0.5	0.8	97	156
		Sτθ	0	0	97	156
		Sz	35	0	164	260
		Sbθdp	0.5	32	247	391
		Sτdp	1.7	0.7	97	156
		Srokz	-9	0	164	260
		SS	180	218	247	391

Table 3.3-3(g) Stress resultants on Flexible Plates for the load combinations.

Load Combinations	Torus Angle,θ	Stress Comp.	Plate Stress, MPa		Allowable Limit, MPa	
			Top	Middle	SS316LNIG	Inco-625
Category-IV (1) (DW + THL11 + VDE-I + SL2) **Primary Stress Only**	θ = 0	Sbr	137	212	411	650
		Sbθ	0	0	411	650
		Sτr	0.7	0.9	164	260
		Sτθ	0	0	164	260
		Sz	42	0	274	434
		Sbθdp	0.5	32	411	650
		Sτdp	1.7	0.7	164	260
		Srokz	35	0	274	434
		SS	215	244	411	650
	θ = 45	Sbr	132	207	411	650
		Sbθ	192	236	411	650
		Sτr	0.6	0.9	164	260
		Sτθ	15	24	164	260
		Sz	42	0	274	434
		Sbθdp	0.5	32	411	650
		Sτdp	1.7	0.7	164	260
		Srokz	25	0	274	434
		SS	392	477	411	650
	θ = 90	Sbr	119	194	411	650
		Sbθ	271	333	411	650
		Sτr	0.6	0.8	164	260
		Sτθ	21	33	164	260
		Sz	42	0	274	434
		Sbθdp	0.5	32	411	650
		Sτdp	1.7	0.7	164	260
		Srokz	0	0	274	434
		SS	434	564	411	650
	θ = 135	Sbr	106	182	411	650
		Sbθ	192	236	411	650
		Sτr	0.5	0.8	164	260
		Sτθ	15	24	164	260
		Sz	42	0	274	434
		Sbθdp	0.5	32	411	650
		Sτdp	1.7	0.7	164	260
		Srokz	-25	0	274	434
		SS	316	452	411	650
	θ = 180	Sbr	100	176	411	650
		Sbθ	0	0	411	650
		Sτr	0.5	0.7	164	260
		Sτθ	0	0	164	260
		Sz	42	0	274	434
		Sbθdp	0.5	32	411	650
		Sτdp	1.7	0.7	164	260
		Srokz	-35	0	274	434
		SS	104	209	411	650

Table 3.3-4(a) Stress on the Joint Bolts for the load combinations.

Load Combinations	Torus Angle,_	Stress Comp.	Plate Stress, MPa		Allowable Limit, MPa	
			Top(12-M72)	Middle(14-M60)	SS316LNIG	Inco-718
Category I (1) Assembly at RT (DW and Radial Mismatch Disp. 5mm)	Primary Stress	Sz0	128	0	137	687
		Sbr	2	0.7	137	687
		Sτr	0.6	0.2	82	412
		SS	128	0.8	137	687
Category I (2) Normal Operation-1 (DW + THL11 + THL12) at 100 C	Primary Stress	Sz0	128	0	137	687
		Sbr	9	7	137	687
		Sτr	4	2	82	412
		Sbθdp	0.8	21	137	687
		Sτdp	0.3	0.1	82	412
		SS	138	28	137	687
Category I (3) Normal Operation-2 (DW + THL21 + THL22) at 200 C	Primary Stress	Sz0	128	0	137	687
		Sbr	14	10	137	687
		Sτr	5	2	82	412
		Sbθdp	0.8	21	137	687
		Sτdp	0.3	0.1	82	412
		SS	141	31	206	687

Note : 1) The total stress of SS includes the stresses due to TF case overturning deformation effect.

2) Stress Components mean as follows;

Sz0 : Vertical Tensile Stress Component due to Vertical Force
Sbr : Radial Bending Stress Component due to Radial Force and Displacement
Sbθ : Toroidal Bending Stress Component due to Toroidal Force and Displacement
Sτr : Radial Shear Stress Component due to Radial Force and Displacement
Sτθ : Toroidal Shear Stress Component due to Toroidal Force and Displacement
Sbθdp : Toroidal Bending Stress Component due to TF Coil Overturning Displacement
Sτdp : Toroidal Shear Stress Component due to TF Coil Overturning Displacement
Szrok : Vertical Tensile Stress Component due to VV Rocking Movement
SS : Total Equivalent Stress

Table 3.3-4(b) Stress on the Joint Bolts for the load combinations.

Load Combinations	Torus Angle,_	Stress Comp.	Plate Stress, MPa		Allowable Limit, MPa	
			Top(12-M72)	Middle(14-M60)	SS316LNIG	Inco-718
Category I (4) Normal Operation-3 (DW + THL11 + THL12 + VDE-I) Primary Stress Only	θ = 0	Sz0	182	0	137	687
		Sbr	10	7	137	687
		Sbθ	0	0	137	687
		Sτr	4	2	82	412
		Sτθ	0	0	82	412
		Sbθdp	0.8	21	137	687
		Sτdp	0.3	0.1	82	412
		Szrok	55	0	137	687
		SS	248	28	137	687
	θ = 45	Sz0	182	0	137	687
		Sbr	10	7	137	687
		Sbθ	66	30	137	687
		Sτr	4	2	82	412
		Sτθ	19	10	82	412
		Sbθdp	0.8	21	137	687
		Sτdp	0.3	0.1	82	412
		Szrok	39	0	137	687
		SS	301	63	137	687
	θ = 90	Sz0	182	0	137	687
		Sbr	9	7	137	687
		Sbθ	94	43	137	687
		Sτr	4	2	82	412
		Sτθ	27	15	82	412
		Sbθdp	0.8	21	137	687
		Sτdp	0.3	0.1	82	412
		Szrok	0	0	137	687
		SS	293	78	137	687
	θ = 135	Sz0	182	0	137	687
		Sbr	9	7	137	687
		Sbθ	66	30	137	687
		Sτr	3	2	82	412
		Sτθ	19	10	82	412
		Sbθdp	0.8	21	137	687
		Sτdp	0.3	0.1	82	412
		Szrok	-39	0	137	687
		SS	224	63	137	687
	θ = 180	Sz0	182	0	137	687
		Sbr	9	7	137	687
		Sbθ	0	0	137	687
		Sτr	3	2	82	412
		Sτθ	0	0	82	412
		Sbθdp	0.8	21	137	687
		Sτdp	0.3	0.1	82	412
		Szrok	-55	0	137	687
		SS	137	28	137	687

Table 3.3-4(c) Stress on the Joint Bolts for the load combinations.

Load Combinations	Torus Angle,_	Stress Comp.	Plate Stress, MPa		Allowable Limit, MPa	
			Top(12-M72)	Middle(14-M60)	SS316LNIG	Inco-718
Category II (1) Anticipated Upset Condition (DW + THL11 + THL12 + VDE-II) Primary Stress Only	θ = 0	Sz0	196	0	137	687
		Sbr	10	7	137	687
		Sbθ	0	0	137	687
		Sτr	4	2	82	412
		Sτθ	0	0	82	412
		Sbθdp	0.8	21	137	687
		Sτdp	0.3	0.1	82	412
		Szrok	70	0	137	687
		SS	277	28	137	687
	θ = 45	Sz0	196	0	137	687
		Sbr	10	7	137	687
		Sbθ	84	38	137	687
		Sτr	4	2	82	412
		Sτθ	24	13	82	412
		Sbθdp	0.8	21	137	687
		Sτdp	0.3	0.1	82	412
		Szrok	49	0	137	687
		SS	344	73	137	687
	θ = 90	Sz0	196	0	137	687
		Sbr	9	7	137	687
		Sbθ	119	54	137	687
		Sτr	4	2	82	412
		Sτθ	34	18	82	412
		Sbθdp	0.8	21	137	687
		Sτdp	0.3	0.1	82	412
		Szrok	0	0	137	687
		SS	334	92	137	687
	θ = 135	Sz0	196	0	137	687
		Sbr	9	7	137	687
		Sbθ	84	38	137	687
		Sτr	3	2	82	412
		Sτθ	24	13	82	412
		Sbθdp	0.8	21	137	687
		Sτdp	0.3	0.1	82	412
		Szrok	-49	0	137	687
		SS	247	72	137	687
	θ = 180	Sz0	196	0	137	687
		Sbr	9	7	137	687
		Sbθ	0	0	137	687
		Sτr	3	2	82	412
		Sτθ	0	0	82	412
		Sbθdp	0.8	21	137	687
		Sτdp	0.3	0.1	82	412
		Szrok	-70	0	137	687
		SS	137	28	137	687

Table 3.3-4(d) Stress on the Joint Bolts for the load combinations.

Load Combinations	Torus Angle,_	Stress Comp.	Plate Stress, MPa		Allowable Limit, MPa	
			Top(12-M72)	Middle(14-M60)	SS316LNIG	Inco-718
Category II (2) Anticipated Upset Condition (DW + THL11 + THL12 + VDE-I + SL1) Primary Stress Only	θ = 0	Sz0	201	0	137	687
		Sbr	10	7	137	687
		Sbθ	0	0	137	687
		Sτr	4	2	82	412
		Sτθ	0	0	82	412
		Sbθdp	0.8	21	137	687
		Sτdp	0.3	0.1	82	412
		Szrok	110	0	137	687
		SS	322	28	137	687
	θ = 45	Sz0	201	0	137	687
		Sbr	10	7	137	687
		Sbθ	133	61	137	687
		Sτr	4	2	82	412
		Sτθ	38	21	82	412
		Sbθdp	0.8	21	137	687
		Sτdp	0.3	0.1	82	412
		Szrok	78	0	137	687
		SS	430	99	137	687
	θ = 90	Sz0	201	0	137	687
		Sbr	9	7	137	687
		Sbθ	188	86	137	687
		Sτr	4	2	82	412
		Sτθ	53	29	82	412
		Sbθdp	0.8	21	137	687
		Sτdp	0.3	0.1	82	412
		Szrok	0	0	137	687
		SS	415	129	137	687
	θ = 135	Sz0	201	0	137	687
		Sbr	9	7	137	687
		Sbθ	133	61	137	687
		Sτr	3	2	82	412
		Sτθ	38	21	82	412
		Sbθdp	0.8	21	137	687
		Sτdp	0.3	0.1	82	412
		Szrok	-78	0	137	687
		SS	279	99	137	687
	θ = 180	Sz0	201	0	137	687
		Sbr	9	7	137	687
		Sbθ	0	0	137	687
		Sτr	3	2	82	412
		Sτθ	0	0	82	412
		Sbθdp	0.8	21	137	687
		Sτdp	0.3	0.1	82	412
		Szrok	-110	0	137	687
		SS	101	28	137	687

Table 3.3-4(e) Stress on the Joint Bolts for the load combinations.

Load Combinations	Torus Angle,_	Stress Comp.	Plate Stress, MPa		Allowable Limit, MPa	
			Top(12-M72)	Middle(14-M60)	SS316LNIG	Inco-718
Category III (1) Unlikely Upset Condition (DW + THL11 + THL12 + VDE-III) Primary Stress Only	θ = 0	Sz0	219	0	137	687
		Sbr	10	7	137	687
		Sbθ	0	0	137	687
		Sτr	4	2	82	412
		Sτθ	0	0	82	412
		Sbθdp	0.8	21	137	687
		Sτdp	0.3	0.1	82	412
		Szrok	92	0	137	687
		SS	322	28	137	687
	θ = 45	Sz0	219	0	137	687
		Sbr	10	7	137	687
		Sbθ	111	51	137	687
		Sτr	4	2	82	412
		Sτθ	31	17	82	412
		Sbθdp	0.8	21	137	687
		Sτdp	0.3	0.1	82	412
		Szrok	65	0	137	687
		SS	411	87	137	687
	θ = 90	Sz0	219	0	137	687
		Sbr	9	7	137	687
		Sbθ	156	72	137	687
		Sτr	4	2	82	412
		Sτθ	44	24	82	412
		Sbθdp	0.8	21	137	687
		Sτdp	0.3	0.1	82	412
		Szrok	0	0	137	687
		SS	398	112	137	687
	θ = 135	Sz0	219	0	137	687
		Sbr	9	7	137	687
		Sbθ	111	51	137	687
		Sτr	3	2	82	412
		Sτθ	31	17	82	412
		Sbθdp	0.8	21	137	687
		Sτdp	0.3	0.1	82	412
		Szrok	-65	0	137	687
		SS	284	87	137	687
	θ = 180	Sz0	219	0	137	687
		Sbr	9	7	137	687
		Sbθ	0	0	137	687
		Sτr	3	2	82	412
		Sτθ	0	0	82	412
		Sbθdp	0.8	21	137	687
		Sτdp	0.3	0.1	82	412
		Szrok	-92	0	137	687
		SS	138	28	137	687

Table 3.3-4(f) Stress on the Joint Bolts for the load combinations.

Load Combinations	Torus Angle,_	Stress Comp.	Plate Stress, MPa		Allowable Limit, MPa	
			Top(12-M72)	Middle(14-M60)	SS316LNIG	Inco-718
Category III (2) Unlikely Upset Condition (DW + THL11 + THL12 + VDE-II + SL1) Primary Stress Only	θ = 0	Sz0	215	0	137	687
		Sbr	10	7	137	687
		Sbθ	0	0	137	687
		Sτr	4	2	82	412
		Sτθ	0	0	82	412
		Sbθdp	0.8	21	137	687
		Sτdp	0.3	0.1	82	412
		Szrok	125	0	137	687
		SS	351	28	137	687
	θ = 45	Sz0	215	0	137	687
		Sbr	10	7	137	687
		Sbθ	150	69	137	687
		Sτr	4	2	82	412
		Sτθ	43	23	82	412
		Sbθdp	0.8	21	137	687
		Sτdp	0.3	0.1	82	412
		Szrok	88	0	137	687
		SS	474	109	137	687
	θ = 90	Sz0	215	0	137	687
		Sbr	9	7	137	687
		Sbθ	213	97	137	687
		Sτr	4	2	82	412
		Sτθ	60	33	82	412
		Sbθdp	0.8	21	137	687
		Sτdp	0.3	0.1	82	412
		Szrok	0	0	137	687
		SS	457	143	137	687
	θ = 135	Sz0	219	0	137	687
		Sbr	9	7	137	687
		Sbθ	150	69	137	687
		Sτr	3	2	82	412
		Sτθ	43	23	82	412
		Sbθdp	0.8	21	137	687
		Sτdp	0.3	0.1	82	412
		Szrok	-88	0	137	687
		SS	302	109	137	687
	θ = 180	Sz0	215	0	137	687
		Sbr	9	7	137	687
		Sbθ	0	0	137	687
		Sτr	3	2	82	412
		Sτθ	0	0	82	412
		Sbθdp	0.8	21	137	687
		Sτdp	0.3	0.1	82	412
		Szrok	-125	0	137	687
		SS	101	28	137	687

Table 3.3-4(g) Stress on the Joint Bolts for the load combinations.

Load Combinations	Torus Angle,_	Stress Comp.	Plate Stress, MPa		Allowable Limit, MPa	
			Top(12-M72)	Middle(14-M60)	SS316LNIG	Inco-718
Category IV (1) Extremely Unlikely Event Condition (DW + THL11 + THL12 + VDE-I + SL2) Primary Stress Only	θ = 0	Sz0	259	0	206	959
		Sbr	11	8	206	959
		Sbθ	0	0	206	959
		Sτr	4	2	124	412
		Sτθ	0	0	124	412
		Sbθdp	0.8	21	206	959
		Sτdp	0.3	0.1	124	412
		Szrok	275	0	206	959
		SS	545	29	206	959
	θ = 45	Sz0	259	0	206	959
		Sbr	10	8	206	959
		Sbθ	331	152	206	959
		Sτr	4	2	124	412
		Sτθ	94	51	124	412
		Sbθdp	0.8	21	206	959
		Sτdp	0.3	0.1	124	412
		Szrok	194	0	206	959
		SS	820	209	206	959
	θ = 90	Sz0	259	0	206	959
		Sbr	9	7	206	959
		Sbθ	469	215	206	959
		Sτr	4	2	124	412
		Sτθ	133	73	124	412
		Sbθdp	0.8	21	206	959
		Sτdp	0.3	0.1	124	412
		Szrok	0	0	206	959
		SS	787	284	206	959
	θ = 135	Sz0	259	0	206	959
		Sbr	8	7	206	959
		Sbθ	331	152	206	959
		Sτr	3	2	124	412
		Sτθ	94	51	124	412
		Sbθdp	0.8	21	206	959
		Sτdp	0.3	0.1	124	412
		Szrok	-194	0	206	959
		SS	450	208	206	959
	θ = 180	Sz0	259	0	206	959
		Sbr	8	6	206	959
		Sbθ	0	0	206	959
		Sτr	3	2	124	412
		Sτθ	0	0	124	412
		Sbθdp	0.8	21	206	959
		Sτdp	0.3	0.1	124	412
		Szrok	-275	0	206	959
		SS	10	27	206	959

Table 3.3-5(a) Primary Stress on Plate as a function of Mechanical Stiffness Ratios of kkr' and kkθ'

Load Combination	Load Category	Max. Stress on Plate, (MPa)						Allowable Limit at 120 C, (MPa) (**Inco-625**)
		(kkr', kkθ') =(0.10, 0.20)		**(kkr', kkθ') =(0.24, 0.46)**		(kkr', kkθ') =(0.30, 0.60)		
		Top	Mid	**Top**	**Mid**	Top	Mid	
DW	I	41	16	**41**	**19**	41	21	325
DW(+THL1)		140	185	**140**	**226**	140	243	
DW(+THL2)		177	244	**177**	**297**	177	319	
DW+VDE-I		213	255	**203**	**293**	199	307	
DW+VDE-II	II	233	273	**220**	**311**	214	324	
DW+VDE-I +SL-1		281	324	**261**	**361**	252	372	
DW+VDE-III	III	262	301	**245**	**338**	238	350	391
DW+VDE-II +SL-1		301	343	**277**	**379**	268	389	
DW+VDE-I +SL-2	IV	485	533	**434**	**564**	412	567	650

Note : 1) (kkr', kkθ') mean mechanical stiffness ratios of kr2/kr1 in radial direction and of kθ2/kθ1 in toroidal direction.

2) Combinations of mechanical stiffness ratios are corresponding to followings:

Ratio (kkr', kkθ')	Thickness (t1, t2)	Width (w1, w2)	
(0.10, 0.20)	(30 mm, 20.5mm)	(500 mm, 490 mm)	
(0.24, 0.46)	(30 mm, 25 mm)	(500 mm, 600 mm)	Reference
(0.30, 0.60)	(30 mm, 26.8mm)	(500 mm, 643 mm)	

3) Suffixes 1 and 2 indicate to upper hanging support plates and middle radial stopper, respectively.

Table 3.3-5(b) Primary Stress on Bolt as a function of Mechanical Stiffness Ratios of kkr' and kkθ'

Load Combination	Load Category	Max. Stress on Plate, (MPa)						Allowable Limit at 120 C, (MPa) (**Inco-718**)
		(kkr', kkθ') =(0.10, 0.20)		**(kkr', kkθ') =(0.24, 0.46)**		(kkr', kkθ') =(0.30, 0.60)		
		Top	Mid	**Top**	**Mid**	Top	Mid	
DW	I	128	0.4	**128**	**0.8**	128	1	687
DW(+THL1)		138	13	**138**	**28**	138	37	
DW(+THL2)		141	14	**141**	**31**	141	41	
DW+VDE-I		315	41	**301**	**78**	296	96	
DW+VDE-II	II	361	49	**344**	**92**	324	112	
DW+VDE-I +SL-1		454	70	**430**	**129**	419	156	
DW+VDE-III	III	434	60	**411**	**112**	402	136	
DW+VDE-II +SL-1		504	78	**474**	**143**	461	173	
DW+VDE-I +SL-2	IV	889	158	**820**	**284**	791	340	959

Note : The bolt stresses include the shearing stress components assuming no friction forces between the joint flanges.

Table 3.3-5(c) Primary Stress on Bolt as a function of Mechanical Stiffness Ratios of kkr' and kkθ'

Load Combination	Load Category	Max. Stress on Plate, (MPa)						Allowable Limit at 120 C, (MPa) **(Inco-718)**
		(kkr', kkθ') =(0.10, 0.20)		**(kkr', kkθ') =(0.24, 0.46)**		(kkr', kkθ') =(0.30, 0.60)		
		Top	Mid	**Top**	**Mid**	Top	Mid	
DW	I	128	0.3	**128**	**0.7**	128	0.9	687
DW(+THL1)		138	12	**138**	**28**	138	37	
DW(+THL2)		141	14	**141**	**30**	141	40	
DW+VDE-I		310	37	**298**	**71**	293	87	
DW+VDE-II	II	356	43	**340**	**82**	333	101	
DW+VDE-I +SL-1		447	61	**422**	**114**	412	138	
DW+VDE-III	III	426	53	**404**	**99**	396	121	
DW+VDE-II +SL-1		493	67	**464**	**125**	453	152	
DW+VDE-I +SL-2	IV	858	134	**796**	**242**	769	290	959

Note : The bolt stresses include no shearing stress component assuming the enough friction forces between the joint flanges to resist the external horizontal loads.

Table 3.3-6 Buckling Strength and Safety Factor for several Load Combinations

Load Combinations	Load Category	Max. Reaction Force, Fv (MN)	Buckling Load, Pcr (MN)	Safety Factor, mk	Allowable Limit [8]
DW	I	+5.56	-18.5	∞	> 3
DW (+THL)		+5.56	-18.5	∞	
DW+VDE-I		+3.17	-18.5	∞	
DW+VDE-II	II	+2.56	-18.5	∞	> 3
DW+VDE-I +SL-1		+1.72	-18.5	∞	
DW+VDE-III	III	+1.56	-18.5	∞	> 2.5
DW+VDE-II +SL-1		+1.72	-18.5	∞	
DW+VDE-I +SL-2	IV	-0.167	-18.5	111	> 1.5

Note : 1) The vertical component of all VDE forces is conservatively considered to be upward only for the buckling assessment of the flexible plates.

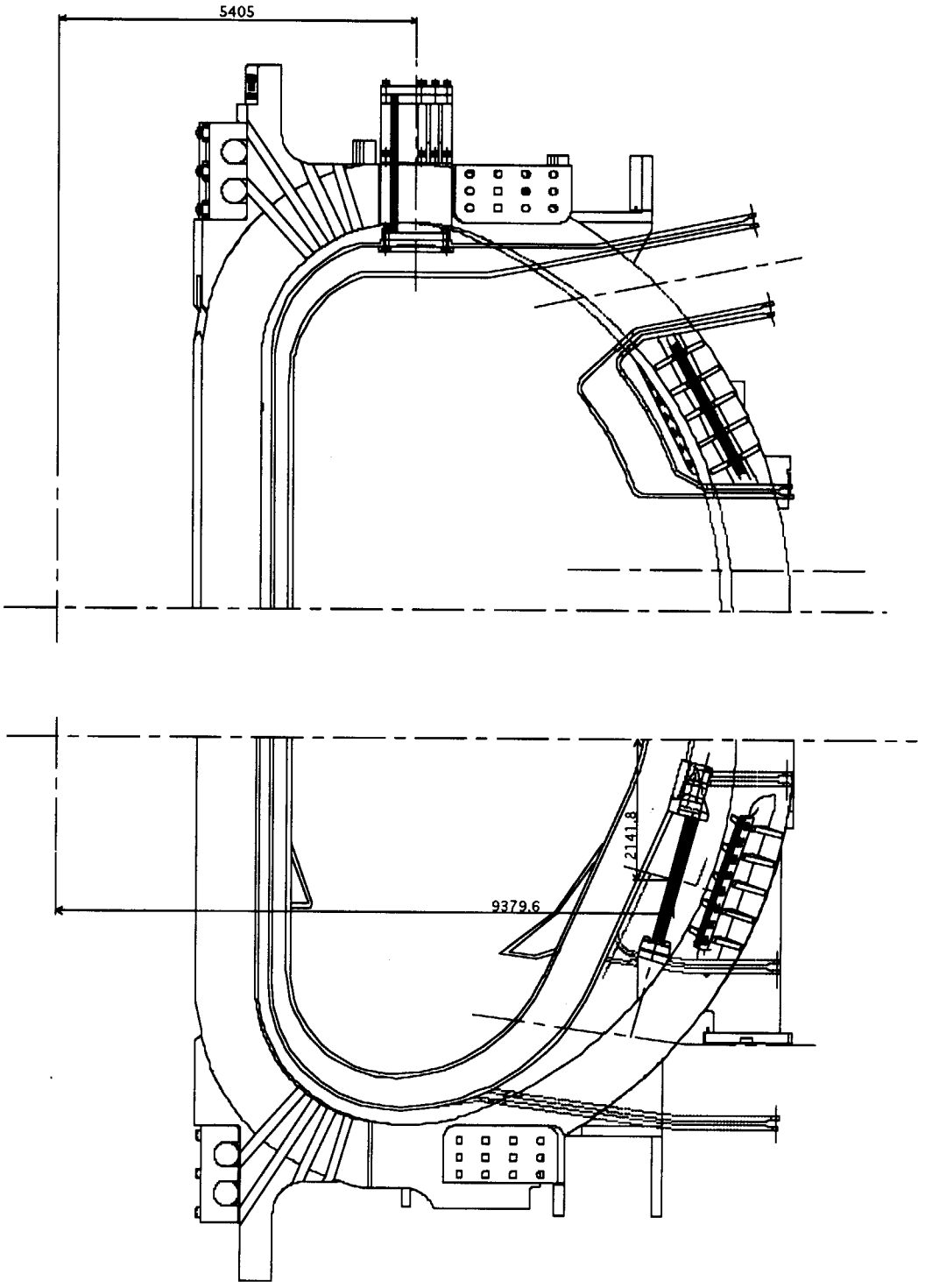

Fig. 3.1-1 Overall VV Support System with Top Hanging Support and Mid Radial Stopper

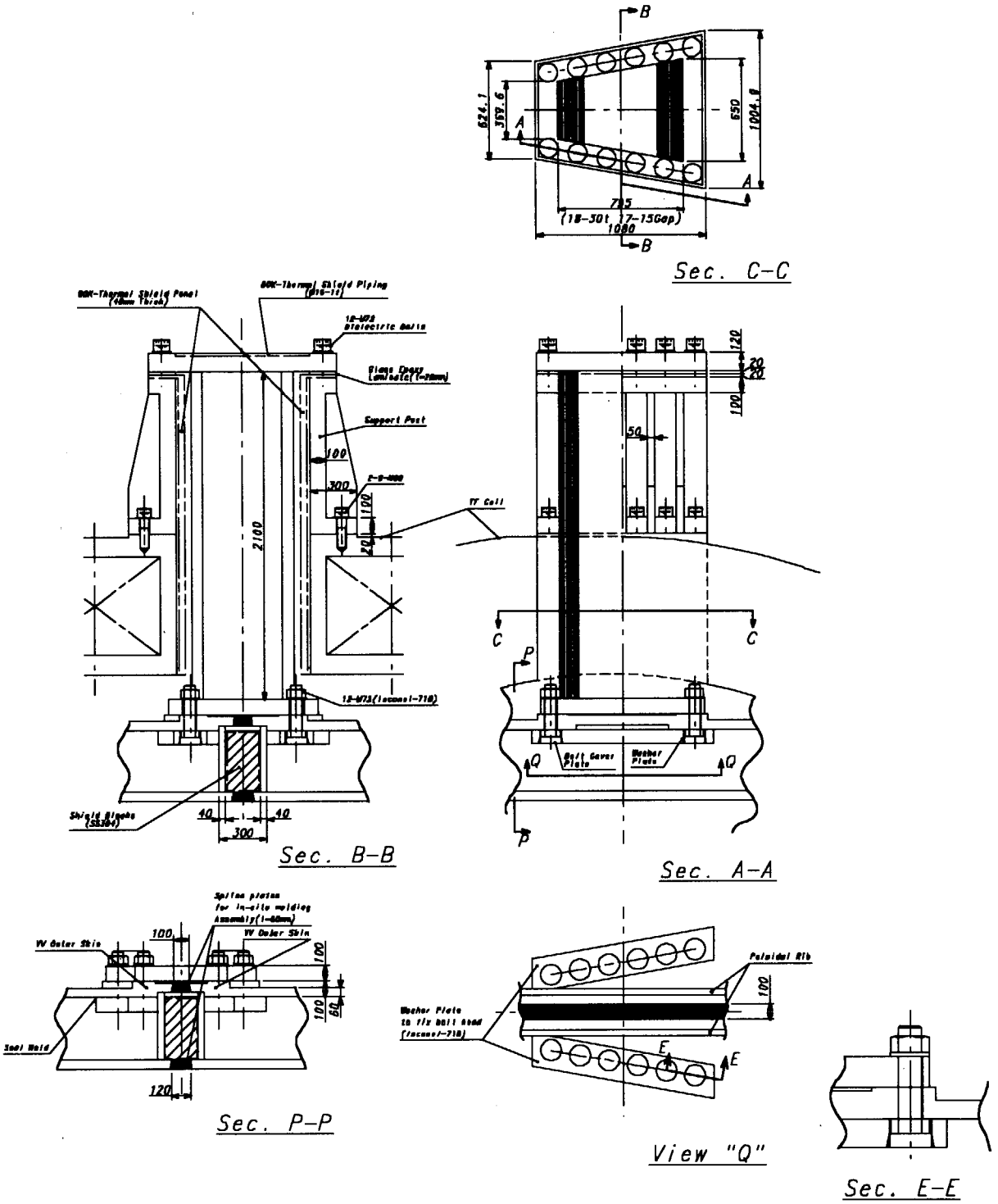

Fig. 3.1-2 Detailed Cross-Sections of Top Hanging VV Support with Flexible Plates

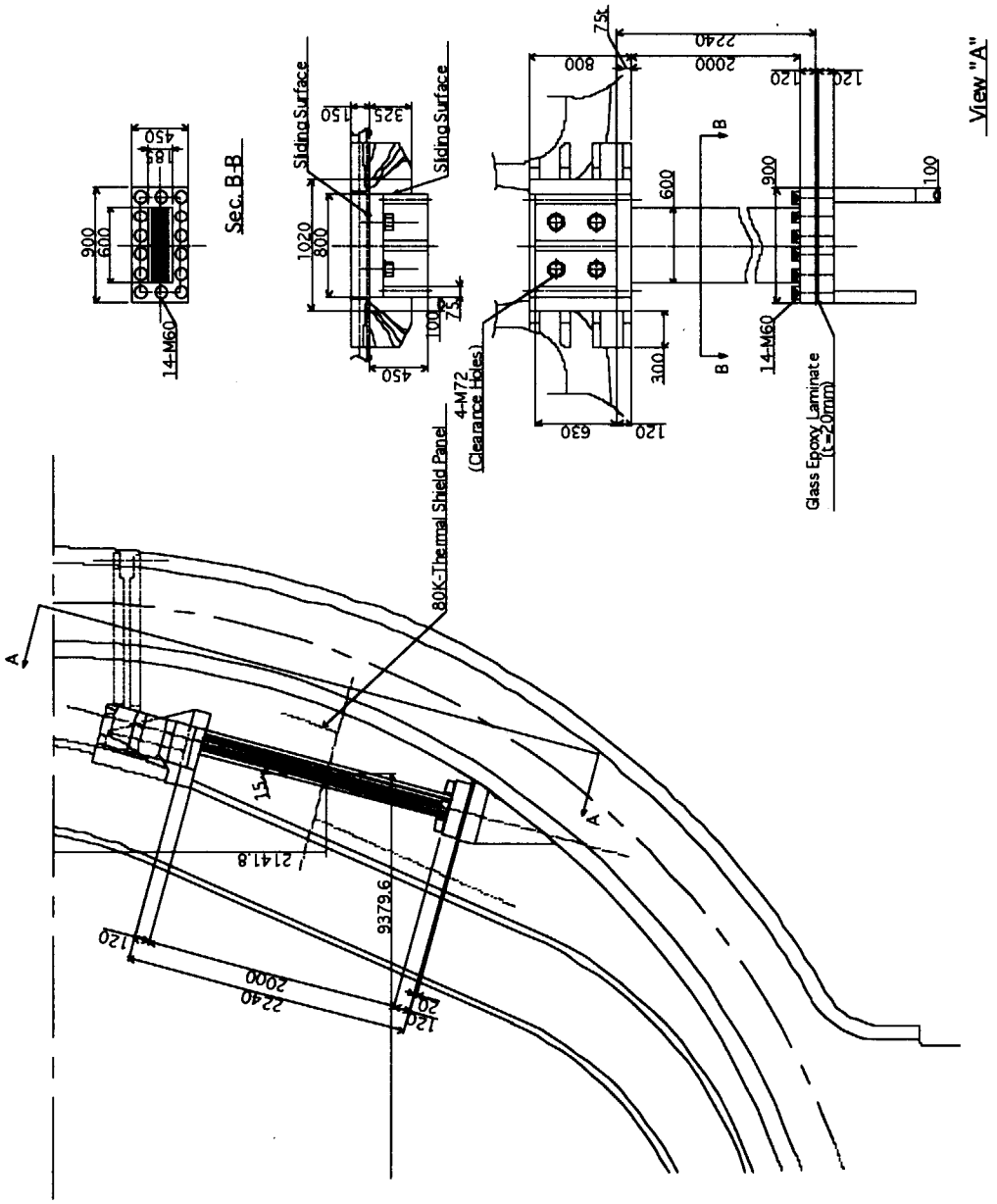

Fig. 3.1-3 Detailed Cross-Sections of VV Middle Radial Stopper with Flexible Plates

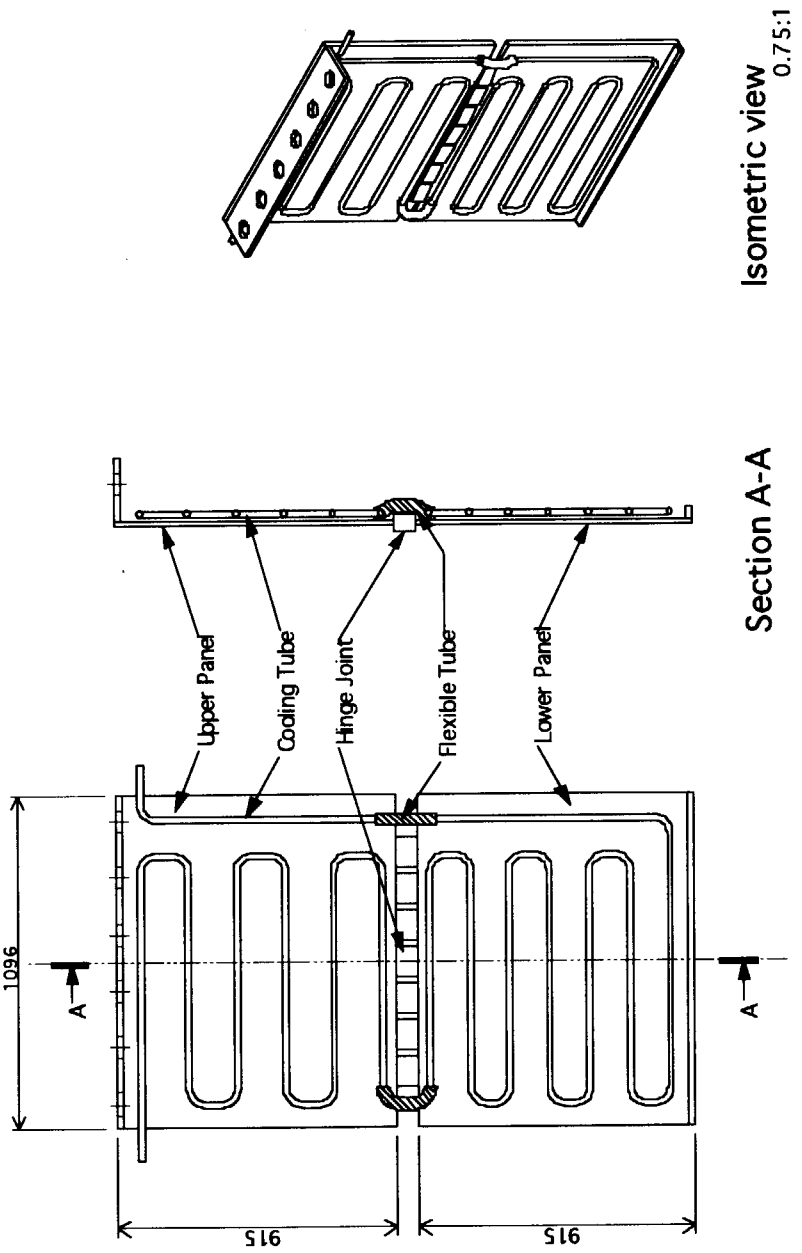

Fig.3.1-4 Schematic Drawing of Thermal Shield Panel

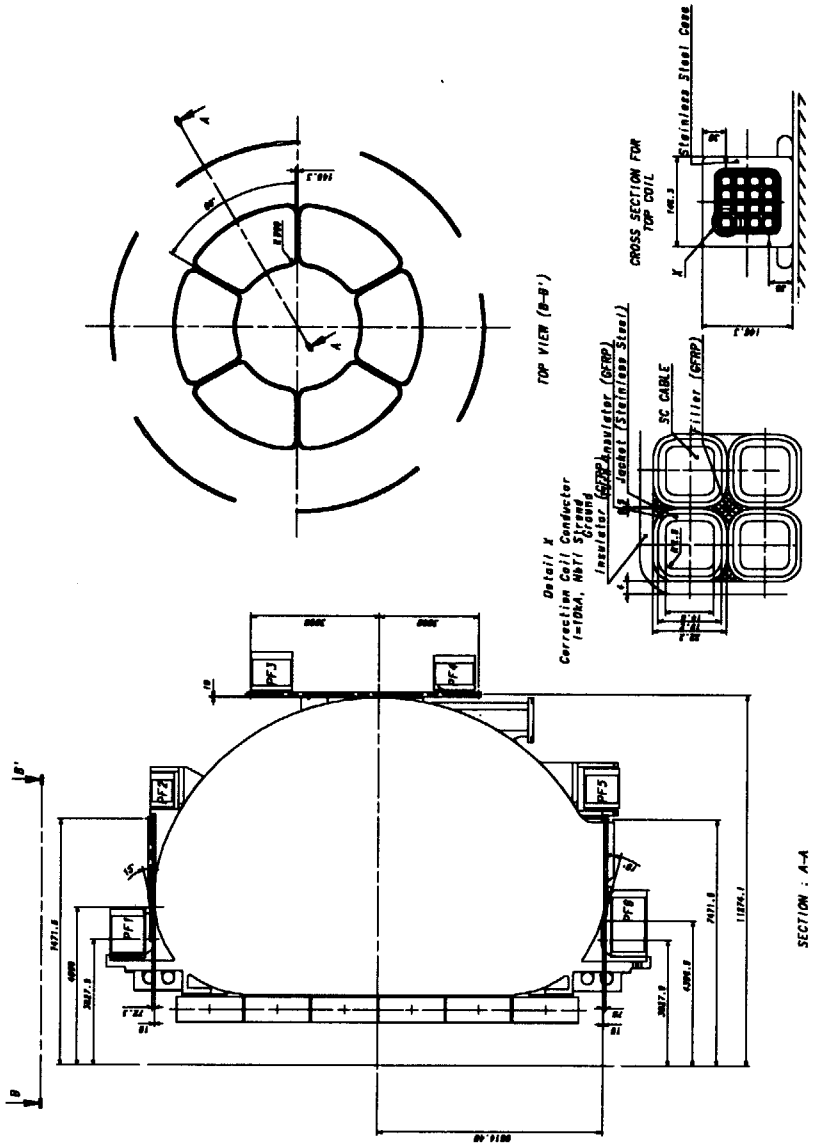

Fig. 3.1-5(a) Modification of Top CC Winding Configuration

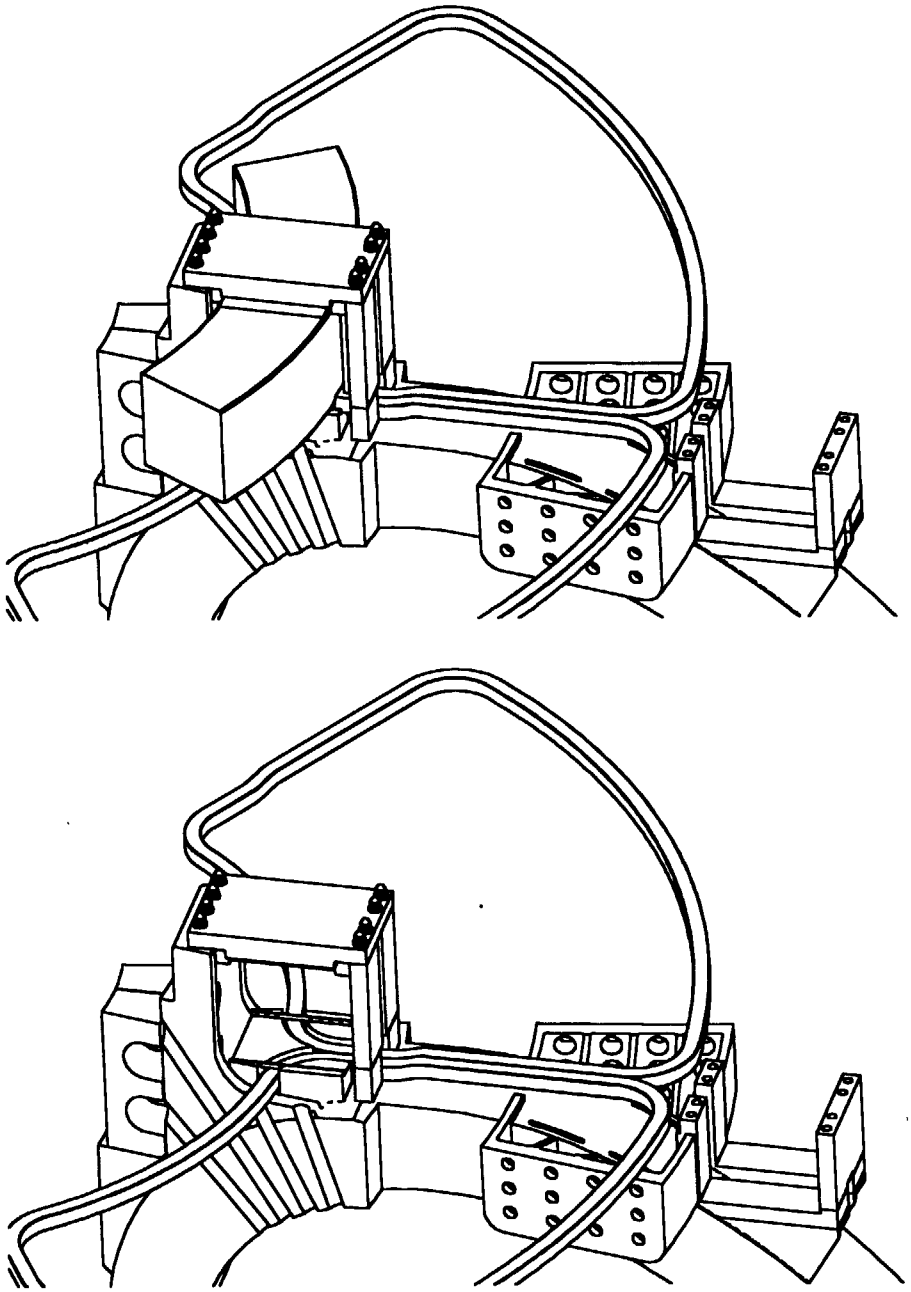

Fig. 3.1-5(b) Modification of Top CC Radial Spans Arrangement

Case	t1 (m)	W (m)	L (m)	T1 (K)	Remarks
1	0.03	0.5	2.1	80	Top Hanging Support
2	0.025	0.6	2.0	4	Middle Radial Stopper

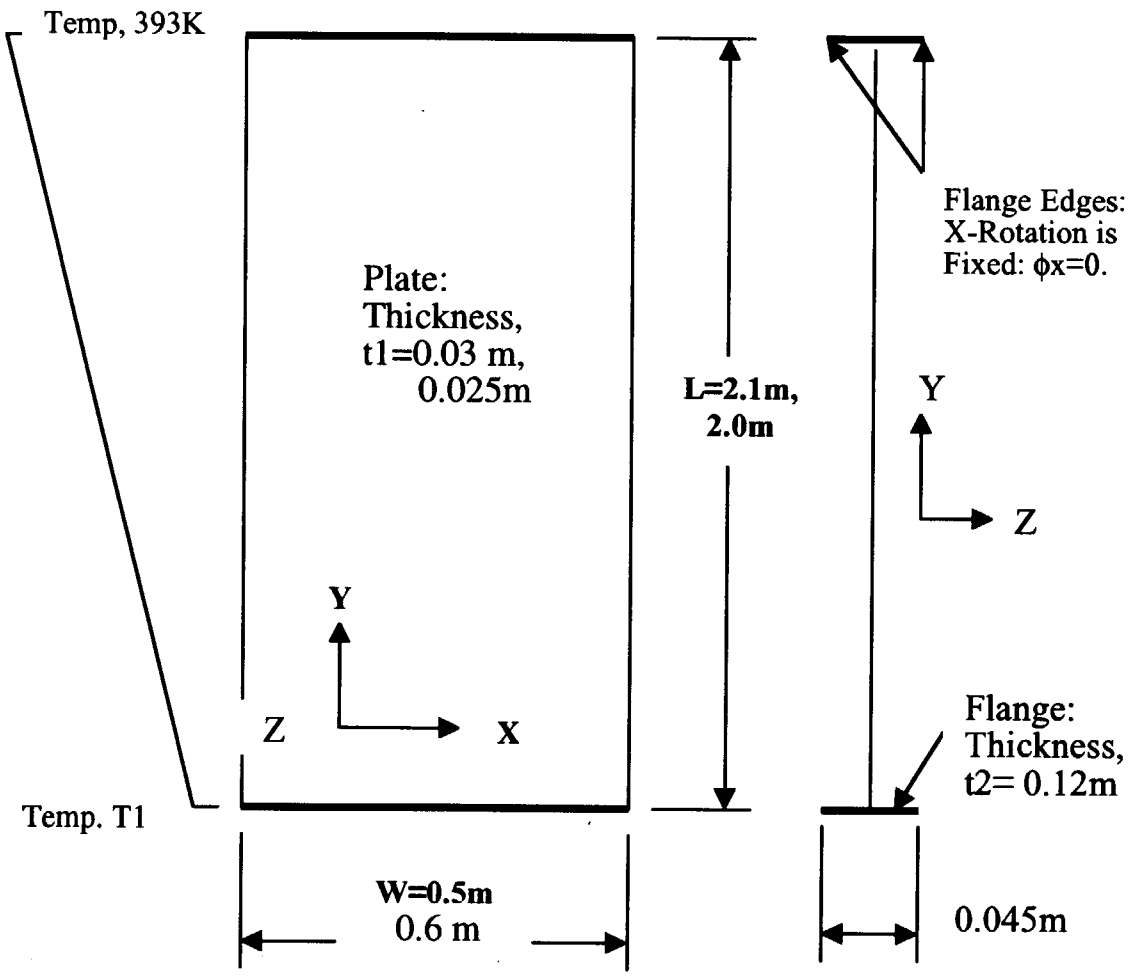

Fig.3.3-1 FEM Model and Boundary Conditions for Thermal Stress Calculations on Plate due to Vertical Temperature Gradient

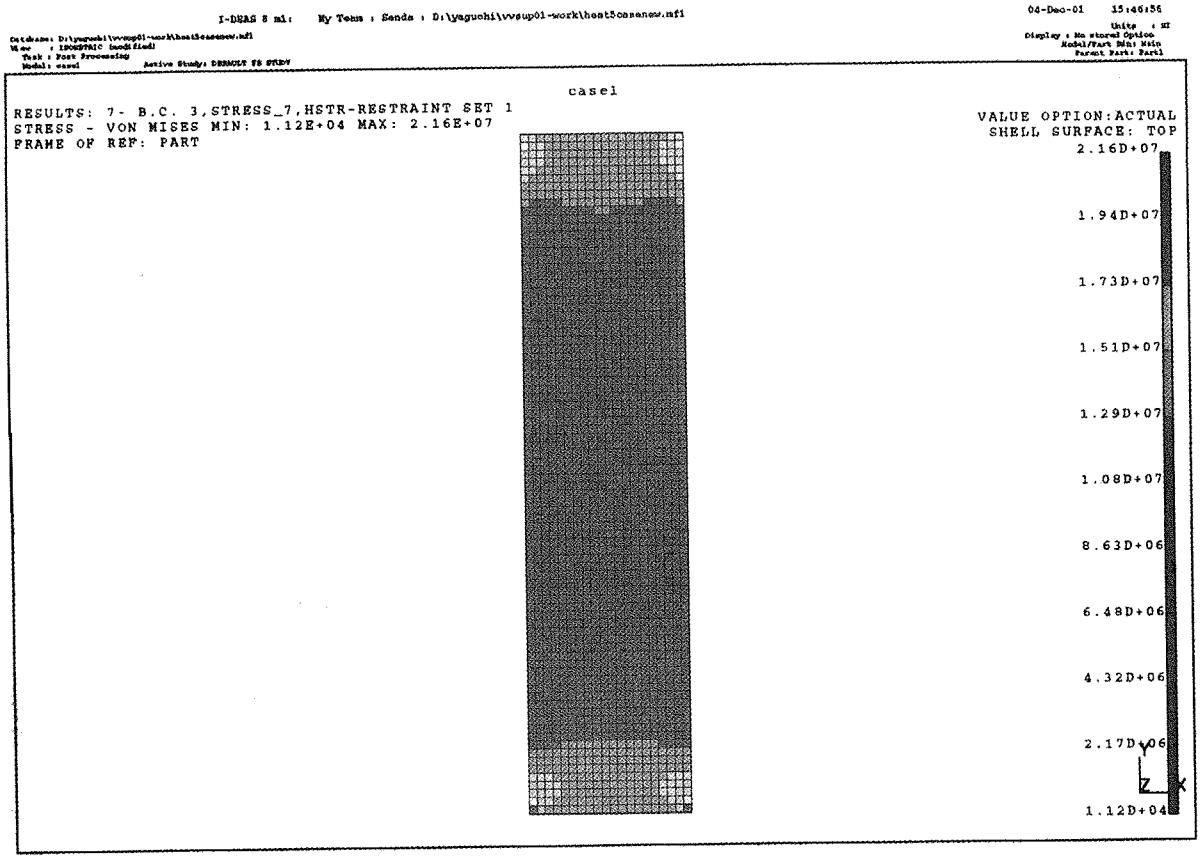

Fig. 3.3-2(a) In-plane Thermal Stress on Flexible Plate (with 30 mm Thickness and 500 mm Width) of Top Hanging Support due to Vertical Temperature Gradient from 80 K to 400 K

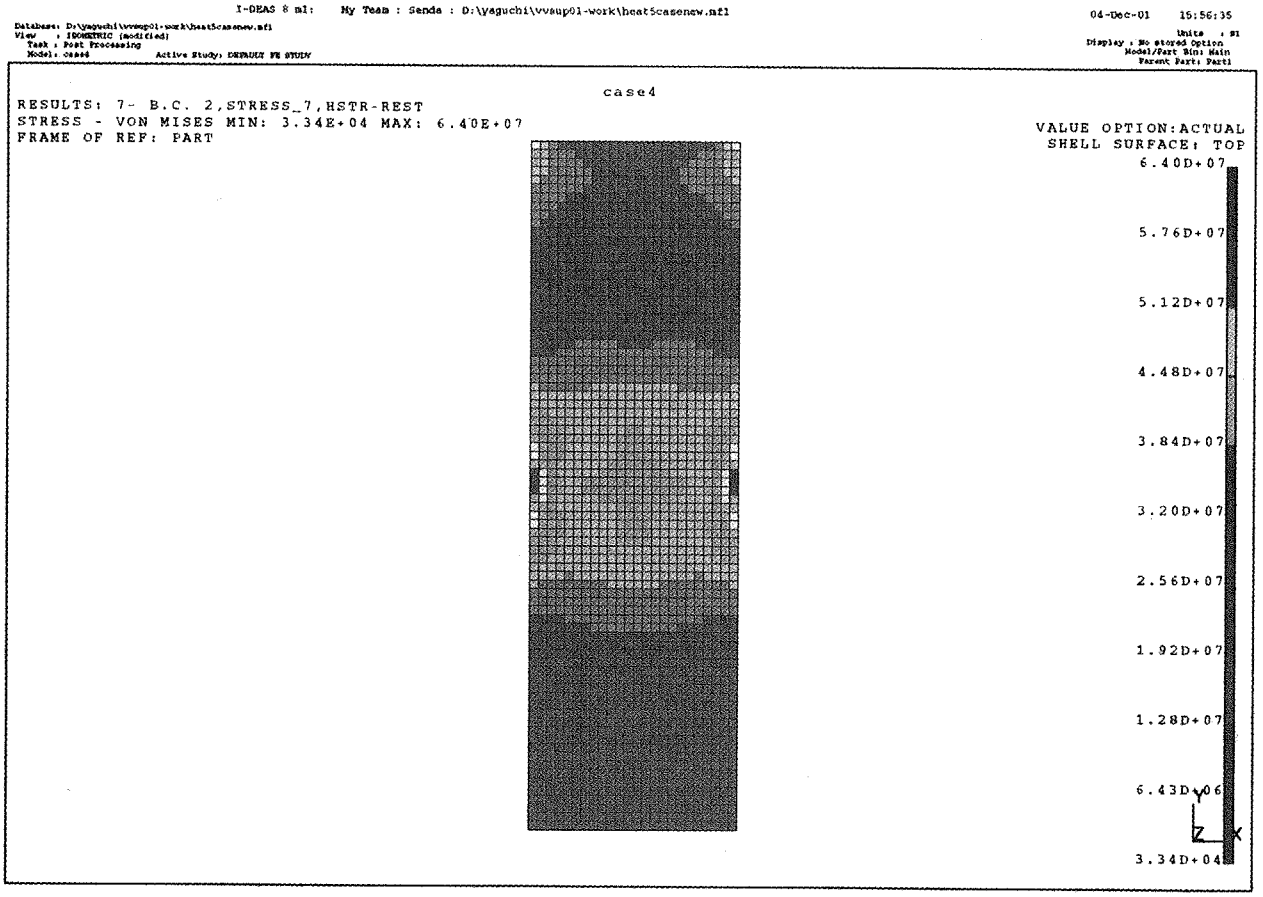

Fig. 3.3-2(b) In-plane Thermal Stress on Flexible Plate of Mid Radial Stopper Plate (with 25 mm Thickness and 600 mm Width) due to Vertical Temperature Gradient from 4 K to 400 K

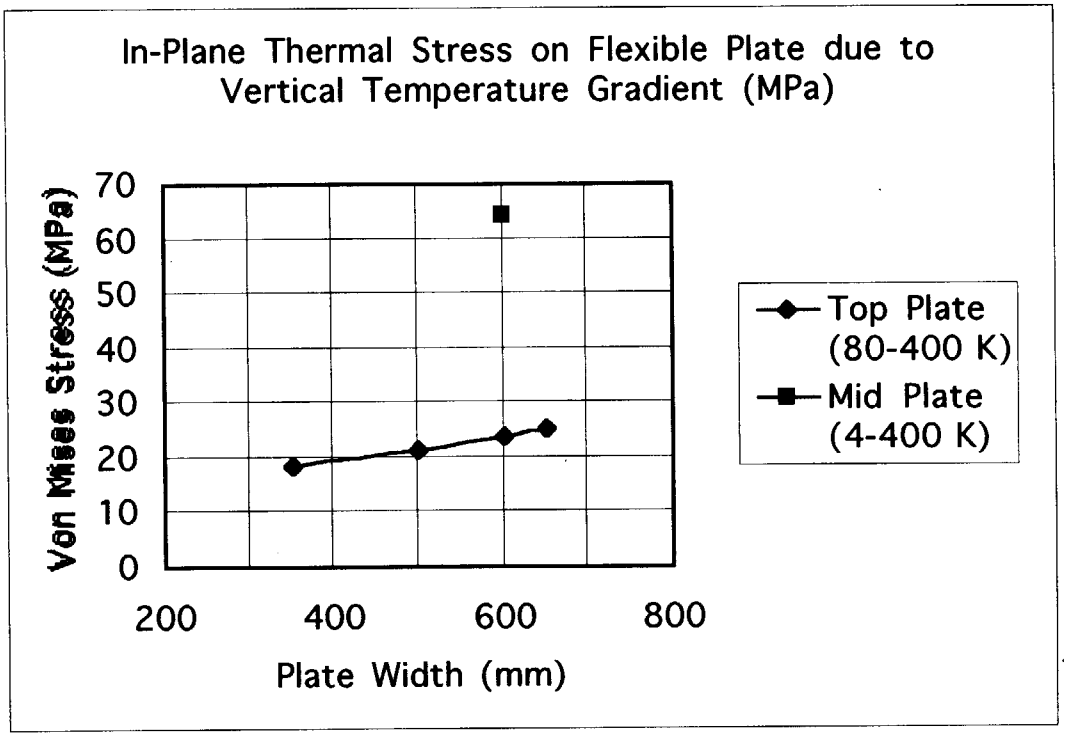

Fig. 3.3-2(c) Max. In-Plane Thermal Stress on Top Hanging Flexible Plates due to Temperature Gradient from 80 K to 400 K as a function Plate Width

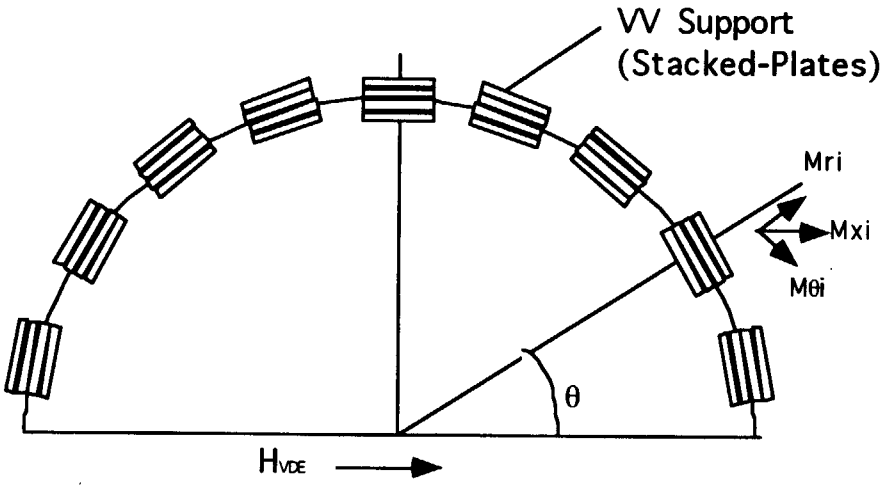

Fig. 3.3-3 VV Support Location in Toroidal Direction

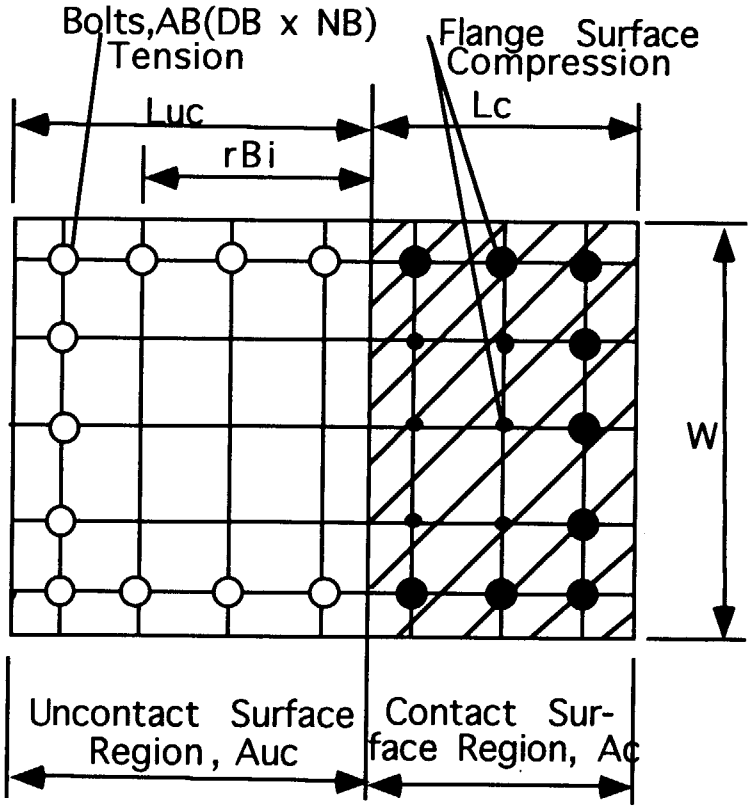

Fig. 3.3-4 Schematic drawing of flange/bolts behaviors at the loading

4. Investigation of Compressive Type Support in Divertor Region

The compressive type support concept using the region of alternate divertor port is another option of VV support design. Two designs are investigated for the compressive VV support. One is mounted on TF inter-coil structures (OIS) and the other is on cryostat ring.

4.1 Support System on TF Coil Outer Inter-coil Structure

4.1.1 Configuration

The compressive type support on TF coil OIS is shown in Fig.4.1-1～Fig.4.1-3. The VV support system consists of nine supports in toroidal direction. Each support has sixteen flexible plates. The main parameters of the support system are as follows;

Table 4.1-1 Main Parameters of VV Support System on TF coil OIS

	VV Support
Number of supports	9
Dimensions of flexible plate length×width×thickness	2000×1400×30 [mm]
Number of flexible plates	16
Material of flexible plates	SS316LN
Material of bolt	Inconel 718

The flexible support is sustained on the TF coil outer inter-coil structures which are located in divertor port region between TF coils.

As the support is located in field joint regions, the connection flanges of VV wall and TF coil case are divided into two parts in order not to weld the connection flanges at VV initial assembly. The flanges of flexible plates are bolted to the connection flanges of VV wall with insulation shims.

A thermal anchor of gas helium is attached in the middle of flexible plates.

4.1.2. Structural Assessment of Support System

(1) Membrane stress

Membrane stress of flexible plate includes vertical compressive and horizontal shear stresses. The vertical compressive stresses can be obtained by dividing total vertical downward load by area of all flexible plates.

The horizontal shear loads are produced by horizontal swaying displacement due to seismic and VDE events. The horizontal loads can be calculated by multiplying spring constants of the flexible plate by displacement of VV swaying movement. In the calculation of horizontal displacements, it is assumed that the VV is a rigid structure, therefore the displacement is the resultant of shear and bending deformation of the flexible plates, shown in chapter 3. The spring constant of a flexible plate for horizontal displacement is given as follows;

$$\frac{1}{\frac{L^3}{12EI}+\frac{L}{KAG}} \tag{4.1-1}$$

where E : Young's modulus (200GPa)
I : Moment of inertia ($6.86\times10^{-3}m^4$)
L : Length of flexible plate (1.4m)
A : Area of cross section of flexible plate ($0.042m^2$)
G : Shear modulus (77GPa)

Supposing two spring constants of flexible plate about principal axes of the cross section are k_r and k_θ, the transformed spring constant in the horizontal displacement direction is as follows;

$$k_r\cos^2\theta + k_\theta\sin^2\theta \tag{4.1-2}$$

where θ is the angle between a principal axis of a flexible plate and the VV horizontal displacement direction. The total spring constant can be obtained by the summation of spring constants of all flexible plate supports. The shear and bending loads of each support are obtained by multiplying the VV displacement and the corresponding spring constants.

The maximum shear stress appears at the VV support perpendicular to the movement direction. Table 4.1-2 shows the membrane stresses of flexible plates for load combinations. All VV supports sustain the vertical load and about a half of the VV supports sustain the horizontal load. The shear force of the plate in the radial direction is negligible because it is two order less than that of circumferential direction.

The resultant stress intensity of compressive and shear stresses is given by a following formula.

$$2\sqrt{\left(\frac{\sigma}{2}\right)^2+\tau^2} \tag{4.1-3}$$

The stress intensities of the flexible plate are within the allowable values, shown in Table 4.1-2.

(2) Bending stress

Two kinds of bending stresses are induced in the flexible plate. One is due to the vertical downward load under the bending deformation caused by the difference of thermal displacement between VV and TF coil. The other is due to the horizontal load caused by VV movement.

(i) Bending stress due to vertical downward load with deformation of thermal displacement

The relative thermal displacements between VV and TF coil at cooling down are as follows;

Normal operation(100℃) 40.9 mm

Baking (200℃) 56.9 mm

The bending moment and stress are obtained by following formula.

Bending moment

$$M = 6EI\delta / L^2$$

Bending stress

$$\sigma = 3E\delta t / L^2$$

where E: Young's modulus

δ : Relative displacement between VV and TF coil due to thermal contraction

t : Thickness of flexible plate

L : Length of flexible plate

The maximum bending moment of the flexible plate with deformation of thermal displacement is as follows;

$$M = \frac{Pl}{2} \frac{\sin(-\kappa L/2)}{\frac{\kappa L}{2}\cos(\kappa L/2) - \sin(\kappa L/2)} \qquad (4.1\text{-}4)$$

$$\kappa^2 = \frac{P}{EL}$$

where P is the vertical downward load. The maximum bending stress appears at the point

$$P \geq EI\pi^2 / L^2 \qquad Z = L/2 - \pi^2 / L^2$$

$$P \leq EI\pi^2 / L^2 \qquad Z = 0$$

where Z is the coordinate of longitudinal direction of the flexible plate. In this design, maximum bending stress is induced at the edge of the flexible plate because of the condition of P $\leqq$ EI π^2 / L^2. Table 4.1-3 shows the bending stress due to vertical downward load with deformation of thermal displacement. The bending stresses are 155～273MPa which are more than half of total primary stresses.

(ii) Bending stress due to horizontal load

VV movements due to horizontal load are horizontal swaying and vertical rocking assuming that VV is a rigid structure.

The stiffness of the flexible support in the radial direction is much smaller than that in circumferential direction. Therefore horizontal load caused by swaying movement is mainly sustained by the supports perpendicular to the movement direction and the maximum bending stress is induced in the flexible plates of the supports. Table 4.1-3 shows the bending stress due to horizontal load. The stresses are 21～105 MPa which are similar magnitude as membrane stress except tha case of Cat. IV event.

For the rocking movement, the maximum stress is induced in the flexible

supports parallel to the movement direction. The dominant stress of flexible plate is membrane one of 4 MPa. The bending stress due to rocking movement is negligible to calculate the primary stress because the location of the maximum bending stress is different from that due to swaying movement.

(iii) Bending stress due to TF coil deformation

The bending stress due to the deformation of TF coil OIS is also calculated from the rotation of the VV support around the radial direction of the machine. The TF coil rotation was calculated to be 7.87×10-4rad[11]. The bending stress of the flexible plate due to the rotation of TF coil OIS is calculated to be 55MPa. The stresses shown in Table 4.1-3 include the bending stress due to the deformation TF coil OIS as primary stress.

(3) In-plane thermal stress

In-plane thermal stress due to non-uniform temperature distribution has been calculated using FEM analysis. Figures 4.1-4 and 4.1-5 show the analysis model and the boundary condition, respectively. The analysis model includes a flexible plate and the corresponding flange. Thermal anchor of 80K helium gas is located in the middle of the flexible plate in the longitudinal direction.

Figures 4.1-6 and 4.1-7 show the deformation and the maximum shear stress profiles in the flexible plate. The plate deforms in the middle of the plate and the maximum Tresca stress of 105 MPa is induced at that point. The stress of the plate edge is almost the same as that in the middle of the plate. The in-plane thermal stresses are evaluated as secondary stress for the assessment, shown in Table 4.1-4. The primary plus secondary stresses are within the allowable values.

4.1.3 Buckling Assessment

The buckling load is calculated from the formula of elastic buckling of bar under the condition of both fixed ends. In the buckling theory, the equivalent length of the bar for the condition is 0.5L. In reality, recommended length of the load calculation is 0.65L because the ends are not completely fixed. The buckling load N is given as follows;

$$N = \frac{\pi^2 EI}{(0.65L)^2} n = 5.30 \times 10^8 [N] \qquad (4.1\text{-}5)$$

where n is total number of flexible plates.

Transverse buckling moment can be obtained as follows for rectangular plate with the condition of both fixed ends.

$$Mcr = 2.56 \times \frac{2\pi}{L} \times \sqrt{EIGJ} = 6.28 \times 10^6 [N] \qquad (4.1\text{-}6)$$

where I is moment of inertia of the cross section about the central axis parallel to plane of buckling and GJ is stiffness of torsion. The transverse buckling load is given by dividing buckling moment by plate length.

Table 4.1-5 shows the load factor (safety factor on buckling strength) for longitudinal and transverse buckling. The calculated load factors are within the

allowable values.

4.1.4 Natural Frequency

Two vibration modes are considered for horizontal movement; swaying and rocking movements. The natural frequency can be obtained by the total spring constant of the horizontal movements. The spring constants and the natural frequency are as follows;

Spring constant of swaying movement 6.29×10^{10} N/m
Spring constant of rocking movement 1.84×10^{12} N/m
Equivalent horizontal spring constant 6.08×10^{10} N/m
Natural frequency

$$f = \frac{1}{2\pi}\sqrt{\frac{k}{M}} = 3.92[Hz] \qquad 4.1-$$

4.1.5 Heat Load Assessment of Support System

Heat loads from VV to thermal anchor and that from thermal anchor to TF coil are given by following formulas.

$$Q_1 = \frac{A}{L_1}\int_4^{80}\lambda(t)dt$$
$$Q_2 = \frac{A}{L_1}\int_{80}^{300}\lambda(t)dt \qquad 4.1-$$

where L1 and L2 are lengths of heat conduction, and A is the area of flexible plates. Supposing that the flexible plates are made of Inconel 625 and the thermal anchor is located in the middle of a flexible plate, total heat load of the support to TF coil is as follows;

$$Q_1 = \frac{0.03\times1.4\times16\times9}{1}\times324.5 = 1.96\times10^3[W] \qquad (80K\rightarrow4K)$$

Total heat load to thermal anchor is

$$Q_2 = \frac{0.03\times1.4\times16\times9}{1}\times2829.4 = 17.1\times10^3[W] \qquad (300K\rightarrow80K)$$

4.1.6 Bolt Stress Assessment

The tensile stresses of bolt are produced by upward electromagnetic load and by bending moment due to the relative thermal displacement between TF coil OIS and VV wall. Horizontal load also causes the tensile stresses of bolts by bending moment due to the shear load of swaying displacement. The shear load between flanges is sustained by friction between flanges.

The strength of Inconel 718 for bolt material is

100℃ Yield strength 1030 MPa Ultimate strength 1370 MPa

4K Yield strength 1350 MPa Ultimate strength 1600 MPa

The integrity assessment of bolt has been performed for the bolts of the support flange. According to the criteria of ASME Sec. III-NB, allowable value in operation condition is two third of yield strength (2/3 σ y =687MPa). Initial pre-load stress of bolt is assumed to be 500 MPa in this design.

(1) Tensile load of bolts due to bending moment at cooling down

Shear load F_1 of a flexible plate edge is

$$F_1 = \frac{12EI\delta}{L^3} \qquad (4.1\text{-}9)$$

where E、 I、 δ 、 and L are Young's modulus, moment of inertia, thermal displacement, and length of flexible plate, respectively. The total shear load of sixteen flexible plates of a VV support is 0.67 MN.

The tensile load F_2 of flange edge due to the shear load is

$$F_2 = \frac{F_1 \times \frac{L}{2}}{L_{flange}} = 0.62[MN] \qquad (4.1\text{-}10)$$

where L_{flange} is the length between the location of bolt and the flange edge. The tensile load of bolt due to bending moment can be obtained assuming that ten bolts along a flange edge sustain the total tensile load of F_2.

For the cases of seismic and VDE events, upward load is sustained by bolts when the upward load exceeds the total weight. Table 4.1-6 shows upward loads for load combinations. Only in the case of Cat.IV event, the upward load exceeds the total weight but is negligible small.

(2) Tensile load of bolts due to swaying and rocking movement

For the case of swaying movement, the maximum shear load is induced for the support perpendicular to the swaying movement displacement. The maximum shear load F_3 in θ direction is 6.56 MN under the condition of horizontal load of 30MN. Supposing that a half of bolts of the VV support flange sustain the moment, the total tensile load F_4 of six bolts at the flange edge is given as follows;

$$F_3 \times L = 6F_4 \times L_{flange} + 2(0.875^2 F_4 L_{flange} + 0.75^2 F_4 L_{flange} + 0.625^2 F_4 L_{flange}) + 6 \times 0.5^2 F_4 L_{flange}$$

where L_{flange} is the length between the location of bolt and the flange edge.

The maximum tensile stress of bolts due to swaying movement for the horizontal load of 30 MN is

$$F_4 \ / \ (\pi d2/4) = 181 \times 10^6 \text{ (Pa)}$$

The maximum tensile load of a VV support due to rocking movement is 2.7 MN

which is induced in the VV support parallel to the movement direction. Thirty six bolts of a support flange sustain the tensile load. The tensile stress of the bolt is

$$2.7\times10^{6}/\ (\pi d^{2}/4)\ /36 = 17.0\times10^{6}\ (\mathrm{Pa})$$

(3) Proof bolt stress

Bolt is tightened with an initial pre-load of F_i which is usually greater than that due to applied load of F_{applid}. The poof bolt stress F_{bolt} is given as follows;

$$F_{bolt} = F_i + \frac{k_{bolt} \times F_{applied}}{(k_{bolt} + k_{flange})} \qquad (4.1\text{-}11)$$

where k_{bolt} and k_{flange} are spring constants of bolt and flange, respectively. In order to estimate the spring constant of flange, the compressed area of flange is assumed to be three times the bolt-hole diameter.

Table 4.1-6 shows the stresses of bolt for load combinations. The initial pre-load of bolt is assumed to be 500MPa in the calculation. The tensile stress due to horizontal load is the summation of loads due to swaying and rocking movement. All of bolt stresses are within the allowable values of ASME Sec. III.

(4) Friction support of shear load between flanges

Shear load between flanges due to horizontal load is sustained by friction between flanges. Because the bolt hole of flanges should be a little larger than the bolt cross section for assembly adjustment of flange contact. As the initial pre-load of bolt is 500 MPa, the compression between flanges is as follows;

$$500\times\ (\pi d^{2}/4)\ \times36 = 80.8\quad [\mathrm{MN}]/\mathrm{support}$$

According to ASME Sec. III NF, the friction factor between flanges is 0.25 for clean- surface condition (5). The friction factor is assumed to be half of the friction factor because some shims will be inserted between the flanges.

Table 4.1-7 shows the upward loads due to weight, electromagnetic and seismic load, and due to swaying and rocking movement. The friction force depends on the compression between flanges. If the friction is larger than shear load, the friction can sustain the shear load. Table 4.1-8 shows the comparison between shear load and friction. The friction can sustain the shear load except the case of Cat. IV. For the case of Cat. IV events, the machine is not required to be operatable after these events however no significant releases should occur. Even if the shear load exceeds the friction force for the specific support perpendicular to the movement direction, horizontal load can be sustained by the supports as a whole. No significant damage of the machine is expected to occur.

Table 4.1-2 Membrane stress intensity of flexible plate of VV support on TF OIS

Cat.	Load Combination	Vertical Load		Horizontal load			Mem-brane stress intensity (MPa)	Mem-brane allow-ables SS316 LN
		Total load (MN)	Com-pres-sion (MPa)	Total load (MN)	Max. load/ support (MN)	Shear stress (MPa)		
I	Weight(100℃)	100	16.5	-	-	-	16.5	Sm
	Baking(200℃)	100	16.5	-	-	-	16.5	=207
	Weight +VDEI	143	23.6	15	3.3	4.9	25.5	
II	Weight +VDEII	154	25.4	19	4.2	6.2	28.2	Sm
	Weight+VDEI+SL1	158	26.1	30	6.6	9.8	32.6	=207
III	Weight +VDEIII	172	28.4	25	5.5	8.1	32.7	1.2Sm
	Weight+VDEII+SL1	173	28.5	34	7.4	11.1	35.5	=248
IV	Weight+VDEI+SL2	203	33.5	75	16.4	24.4	59.2	2*Sm= 414

Table 4.1-3 Primary stress intensity of flexible plate of VV support on TF OIS

Cat.	Load combination	Vertical load		Horizontal load		Mem-brane stress intensity (MPa)	Mem-brane+ bending stress intensity (MPa)*	Primary stress allow-able SS316 LN
		Total load (MN)	Bend-ing stress (MPa)	Total load (MN)	Bend-ing stress (MPa)			
I	Weight(100℃)	100	196	0	0	16.5	213	1.5Sm
	Baking(200℃)	100	273	0	0	16.5	290	=311
	Weight +VDEI	143	172	15	21	25.6	274	
II	Weight +VDEII	154	168	19	26	28.2	278	1.5Sm
	Weight+VDEI+SL1	158	167	30	42	32.6	296	=311
III	Weight +VDEIII	172	162	25	35	32.7	285	1.2*1.5S m=373
	Weight+VDEII+SL1	173	162	34	47	35.5	300	
IV	Weight+VDEI+SL2	203	155	75	105	59.2	374	2*1.5Sm =621

* The bending stress of 55MPa due to TF coil deformation is included.

Table 4.1-4 Secondary stress intensity of flexible plate of VV support on TF OIS

Cat.	Load combination	Membrane stress (MPa)	Membrane + bending stress (MPa)	Secondary stress (MPa)	Secondary stress allowable SS316 LN
I	Weight(100℃)	16.5	213	318	3 Sm
	Baking(200℃)	16.5	290	395	=621
	Weight+VDEI	25.6	274	379	
II	Weight+VDEII	28.2	278	383	3 Sm
	Weight+VDEI+SL1	32.6	296	401	=621
III	Weight+VDEIII	32.7	285	390	-
	Weight+VDEII+SL1	35.5	300	405	
IV	Weight+VDEI+SL2	59.2	374	479	-

Table 4.1-5 Buckling load factor of VV support on TF OIS

Cat.	Load combination	Vertical load (Compressive buckling)		Horizontal load (Transverse buckling)		Load factor allowable (ASME Sec. III)
		Total load[MN]	Load factor	Max.load/ support [MN]	Load factor	
I	Weight(100℃)	100	5.3	-	-	
	Baking(200℃)	100	5.3	-	-	3
	Weight+VDEI	143	3.7	3.3	8.6	
II	Weight+VDEII	154	3.4	4.1	6.9	3
	Weight+VDEI+SL1	158	3.4	6.6	4.3	
III	Weight+VDEIII	172	3.1	5.5	5.1	2.5
	Weight+VDEII+SL1	173	3.1	7.4	3.8	
IV	Weight+VDEI+SL2	203	2.6	16.4	1.7	1.5

Table 4.1-6 Tensile stress of bolts of VV support on TF OIS

Cat.	Load combination	Upward load		Horizontal load				Max. tensile load* /bolt [MPa]	Max. tensile stress* /bolt [MPa]	allow-able Inconel 718 ASME Sec.III NB
				Swaying		Rocking				
		Up-ward load/ flange edge [MN]	Ten-sile load/ bolt [MPa]	Shear, load/ sup-port [MN]	Ten-sile load/ bolt [MPa]	Ten-sile load/ sup-port [MN]	Ten-sile load/ bolt [MPa]			
I	Weight(100℃)	0.57	12.7	-		-		12.8	503	2/3 σy = 687
	Baking(200℃)	0.80	17.8	-		-		17.8	505	
	Weight +VDEI	-6.3	12.7	3.3	91	1.4	8.5	103	527	
II	Weight +VDEII	-5.1	12.7	4.2	115	1.7	10.8	127	533	2/3 σy = 687
	Weight+VDEI +SL1	-4.7	12.7	6.6	181	2.7	17.0	194	551	
III	Weight +VDEIII	-3.1	12.7	5.5	151	2.3	14.2	164	543	2/3 σy = 687
	Weight +VDEII +SL1	-3.0	12.7	7.5	205	3.1	19.3	217	557	
IV	Weight +VDEI +SL2	0.3	13.0	16.5	453	6.8	42.5	465	622	Min.(0.7 σu, σy)=957

*The tensile load is the summation of loads due to swaying and rocking movement.

*The tensile stress is proof bolt stress including the initial pre-load of 500 MPa

Table 4.1-7 Shear load between flanges of VV support on TF OIS

Cat.	Load combination	Upward load* [MN]		Horizontal load [MN]				
		Upward load (EM + seismic load)	Upward load (include weight) ／sup-port	Horizontal load (MN)	Load in θ direction due to swaying／support (90°)	Upward load due to rocking／support (90°)	Load in θ direction due to swaying／support (180°)	Upward load due to rocking／sup-port (180°)
I	Weight(100℃)	0	-11	0	0	0	0	0
	Baking(200℃)	0	-11	0	0	0	0	0
	Weight +VDEI	43	-6.3	15	3.3	0.35	1.15	1.35
II	Weight +VDEII	54	-5.1	19	4.2	0.47	1.46	1.71
	Weight+VDEI+SL1	58	-4.7	30	6.6	0.74	2.30	2.70
III	Weight +VDEIII	72	-3.1	25	5.5	0.62	1.92	2.25
	Weight +VDEII +SL1	73	-3.0	34	7.5	0.84	2.61	3.06
IV	Weight +VDEI +SL2	103	0.3	75	16.5	1.85	5.75	6.75

* Minus means downward load.

Table 4.1-8 Shear force and friction between flanges of VV support on TF OIS

Cat.	Load combination	Angle of 90° [MN]			Angle of 160° [MN]		
		Load in θ direction due to swaying ／support	Compression ／support	Friction due to comression／support	Load in θ direction due to swaying ／support	Compression ／support	Friction due to comression／support
I	Weight(100℃)	0	74	9.3	0	74	9.3
	Baking(200℃)	0	74	9.3	0	74	9.3
	Weight +VDEI	3.3	69	8.6	1.15	69	8.5
II	Weight +VDEII	4.2	68	8.4	1.46	68	8.3
	Weight+VDEI+SL1	6.6	67	8.4	2.30	67	8.1
III	Weight +VDEIII	5.5	65	8.2	1.92	65	8.0
	Weight +VDEII +SL1	7.5	65	8.1	2.61	65	7.9
IV	Weight +VDEI +SL2	16.5	61	7.6	5.75	61	7.0

* Initial pre-load of bolt is 500 MPa. Compression of flange is 80.8 MN

* Friction coefficient is assumed to be 0.125 which is a half of that of clean surface.

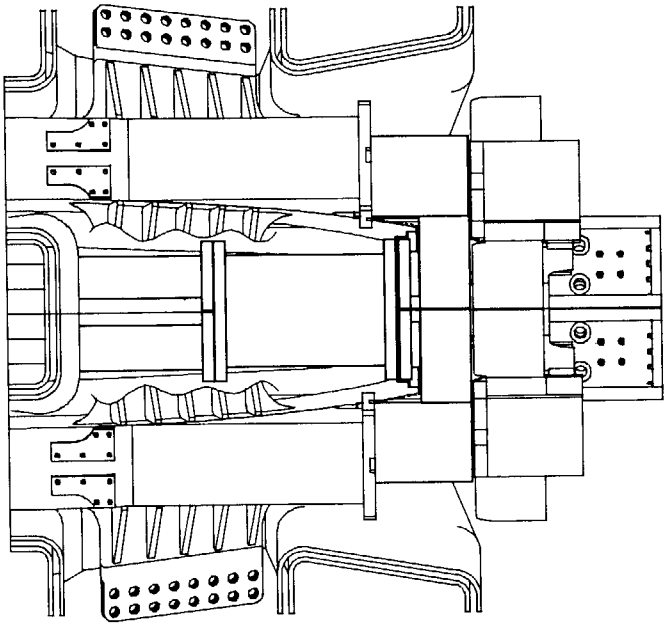

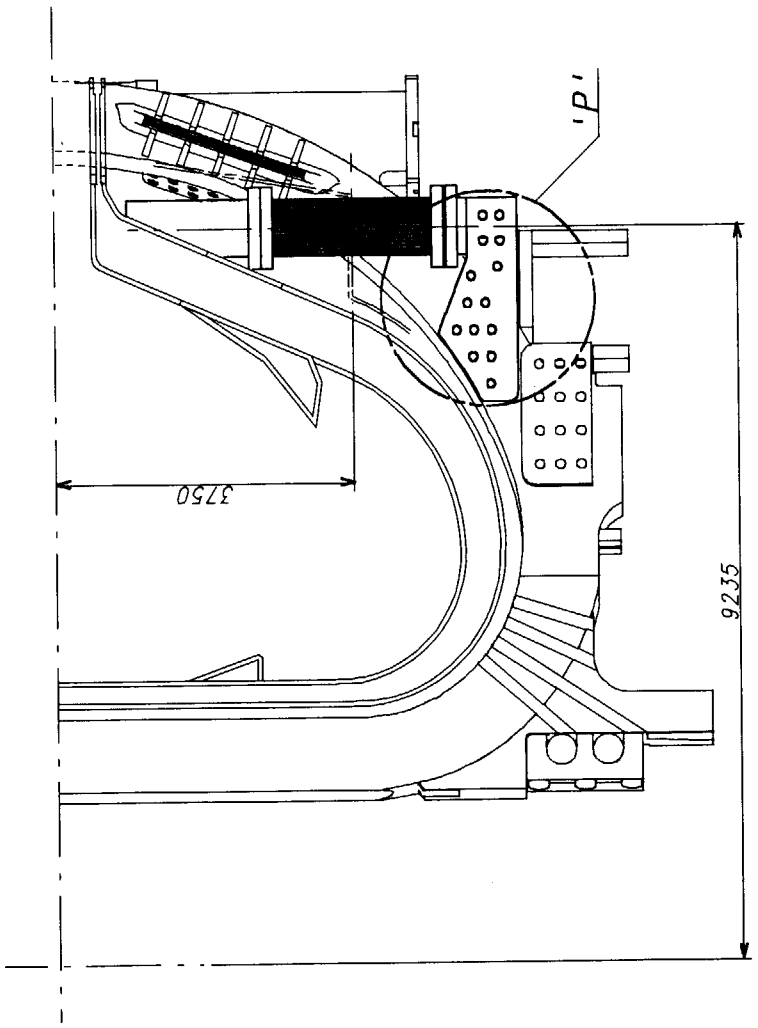

Fig. 4.1-1 VV support structure

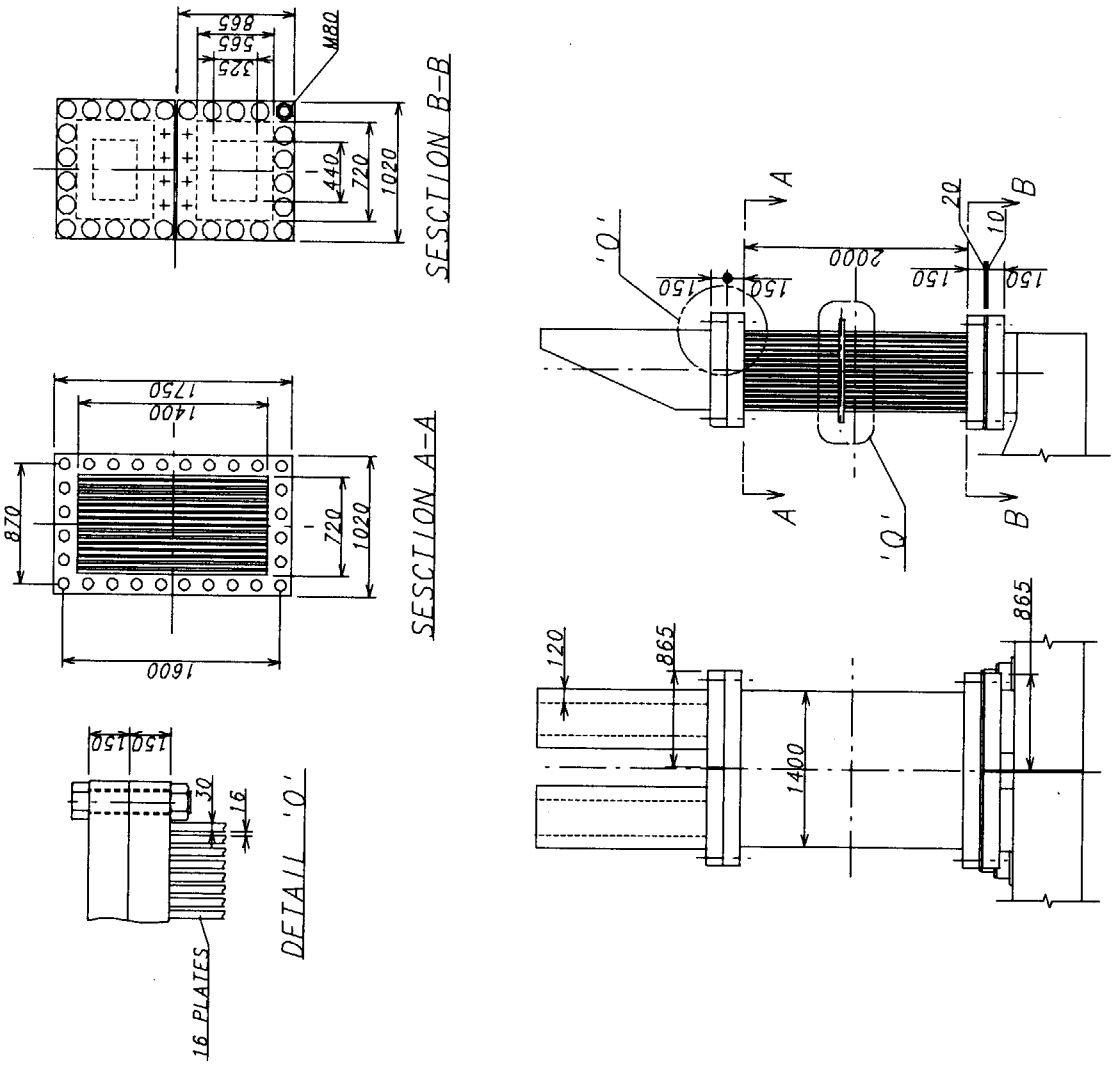

Fig.4.1-2 Flexible plate of VV support

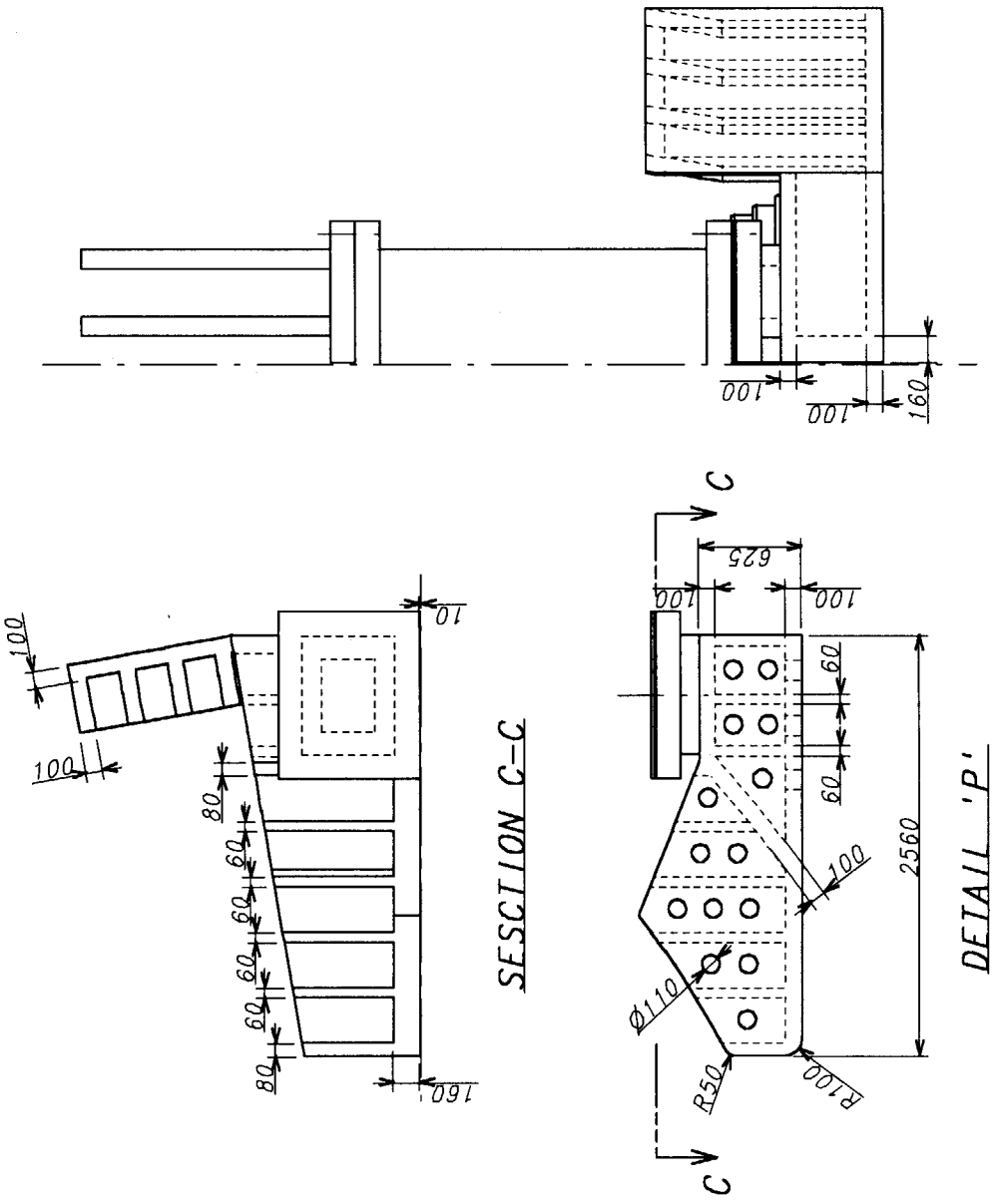

Fig.4.1-3 TF inter-coil structure for VV support

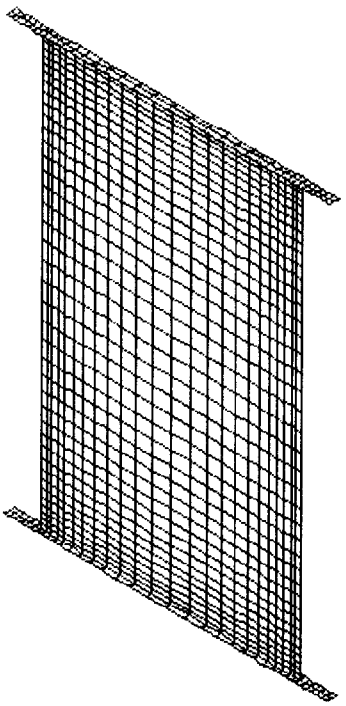

Fig. 4.1-4 Analysis model for in-plane thermal stress

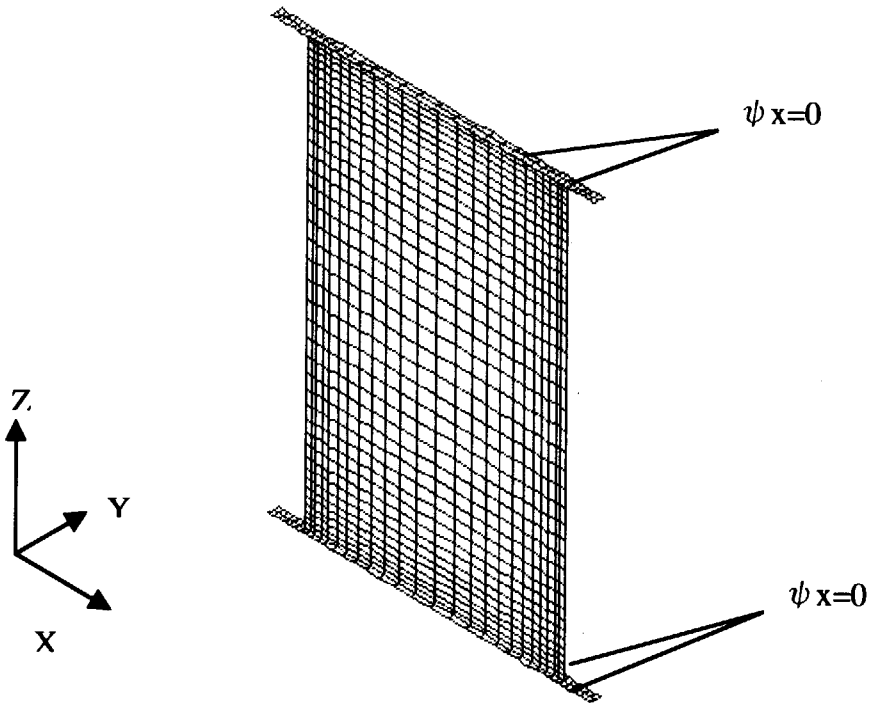

Fig.4.1-5 Analysis condition

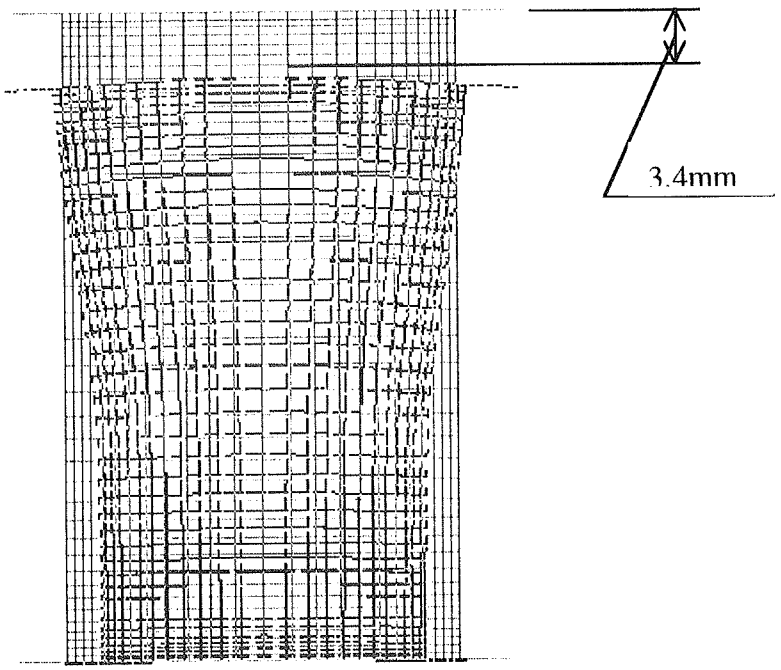

Fig. 4.1-6 Displacement due to cooling down

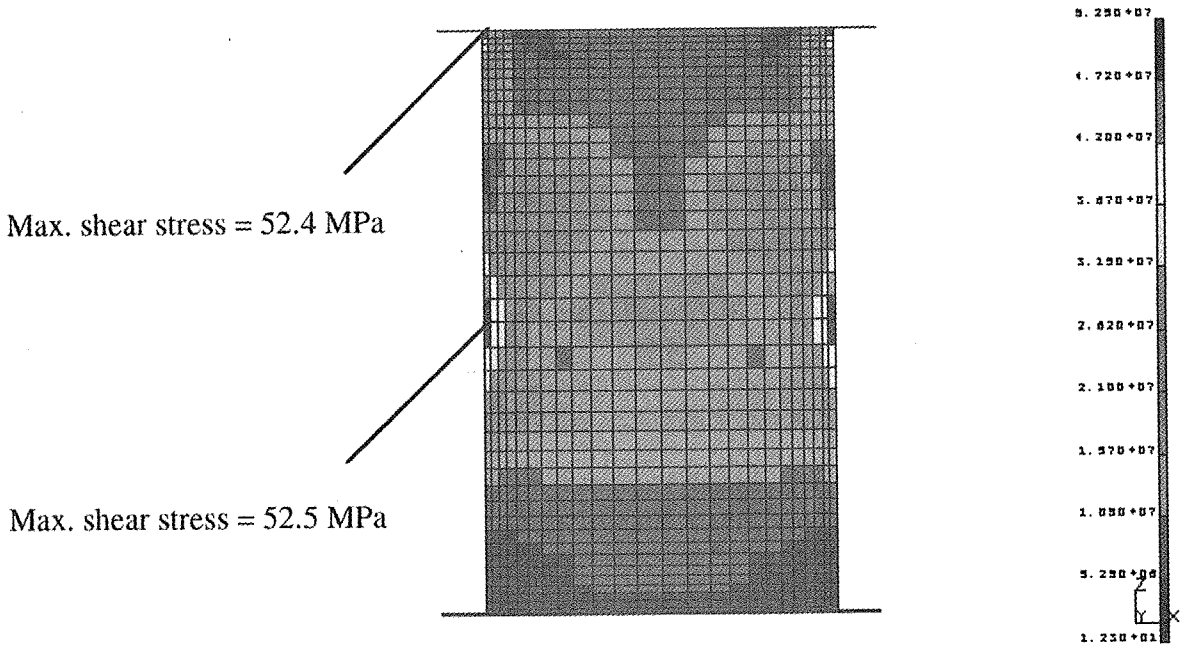

Fig. 4.1-7 Maximum shear stress due to temperature distribution at cooling down

4.2 Support System on Cryostat Ring

4.2.1 Configuration

The compressive type support on cryostat ring using the space of alternate divertor port is shown in Fig.4.2-1～Fig.4.2-3. The VV support system consists of nine supports in toroidal direction. The VV supports have no interaction with TF coil. Therefore, The structural integrity of the VV and TF support increases because of the load reduction for each support.

The main characteristics of the support system are as follows;

(1) The VV supports are connected between VV wall and cryostat ring. The temperature difference between support edges is only 80°C. The stress due to the relative thermal displacement between the support edges is much less than that of the VV support on TF coil OIS.

(2) There is no interference between the VV and TF supports. The TF coil case has no effect on VV support. The increase of reliability of VV support is expected.

(3) The load of TF coil support is also decreased to the weight of coil system and reaction load of VV for plasma disruption.

For locating VV support in PF5 outside, PF5 winging pack turns are changed from 14(R)×16(Z) turns to 12(R)×20(Z) turns in order to make space between VV support and PF5. The sizes of the PF5 coil are changed from 843.2mm(ΔR)×968.8mm(ΔZ) to 725.6mm(ΔR)×1206.0mm(ΔZ). The outboard edge of PF5 moves 118mm to the direction of machine center. It is confirmed that there is no effect on the PF coil performance.

If the space is required between cryostat ring and PF5 coil on the bottom of cryostat for the winding of PF5 coil repair, cryostat ring support may be designed to move the direction of machine outboard.

The design of TF coil support follows that of DDD in ITER FDR [13]. The design loads of the TF support are the weight of coil system and the reaction loads of VDE vertical and horizontal force.

The main parameters of VV and TF support are as follows;

Table 4.2-1 Main Parameters of VV Support System on Cryostat Support Ring

	VV Support	TF Support
Number of supports	9	18
Dimensions of flexible plate length×width×thickness	1500×1200×28 [mm]	2200×1035×25 [mm]
Number of flexible plates	18	22
Material of flexible plates	SS316LN	SS316LN
Material of bolt	Inconel 718	Inconel 718

4.2.2. Structural Assessment of Support System

The structural assessment of the support system is the same as that of the previous section. The results of the assessment of VV and TF support are shown in Table 4.2-1 for membrane stress and Table 4.2-2 for bending stress.

The thermal displacements of VV support between support edges are 12.4 mm for normal operation and 27.9 mm for baking operation. The thermal displacements are much less than that of the VV support on TF coil case.

The membrane and bending stresses for VV and TF coil support are within the allowable values.

Table 4.2-3 shows the secondary stresses of VV and TF flexible plates. The thermal stresses due to non-uniform temperature distribution in the flexible plates are assumed to be 30MPa and 64MPa for VV and TF coil support respectively. The secondary stresses are much less than the allowable values.

The buckling assessment is shown in Table 4.2-4. The VV and TF flexible plate have enough buckling integrity.

The assessment for tensile bolt stresses and shear forces between flanges are also performed as that of previous section. The tensile bolt stresses are almost the same as that of VV support on TF coil OIS. The VV and TF tensile bolt stresses are within the allowable values and the shear loads between flanges can be sustained by friction force between flanges except the case of Cat. IV events.

4.2.3Natural Frequency

Two vibration modes are considered for horizontal movement; swaying and rocking movement. The natural frequency can be obtained by the total spring constant of the horizontal movement. Each spring constant and natural frequency are as follows;

Table 4.2-8 Natural frequencies of VV and TF coil supports

	VV Support	TF Support
Spring constant of swaying movement[N/m]	7.27×10^{10}	5.60×10^{10}
Spring constant of rocking movement [N/m]	1.62×10^{12}	1.27×10^{12}
Equivalent horizontal spring constant [N/m]	6.96×10^{10}	5.36×10^{10}
Natural frequency [Hz]	4.20	3.68

4.3Summary

Compressive type VV supports have been investigated using alternate divertor port region. Two designs have been performed for the compressive VV support concept. One is mounted on TF coil OIS and the other is on cryostat ring.

For both VV supports, the flexible plates stresses, load factors of buckling and bolt stresses are within allowable values for all load combinations. The shear load between flanges can be sustained by friction force between flanges except the case of Cat. IV events.

For the VV support on cryostat ring, the loads of VV and TF supports are decreased comparing with those for the VV support on TF coil OIS. The load of TF coil support is also decreased to the summation of weight of coil system and reaction load for plasma

disruption.

The VV supports of cryostat ring have no load interaction with TF coil performance. The independency is preferable because of no requirement for the structural integrity of TF coil.

Table 4.2-2(a) Membrane stress intensity of VV flexible plate

Cat.	Load Combination	Vertical Load		Horizontal load			Membrane stress intensity (MPa)	Membrane allowables SS316 LN
		Total load (MN)	Compression (MPa)	Total load (MN)	Max. load/support (MN)	Shear stress (MPa)		
I	Weight(100°C)	100	18.4	-	-	-	18.4	Sm
	Baking(200°C)	100	18.4	-	-	-	18.4	=207
	Weight +VDEI	143	26.3	15	3.3	5.4	28.5	
II	Weight +VDEII	154	28.3	19	4.2	6.8	31.4	Sm
	Weight+VDEI+SL1	158	29.1	30	6.6	10.8	36.3	=207
III	Weight +VDEIII	172	31.6	25	5.5	9.0	36.4	1.2Sm
	Weight+VDEII+SL1	173	31.0	34	7.4	12.2	39.5	=248
IV	Weight+VDEI+SL2	203	37.3	75	16.4	27.1	65.8	2*Sm= 414

Table 4.2-2(b) Membrane stress intensity of TF flexible plate

Cat.	Load Combination	Vertical Load		Horizontal load			Membrane stress intensity (MPa)	Membrane allowables SS316 LN
		Total load (MN)	Compression (MPa)	Total load (MN)	Max. load/support (MN)	Shear stress (MPa)		
I	Weight(100°C)	100	9.8	-	-	-	9.8	Sm
	Weight +VDEI	132	12.9	11	1.2	2.9	14.1	=207
II	Weight +VDEII	141	13.7	14	1.5	3.6	15.5	Sm
	Weight+VDEI+SL1	147	14.4	26	2.8	6.8	19.8	=207
III	Weight +VDEIII	154	15.0	18	2.0	4.8	17.8	1.2Sm
	Weight+VDEII+SL1	156	15.2	29	3.1	7.5	21.4	=248
IV	Weight+VDEI+SL2	192	18.8	71	7.7	18.7	41.8	2*Sm= 414

Table 4.2-3(a) Primary stress intensity of VV flexible plate

Cat.	Load combination	Vertical load		Horizontal load		Membrane stress intensity (MPa)	Membrane+ bending stress intensity (MPa)	Primary stress allowable SS316 LN
		Total load (MN)	Bending stress (MPa)	Total load (MN)	Bending stress (MPa)			
I	Weight(100℃)	100	87	0	0	18.4	105	1.5Sm
	Baking(200℃)	100	195	0	0	18.4	213	=311
	Weight +VDEI	143	84	15	91	26.3	201	
II	Weight +VDEII	154	83	19	115	28.3	227	1.5Sm
	Weight+VDEI+SL1	158	83	30	181	29.1	294	=311
III	Weight +VDEIII	172	82	25	151	31.6	265	1.2*1.5Sm=373
	Weight+VDEII+SL1	173	82	34	205	31.0	319	
IV	Weight+VDEI+SL2	203	80	75	453	37.3	572	2*1.5Sm =622

Table 4.2-3(b) Primary stress intensity of TF flexible plate

Cat.	Load combination	Vertical load		Horizontal load		Membrane stress intensity (MPa)	Membrane+ bending stress intensity (MPa)*	Primary stress allowable SS316 LN
		Total load (MN)	Bending stress (MPa)	Total load (MN)	Bending stress (MPa)			
I	Weight(100℃)	100	89	0	0	9.8	98	1.5Sm
	Weight +VDEI	132	89	11	41	14.1	221	=311
II	Weight +VDEII	141	85	14	52	15.5	231	1.5Sm
	Weight+VDEI+SL1	147	85	26	99	19.8	279	=311
III	Weight +VDEIII	154	84	18	69	17.8	249	1.2*1.5Sm=373
	Weight+VDEII+SL1	156	84	29	109	21.4	289	
IV	Weight+VDEI+SL2	192	81	71	271	41.8	453	2*1.5Sm =622

* The bending stress of 80MPa due to TF coil deformation is included.

Table 4.2-4 Secondary stress intensity of VV and TF flexible plates

Cat.	Load combination	VV Flexible Plate		TF Flexible Plate	
		Secondary stress* (MPa)	Allowable SS316LN (MPa)	Secondary stress** (MPa)	Allowable SS316LN (MPa)
I	Weight(100℃)	135	3 Sm	162	3 Sm
	Baking(200℃)	243	=622	-	=622
	Weight+VDEI	231		285	
II	Weight+VDEII	257	3 Sm	295	3 Sm
	Weight+VDEI+SL1	324	=622	343	=622
III	Weight+VDEIII	295	-	313	-
	Weight+VDEII+SL1	349		353	
IV	Weight+VDEI+SL2	602	-	517	-

* The thermal stress of 30MPa due to temperature distribution is included.

** The thermal stress of 64MPa due to temperature distribution is included.

Table 4.2-5(a) Buckling load factor of VV flexible plate

Cat.	Load combination	Vertical load (Compressive buckling)		Horizontal load (Transverse buckling)		Load factor allowable (ASME Sec. III)
		Total load[MN]	Load factor	Max.load/ support [MN]	Load factor	
I	Weight(100℃)	100	7.4	-	-	3
	Baking(200℃)	100	7.4	-	-	
	Weight+VDEI	143	5.2	3.3	21.4	
II	Weight+VDEII	154	4.8	4.1	17.1	3
	Weight+VDEI+SL1	158	4.7	6.6	10.7	
III	Weight+VDEIII	172	4.3	5.5	12.8	2.5
	Weight+VDEII+SL1	173	4.4	7.4	9.5	
IV	Weight+VDEI+SL2	203	3.6	16.4	4.3	1.5

Table 4.2-5(b) Buckling load factor of TF flexible plate

Cat.	Load combination	Vertical load (Compressive buckling)		Horizontal load (Transverse buckling)		Load factor allowable (ASME Sec. III)
		Total load[MN]	Load factor	Max.load/ support [MN]	Load factor	
I	Weight(100℃)	100	5.2	-	-	3
	Weight+VDEI	132	3.9	1.2	20.7	
II	Weight+VDEII	141	3.7	1.5	16.6	3
	Weight+VDEI+SL1	147	3.5	2.8	8.7	
III	Weight+VDEIII	154	3.3	2.0	12.4	2.5
	Weight+VDEII+SL1	156	3.3	3.1	7.8	
IV	Weight+VDEI+SL2	192	2.7	7.7	3.2	1.5

Table 4.2-6(a) Tensile bolt stress of VV support

Cat.	Load combination	Upward load		Horizontal load				Max. tensile load* /bolt [MPa]	Max. tensile stress* /bolt [MPa]	allow-able Inconel 718 ASME Sec.III NB
				Swaying		Rocking				
		Up-ward load/ flange edge [MN]	Ten-sile load/ bolt [MPa]	Shear, load/ sup-port [MN]	Ten-sile load/ bolt [MPa]	Ten-sile load/ sup-port [MN]	Ten-sile load/ bolt [MPa]			
I	Weight(100℃)	0.27	6.0	-		-		6.0	502	2/3 σy = 687
	Baking(200℃)	0.61	13.5	-		-		13.5	504	
	Weight +VDEI	-6.3	6.0	3.3	167	1.4	8.5	173	545	
II	Weight +VDEII	-5.1	6.0	4.2	212	1.7	10.8	218	557	2/3 σy = 687
	Weight+VDEI +SL1	-4.7	6.0	6.6	334	2.7	17.0	340	589	
III	Weight +VDEIII	-3.1	6.0	5.5	278	2.3	14.2	284	575	2/3 σy = 687
	Weight +VDEII +SL1	-3.0	6.0	7.5	376	3.1	19.3	385	601	
IV	Weight +VDEI +SL2	0.3	6.3	16.5	845	6.8	42.5	819	720	Min.(0.7 σu, σ y)=957

*The tensile load is the summation of loads due to swaying and rocking movement.

*The tensile stress is proof bolt stress including the initial pre-load of 500 MPa

Table 4.2-6(b) Tensile bolt stress of TF support

Cat.	Load combination	Upward load		Horizontal load				Max. tensile load* /bolt [MPa]	Max. tensile stress* /bolt [MPa]	allow-able Inconel 718 ASME Sec.III NB
				Swaying		Rocking				
		Up-ward load/ flange edge [MN]	Ten-sile load/ bolt [MPa]	Shear, load/ sup-port [MN]	Ten-sile load/ bolt [MPa]	Ten-sile load/ sup-port [MN]	Ten-sile load/ bolt [MPa]			
I	Weight(100℃)	0.18	6.8	-		-		6.8	502	2/3 σy = 687
	Baking(200℃)	0.18	6.8	-		-		6.8	502	
	Weight +VDEI	-3.2	6.8	1.4	91	1.2	12.8	97	530	
II	Weight +VDEII	-2.6	6.8	1.7	113	1.5	16.2	120	538	2/3 σy = 687
	Weight+VDEI +SL1	-2.3	6.8	3.3	216	2.3	25.6	223	558	
III	Weight +VDEIII	-1.6	6.8	2.3	151	1.9	21.3	158	549	2/3 σy = 687
	Weight +VDEII +SL1	-1.5	6.8	3.6	239	2.6	29.0	246	566	
IV	Weight +VDEI +SL2	0.2	8.7	9.1	594	5.8	64.0	602	644	Min.(0.7 σu , σ y)=957

*The tensile load is the summation of loads due to swaying and rocking movement.

*The tensile stress is proof bolt stress including the initial pre-load of 500 MPa

Table 4.2-7(a) Shear force and friction between flanges of VV support

Cat.	Load combination	Support load at angle of 90 ° due to swaying／support [MN]				Support load at angle of 160 ° due to swaying／support [MN]			
		Load in θ direc-tion	Upward load	Compre ssion	Friction due to comress ion	Load in θ direc-tion	Upward load	Compre ssion	Friction due to comress ion
I	Weight(100℃)	0		70	8.7	0		70	
	Baking(200℃)	0		70	8.7	0		70	
	Weight +VDEI	3.3	0.37	64	8.1	1.15	1.35	63	7.9
II	Weight +VDEII	4.2	0.47	63	7.9	1.46	1.71	62	7.7
	Weight+VDEI+ SL1	6.6	0.74	62	7.8	2.30	2.70	60	7.5
III	Weight +VDEIII	5.5	0.62	61	7.6	1.92	2.25	59	7.4
	Weight +VDEII +SL1	7.5	0.84	61	7.6	2.61	3.06	58	7.3
IV	Weight +VDEI +SL2	16.5	1.85	56	7.0	5.75	6.75	51	6.4

* Initial pre-load of bolt is 500 MPa. Compression of flange is 58.5 MN

* Friction coefficient is assumed to be 0.125 which is a half of that of clean surface.

Table 4.2-7(b) Shear force and friction between flanges of TF support

Cat.	Load combination	Support load at angle of 90 ° due to swaying／support [MN]				Support load at angle of 160 ° due to swaying／support [MN]			
		Load in θ direc-tion	Upward load	Compre ssion	Friction due to comress ion	Load in θ direc-tion	Upward load	Compre ssion	Friction due to comress ion
I	Weight(100℃)	0		59	7.4	0		59	
	Baking(200℃)	0		59	7.4	0		59	
	Weight +VDEI	1.9	1.2	56	7.0	0.95	1.00	56	7.0
II	Weight +VDEII	2.3	1.5	55	6.9	1.20	1.27	55	6.9
	Weight+VDEI+ SL1	3.7	2.3	54	6.8	1.90	2.00	54	6.8
III	Weight +VDEIII	3.1	1.9	54	6.7	1.58	1.67	54	6.7
	Weight +VDEII +SL1	4.2	2.6	53	6.6	2.15	2.27	53	6.6
IV	Weight +VDEI +SL2	9.3	5.8	48	6.0	4.75	5.00	49	6.1

* Initial pre-load of bolt is 500 MPa. Compression of flange is 53.9 MN

* Friction coefficient is assumed to be 0.125 which is a half of that of clean surface.

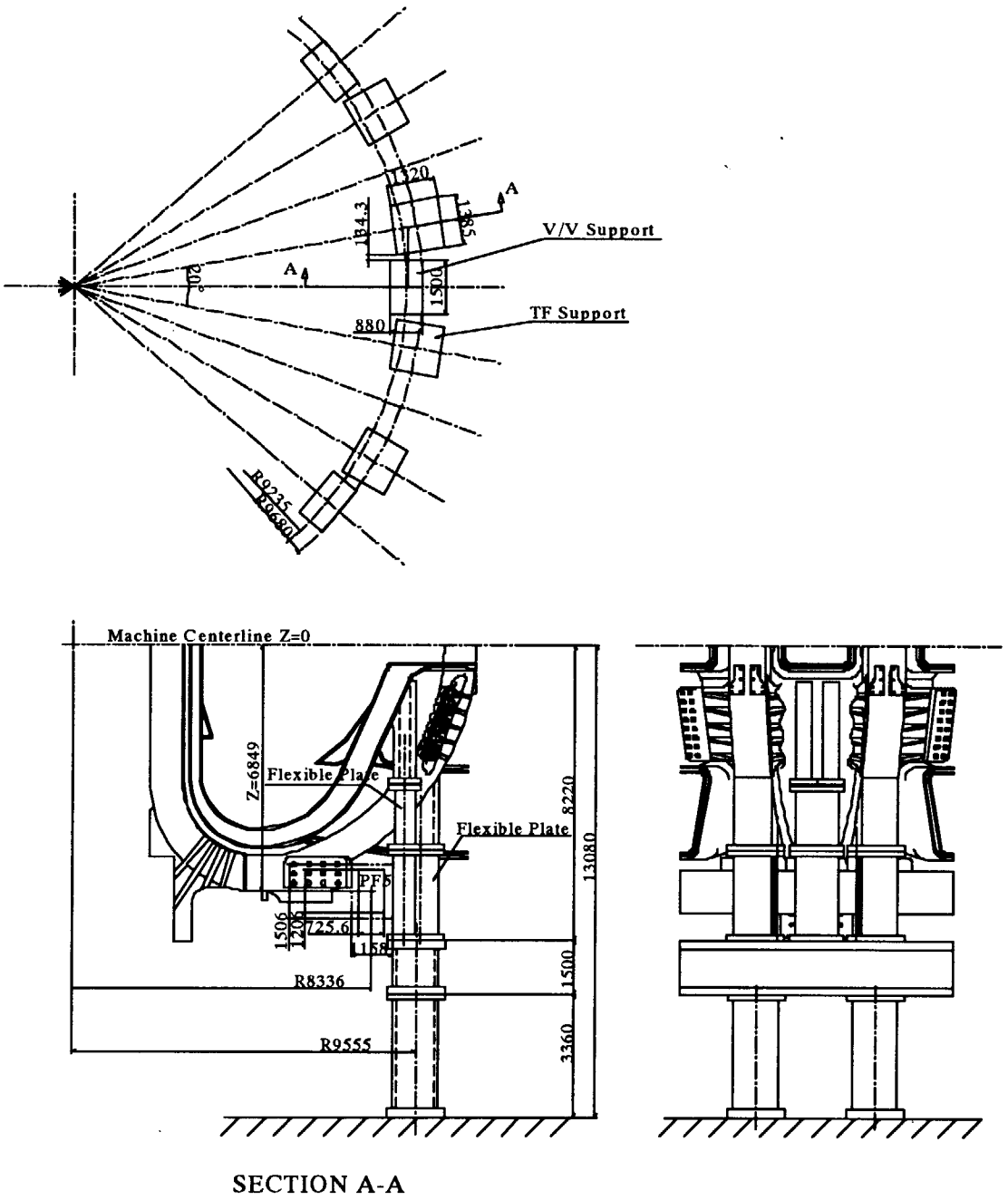

SECTION A-A

Fig 4.2-1 Compressive VV support on cryostat ring

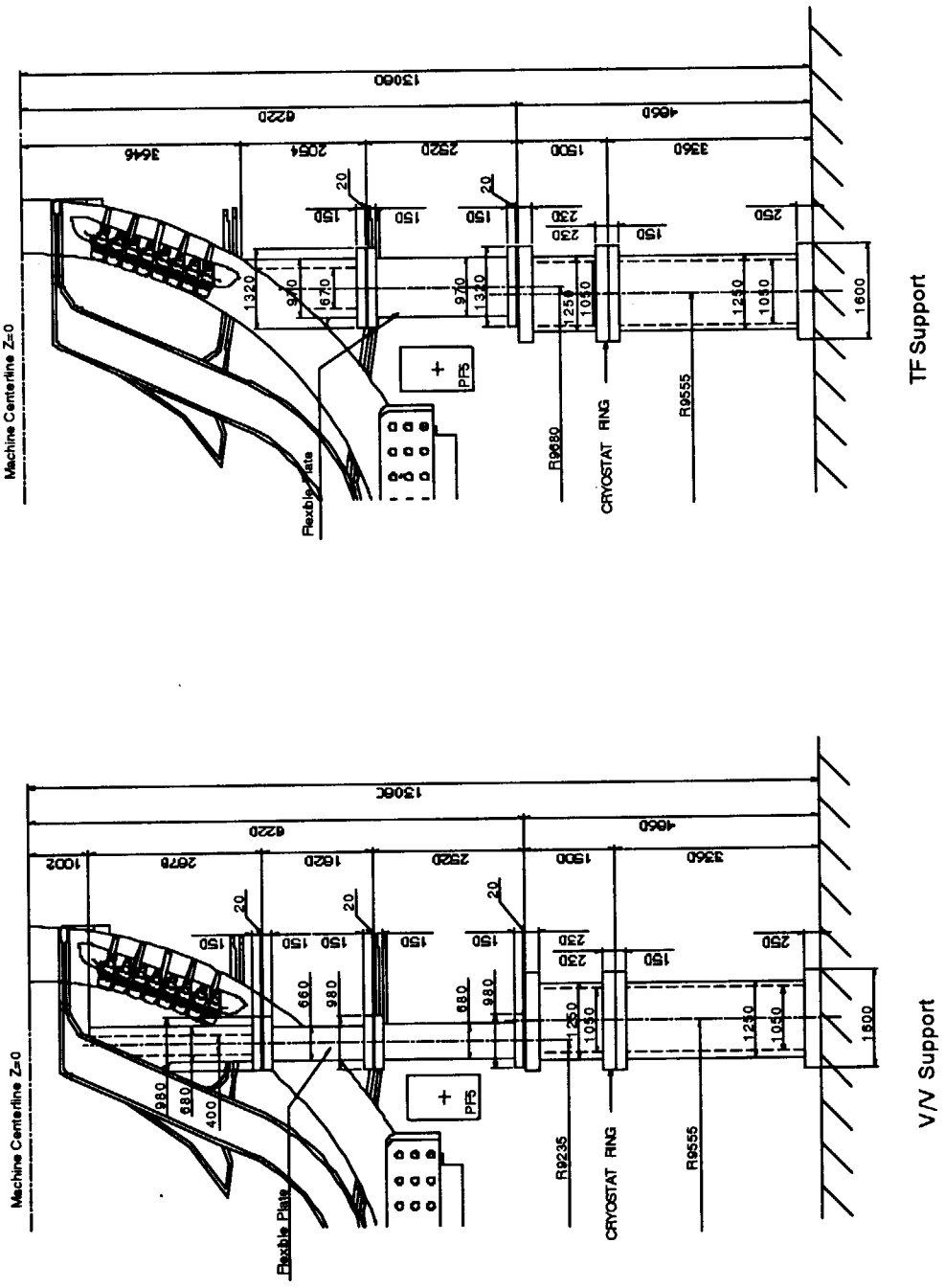

Fig 4.2-2 VV and TF support on cryostat ring

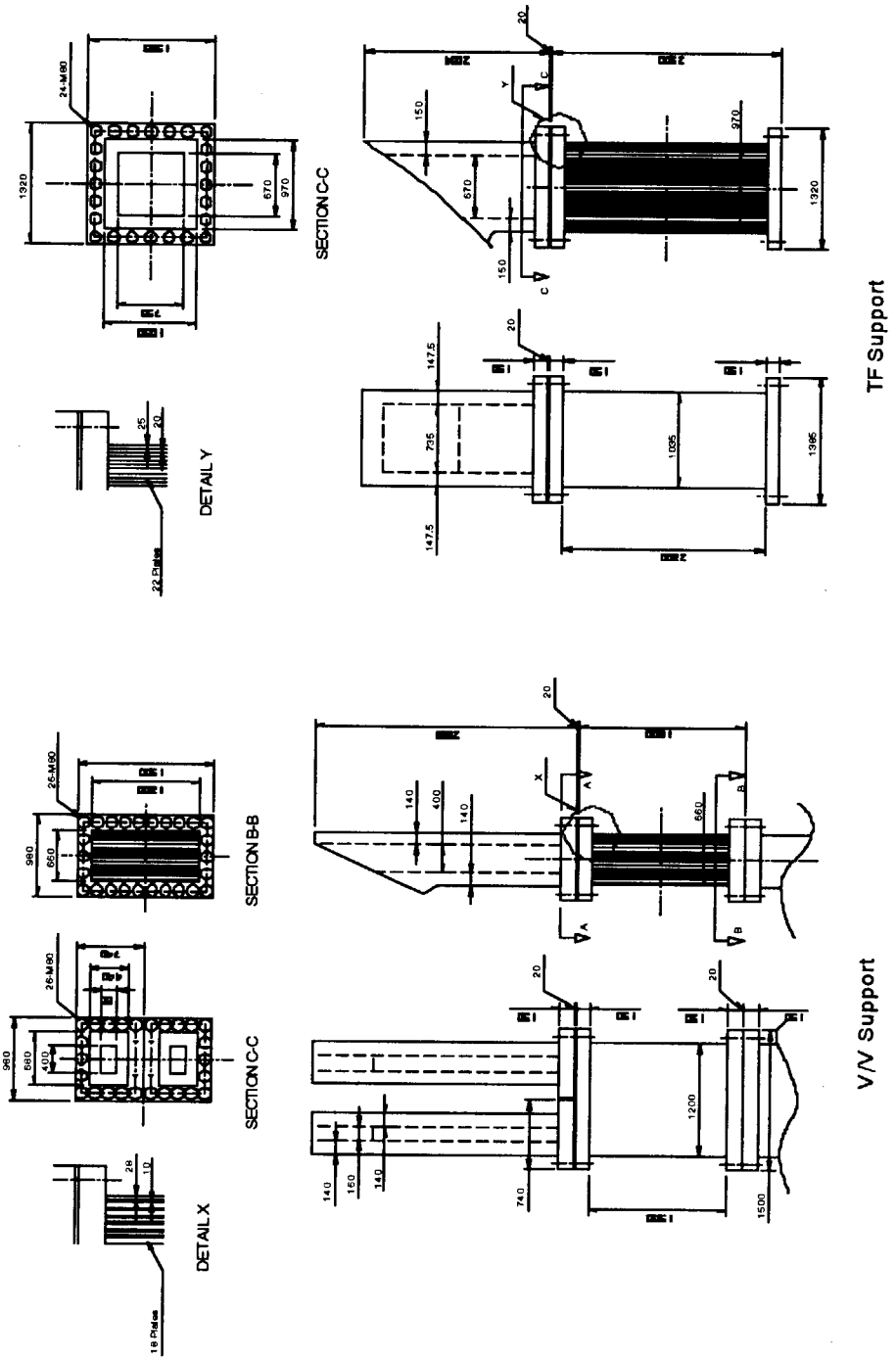

Fig 4.2-3 Flexible plate of VV and TF support

5. Conclusions

Two optional design concepts of VV support have been investigated in order to increase structural integrity of the VV support in current design. The preliminary design study for the VV support concepts has been performed to confirm the structural feasibility. From the studies, following conclusions are drawn.

1) One optional design is a hanging type support that consists of top hanging flexible plates at the top of VV and middle radial stoppers in the middle of outboard VV. Top hanging flexible plates are mounted at the TF inboard top region (R~5400 mm) using the narrow window space surrounded by PF1 and TF coils. Middle radial stoppers are located inside TF coil case around the outboard mid plane. The upper flange connection of the radial stopper should slide in vertical direction to eliminate thermal stress produced by relative thermal displacement between VV wall and TF coil case. Both supports are mounted on 18 locations in toroidal direction. The radial and toroidal reaction loads are shared with both supports. However, the vertical load is sustained by only the hanging support at the top.
2) The other option is a compressive type support that consists of nine VV supports located in alternate divertor port regions in toroidal direction. The location of the VV support corresponds to the position of VV field joint.

   Two designs have been performed for the compressive VV support. One is mounted on TF coil OIS and the other is on cryostat ring. The compressive support on TF coil OIS is dependent on TF coil movement but that on cryostat ring is independent. The loads of VV and TF coil supports are decreased comparing that of support system in which VV support is mounted on TF coil OIS. Stresses of VV support on cryostat ring are less than that on TF coil OIS.
3) All supports have enough structural integrity for all load combinations and the stresses are within the allowable limit. In the optional designs, the stresses produced by the relative thermal displacement between VV wall and TF coil case are considered as primary stress according to ASME Sec. III NF. The stress due to TF coil displacement is also considered as primary stress. The thermal stresses produced by a non-uniform temperature distribution are considered as secondary stress.
4) The restrictions to apply the optional designs are as follows;

   For the hanging type support, the spaces to mount the supports are the TF inboard top region and the VV outboard middle region inside TF case. They are 18 locations in toroidal direction. The location of top VV wall should be moved downward by 100 mm for the joint bolt fastening and thermal shield installation. Top VV outer wall configuration might be flattened for the easy assembly. The top CC radial spans need to be modified from the side edge to the center of the TF case.

   For the compressive type support, the spaces to mount the supports are alternate divertor port regions. Then the divertor ports should be limited to nine ports.

Acknowledgement

The authors would like to express their gratitude to department of ITER Project for their valuable discussions and comments. They would acknowledge Drs. T. Tsunematsu and M. Mori for their support.

References

[1] Design Description Document DDD 1.1 Magnet System, 2.2.3.9 Vacuum Vessel Support, N11 DDD142 01-07-12 R 0.1
[2] R. J. Roark, Formulas for Stress and Strain, 4th Edition, McGraw Hill, New York, 1965
[3] C. T. J. Jong, Displacements of TF coil for PF support and CC analyses performed by RF Home Team, ITER Interface Memorandum, Feb. 27, 2001.
[4] DRG Annex, Load Specification and Combination, p13.
[5] ASME Boiler and Pressure Vessel Code, Sec. VIII, Div. 2
[6] Design Description Document DDD 1.5 Vacuum Vessel, 2.1 VV Design Criteria and Loads, G15 DDD 4 01-06-25 R 0.1
[7] ASME Boiler and Pressure Vessel Code, Sec. III, Subsection-NB-3230
[8] ASME Boiler and Pressure Vessel Code, Sec. III-NB, APPENDIX-F
[9] ASME Boiler and Pressure Vessel Code, Sec. III-NH, APPENDIX-T
[10] Design Description Document DDD 2.7 Thermal Shield, 2.5 Thermal Hydraulic and Thermal Analyses, N27 DDD 6 01-07-17 R 0.1
[11] C.T.J. Jong, Interoffice memorandum,2001.11.
[12] ASME Sec. III NF , 3324.6
[13]Design Description Document DDD 1.1 Magnet System, 2.2.3.8 TF Gravity Support, 11 DDD115 01-06-27 R 0.1

国際単位系 (SI) と換算表

表1　SI基本単位および補助単位

量	名称	記号
長さ	メートル	m
質量	キログラム	kg
時間	秒	s
電流	アンペア	A
熱力学温度	ケルビン	K
物質量	モル	mol
光度	カンデラ	cd
平面角	ラジアン	rad
立体角	ステラジアン	sr

表2　SIと併用される単位

名称	記号
分，時，日	min，h，d
度，分，秒	°，′，″
リットル	l，L
トン	t
電子ボルト	eV
原子質量単位	u

1 eV = 1.60218 × 10^{-19} J

1 u = 1.66054 × 10^{-27} kg

表3　固有の名称をもつSI組立単位

量	名称	記号	他のSI単位による表現
周波数	ヘルツ	Hz	s^{-1}
力	ニュートン	N	$m\cdot kg/s^2$
圧力，応力	パスカル	Pa	N/m^2
エネルギー，仕事，熱量	ジュール	J	N·m
工率，放射束	ワット	W	J/s
電気量，電荷	クーロン	C	A·s
電位，電圧，起電力	ボルト	V	W/A
静電容量	ファラド	F	C/V
電気抵抗	オーム	Ω	V/A
コンダクタンス	ジーメンス	S	A/V
磁束	ウェーバ	Wb	V·s
磁束密度	テスラ	T	Wb/m^2
インダクタンス	ヘンリー	H	Wb/A
セルシウス温度	セルシウス度	℃	
光束	ルーメン	lm	cd·sr
照度	ルクス	lx	lm/m^2
放射能	ベクレル	Bq	s^{-1}
吸収線量	グレイ	Gy	J/kg
線量当量	シーベルト	Sv	J/kg

表4　SIと共に暫定的に維持される単位

名称	記号
オングストローム	Å
バーン	b
バール	bar
ガル	Gal
キュリー	Ci
レントゲン	R
ラド	rad
レム	rem

1 Å = 0.1 nm = 10^{-10} m

1 b = 100 fm^2 = 10^{-28} m^2

1 bar = 0.1 MPa = 10^5 Pa

1 Gal = 1 cm/s^2 = 10^{-2} m/s^2

1 Ci = 3.7 × 10^{10} Bq

1 R = 2.58 × 10^{-4} C/kg

1 rad = 1 cGy = 10^{-2} Gy

1 rem = 1 cSv = 10^{-2} Sv

表5　SI接頭語

倍数	接頭語	記号
10^{18}	エクサ	E
10^{15}	ペタ	P
10^{12}	テラ	T
10^{9}	ギガ	G
10^{6}	メガ	M
10^{3}	キロ	k
10^{2}	ヘクト	h
10^{1}	デカ	da
10^{-1}	デシ	d
10^{-2}	センチ	c
10^{-3}	ミリ	m
10^{-6}	マイクロ	μ
10^{-9}	ナノ	n
10^{-12}	ピコ	p
10^{-15}	フェムト	f
10^{-18}	アト	a

（注）

1. 表1－5は「国際単位系」第5版，国際度量衡局 1985年刊行による。ただし，1 eVおよび1 uの値はCODATAの1986年推奨値によった。
2. 表4には海里，ノット，アール，ヘクタールも含まれているが日常の単位なのでここでは省略した。
3. barは，JISでは流体の圧力を表わす場合に限り表2のカテゴリーに分類されている。
4. EC閣僚理事会指令ではbar，barnおよび「血圧の単位」mmHgを表2のカテゴリーに入れている。

換算表

力	N(=10^5 dyn)	kgf	lbf
	1	0.101972	0.224809
	9.80665	1	2.20462
	4.44822	0.453592	1

粘度　1 Pa·s(N·s/m^2) = 10 P(ポアズ)(g/(cm·s))

動粘度　1 m^2/s = 10^4 St(ストークス)(cm^2/s)

圧力	MPa(=10 bar)	kgf/cm^2	atm	mmHg(Torr)	lbf/in^2(psi)
	1	10.1972	9.86923	7.50062 × 10^3	145.038
	0.0980665	1	0.967841	735.559	14.2233
	0.101325	1.03323	1	760	14.6959
	1.33322 × 10^{-4}	1.35951 × 10^{-3}	1.31579 × 10^{-3}	1	1.93368 × 10^{-2}
	6.89476 × 10^{-3}	7.03070 × 10^{-2}	6.80460 × 10^{-2}	51.7149	1

エネルギー・仕事・熱量	J(=10^7 erg)	kgf·m	kW·h	cal(計量法)	Btu	ft·lbf	eV
	1	0.101972	2.77778 × 10^{-7}	0.238889	9.47813 × 10^{-4}	0.737562	6.24150 × 10^{18}
	9.80665	1	2.72407 × 10^{-6}	2.34270	9.29487 × 10^{-3}	7.23301	6.12082 × 10^{19}
	3.6 × 10^6	3.67098 × 10^5	1	8.59999 × 10^5	3412.13	2.65522 × 10^6	2.24694 × 10^{25}
	4.18605	0.426858	1.16279 × 10^{-6}	1	3.96759 × 10^{-3}	3.08747	2.61272 × 10^{19}
	1055.06	107.586	2.93072 × 10^{-4}	252.042	1	778.172	6.58515 × 10^{21}
	1.35582	0.138255	3.76616 × 10^{-7}	0.323890	1.28506 × 10^{-3}	1	8.46233 × 10^{18}
	1.60218 × 10^{-19}	1.63377 × 10^{-20}	4.45050 × 10^{-26}	3.82743 × 10^{-20}	1.51857 × 10^{-22}	1.18171 × 10^{-19}	1

1 cal = 4.18605 J（計量法）

= 4.184 J （熱化学）

= 4.1855 J （15 °C）

= 4.1868 J（国際蒸気表）

仕事率　1 PS（仏馬力）

= 75 kgf·m/s

= 735.499 W

放射能	Bq	Ci
	1	2.70270 × 10^{-11}
	3.7 × 10^{10}	1

吸収線量	Gy	rad
	1	100
	0.01	1

照射線量	C/kg	R
	1	3876
	2.58 × 10^{-4}	1

線量当量	Sv	rem
	1	100
	0.01	1

（86年12月26日現在）

Alternatives of ITER Vacuum Vessel Support System